

THE VIBRATIONAL SPECTRUM OF A MONATOMIC, FACE-CENTERED CUBIC
CRYSTAL LATTICE

Thesis by
Robert B. Leighton

In Partial Fulfilment of the Requirements for the
Degree of Doctor of Philosophy

California Institute of Technology
Pasadena, California

1947

ACKNOWLEDGMENT

The author wishes to express his deep gratitude to Prof. William V. Houston, who first suggested this problem, and who rendered invaluable aid during the progress of the work, and to Prof. Paul S. Epstein, whose interest and suggestions were very helpful in the later stages of the analysis.

CONTENTS

	Page
ACKNOWLEDGMENT	ii
LIST OF ILLUSTRATIONS	vi
INTRODUCTION	viii
SECTION I. THE EQUATIONS OF MOTION OF A FACE-CENTERED CRYSTAL	
LATTICE	1
1. Introduction	1
2. Notation	1
3. Kinetic Energy of the Face-Centered Cubic Lattice	3
4. Potential Energy of the Face-Centered Cubic Lattice	4
5. The Born - von Karman Boundary Condition	4
6. Lagrangian Function in Terms of the Normal Coordinates	6
7. The Lagrangian Equations of Motion	9
8. The Propagation Vector	9
9. The Secular Determinant	11
SECTION II. GENERAL PROPERTIES OF THE SECULAR DETERMINANT 14	
1. Introduction	14
2. Definition of the Continuous Distribution Function $N(\nu)$	15
3. Symmetry Properties of the Secular Determinant	16
4. Periodicity Properties of the Roots of the Secular Determinant	17
5. Range of Variation of $(l_m n)$	18
6. Special Solutions of the Secular Determinant	20
7. Orthogonality of Surfaces and Symmetry Planes	23

Contents (Cont'd.)

	Page
SECTION III. THE SURFACES OF CONSTANT FREQUENCY	29
1. Introduction	29
2. Fundamental Region of Symmetry and Periodicity	29
3. Contours for $\gamma/a = 0$	30
4. Complete Identification of the Branches	42
5. Contours for $\gamma/a = -0.1$	46
6. Nature of the Contours Near the Origin	48
SECTION IV. THE FREQUENCY SPECTRUM OF A FACE-CENTERED CUBIC CRYSTAL LATTICE	51
1. Introduction	51
2. Construction of the Constant-Frequency Surfaces	51
3. Measurement of Volumes	53
4. The Frequency Spectrum	57
5. The Frequency Spectrum for Low Frequencies	59
SECTION V. ATOMIC FORCE CONSTANTS	63
1. Introduction	63
2. Outline of the Properties of the Elastic Constants	63
3. Elastic Constants of the Monovalent, Cubic Metals	66
4. Evaluation of α and γ	66
SECTION VI. SPECIFIC HEATS OF FACE-CENTERED CUBIC ELEMENTS	71
1. Introduction	71
2. The Specific Heat Integral	71
3. Specific Heats of Face-Centered Cubic Elements	73

Contents (Cont'd.)

	Page
4. θ/β vs. T/β Curves of Very Low Temperatures	75
5. Curves of θ/β vs. T/β and Discussion of Results	77
6. Specific Heat of Silver	79
7. Conclusions	83
ABSTRACT	84
BIBLIOGRAPHY	85

LIST OF ILLUSTRATIONS

Figure	Follows Page
1a. A face-centered cubic lattice	2
1b. The boundary lines of the crystal being treated	2
2. The symmetry planes of the roots of the secular determinant .	17
3. Sine-wave displacements of a chain of mass particles	19
4. The first Brillouin Zone	19
5. A three-dimensional plot of the contours of constant - frequency . . .	42
6. Surfaces near the line $x = y = z$ for one possible correlation of solutions	44
7. Branches I and II make equal angles with the line $x = y = z$.	44
8. Surfaces near the line $x = y = z$ for the other possible correlation of solutions	44
9. Illustration of the degree of approximation to which the results of the analysis of the text correspond to the contours given in Figure 5	46
10. Contours of constant frequency for $\gamma/a = 0$ (Branch I) . . .	48
11. Contours of constant frequency for $\gamma/a = 0$ (Branch II) . .	48
12. Contours of constant frequency for $\gamma/a = 0$ (Branch III) . .	48
13. Contours of constant frequency for $\gamma/a = -0.1$ (Branch I) .	48
14. Contours of constant frequency for $\gamma/a = -0.1$ (Branch II) .	48
15. Contours of constant frequency for $\gamma/a = -0.1$ (Branch III) .	48
16. Constant-frequency contours for $\gamma/a = 0$ and $\gamma/a = -0.1$ neglecting higher order terms in the series expansions of the trigonometric terms of the secular determinant	50

LIST OF ILLUSTRATIONS (Cont'd)

Figure	Follows Page
17. The distribution functions $G_1(\lambda)$ and $G(\lambda)$	59
18. Values of k_1 and k	60
19. Curves of θ/β <u>vs.</u> T/β	77
20. The specific heat of silver	81

INTRODUCTION

Many of the thermal properties of solids can be explained semi-quantitatively by interpreting them in terms of thermal vibrations of the atoms about their mean rest positions. For example, the specific heat is a property which is intimately connected with these thermal vibrations; if the atoms are considered to possess a certain statistical average energy of vibration, the derivative of this average energy with respect to the temperature is proportional to the specific heat. As another example, the electrical resistance of many metals at low temperatures is due to the interaction of the conduction electrons with the vibrating lattice. A quantum-mechanical treatment of the problem of an electron in a perfectly regular lattice gives the result that the electrical resistance is zero, while a more extended treatment including the lattice distortion due to thermal agitation shows that the electrons may be scattered (with an exchange of energy with the vibrating lattice) and correctly accounts for the main features of the empirical data⁽¹²⁾. Other properties of solids that depend wholly or partially upon the thermal vibrations of the atoms are the thermal expansion, the thermal scattering of X-rays (observed in X-ray diffraction), and many of the more complicated phenomena, such as phase changes, melting, order-disorder transitions, and free rotation in crystals, to name but a few.

For many purposes the above properties may be treated adequately by using only the qualitative features of the thermal vibrations, but in certain cases, the experimental data indicate that a more refined treatment is desirable. In particular this is true of the specific heat.

It is the purpose of this paper to study the thermal vibrations of a

face-centered cubic lattice, for which good data on elasticity and specific heat are available, and to attempt to improve the agreement between theoretical and experimental values of specific heats. In order to provide a background against which the results of the present investigation can be evaluated, a few remarks regarding the work of previous investigators may be helpful.

The rough rule of Dulong and Petit, which asserts that the molar heat capacity of a monatomic crystalline solid is equal to $3R$, where R is the gas constant per mole, is given theoretical support by the classical statistics. For, classically, each atom of a solid body would possess, on the average, $3kT$ ergs of vibrational energy at the temperature T , and thus the N_0 atoms in a mole of the solid would possess $3N_0kT$ ergs of energy. Differentiation of this expression with respect to T yields,

$$C_V = 3N_0k = 3R,$$

as indicated above.

Actually, it is known that the heat capacity drops from the Dulong Petit value at high temperatures to zero at the absolute zero. This was first inferred from Nernst's Heat Postulate, and experimentally verified by Nernst's pupils. Einstein⁽⁶⁾ first recognized the importance of treating the atoms of a crystal as quantum-mechanical simple harmonic oscillators. He regarded the atoms of a crystal as being independent three-dimensional oscillators, all having the same frequency ν . Quantum-mechanically, the average energy possessed by a one-dimensional simple harmonic oscillator at the temperature T is

$$(0.1) \quad E_{av.} = +h\nu/2 + h\nu / (e^{h\nu/kT} - 1)$$

The specific heat follows from this expression by differentiation with respect to the temperature and multiplication by the number of oscillators

present in the crystal, which is $3N_0$, since the above expression is for a one-dimensional oscillator:

$$(0.2) \quad C_v = 3N_0 d/dT \left(\frac{h\nu}{2} + \frac{h\nu}{e^{h\nu/kT} - 1} \right) = \frac{3N_0 k h^2 \nu^2}{k^2 T^2} \frac{e^{h\nu/kT}}{(e^{h\nu/kT} - 1)^2}.$$

It will be seen that the specific heat of such a system does indeed vanish at low temperatures, and by expanding the denominator in a Taylor series it can be shown that the specific heat at high temperatures approaches $3R$. The expression (0.2) has an exponential dependence on the reciprocal of the temperature for low temperatures, while actual nonconducting solids show a T^3 dependence upon the temperature in the low temperature range. The difficulty comes in the assumption of a single frequency for all of the oscillators, generally of the order of an infra-red frequency, while actually it is clear that some of the normal frequencies of the solid body will be very low, corresponding to the mechanical vibrations of the crystal as a whole.

By the theory of normal coordinates, each normal mode of vibration may be treated as a separate harmonic oscillator, whose possible energy levels are $(N + \frac{1}{2})h\nu$. The spectrum of possible values of the frequencies of the normal modes of a solid body of a finite size will actually consist of a large number of discrete values, but for the purpose of calculating the specific heat these frequencies are so close together that they may be considered to be continuously distributed according to a distribution law,

$$(0.3) \quad N(\nu) \Delta\nu = \Delta n$$

where Δn is the number of normal frequencies lying in the range ν to $\nu + \Delta\nu$, and $N(\nu)$ is the distribution function. Thus, the approximation of

the actual, discrete frequency spectrum by the continuous distribution function $N(\nu)$ is quite analogous to an approximation of the actual, discrete nature of the atomic lattice by a continuous mass distribution, ρ .

From equations (0.2) and (0.3), the specific heat of Δn oscillators having the frequency ν is,

$$\begin{aligned} \Delta C_V &= \frac{h^2 \nu^2}{kT^2} \frac{e^{h\nu/kT}}{(e^{h\nu/kT} - 1)^2} \Delta n \\ &= \frac{h^2 \nu^2}{kT^2} \frac{e^{h\nu/kT}}{(e^{h\nu/kT} - 1)^2} N(\nu) \Delta \nu, \end{aligned}$$

whence the total specific heat of a body having the frequency distribution $N(\nu)$ is

$$(0.4) \quad C_V = \frac{h^2}{kT^2} \int_0^{\nu_m} \frac{\nu^2 e^{h\nu/kT}}{(e^{h\nu/kT} - 1)^2} N(\nu) d\nu$$

The foregoing considerations were embodied in theories of specific heat by Debye⁽⁴⁾, who assumed that the spectrum of normal frequencies of a crystal was essentially like that of a continuous medium, and by Born and von Karman⁽²⁾, who set up the dynamical equations of motion of the atoms of a crystal, and with a transformation of coordinates arrived at a secular determinant, whose solution would yield the frequency spectrum of the crystalline body.

In the Debye theory it is shown that the distribution function $N(\nu)$ for a continuum is proportional to the square of the frequency:

$$(0.5) \quad N(\nu) = A\nu^2$$

where A is a constant depending upon the velocities of propagation of longitudinal and transverse waves in the solid medium, and upon the volume of the body. The

fact that the total number of normal modes of a crystal containing N_0 atoms is $3N_0$ is provided for by cutting the distribution off abruptly at a maximum frequency ν_m , such that

$$(0.6) \quad \int_0^{\nu_m} A\nu^3 d\nu = A\nu_m^3 / 3 = 3N_0.$$

When the distribution (0.5) is used, and the substitution $x = h\nu/kT$ is made, the specific heat integral (0.4) becomes, for an isotropic continuum,

$$C_v = \frac{A k T^3}{h^3} \int_0^{h\nu_m/kT} \frac{x^4 e^x}{(e^x - 1)^2} dx.$$

Defining a new quantity $\Theta = h\nu_m/k$, called the Debye Characteristic Temperature, and using the relation (0.6), the specific heat may finally be written,

$$C_v = 9R \left(\frac{T}{\Theta} \right)^3 \int_0^{\Theta/T} \frac{x^4 e^x}{(e^x - 1)^2} dx.$$

The Debye theory is thus a one-parameter theory, so that a knowledge of the true specific heat at one temperature should suffice to determine the characteristic temperature, and from this the specific heat at any other temperature. In practice it is found that the value of Θ as calculated from the elastic properties and the density does not agree with that value calculated from specific heat data at the same temperature. This difficulty is usually resolved by choosing a value of Θ that gives good agreement with measured specific heats over the temperature range of interest.

It will be appreciated that, because of the variation of elastic constants with temperature, and because the Debye distribution does not give an adequate

approximation to the actual frequency distribution for a crystal, the quantity Θ cannot be constant with temperature. It has become customary, in discussing the properties of a frequency distribution function, to study, not the specific heat curve defined by the function, but rather the curve of Θ vs. T which would be necessary to make the Debye theory give the same specific heat curve as does the distribution function under consideration. This procedure is followed because Θ is a more sensitive function of the shape of the frequency spectrum than is the specific heat. Thus, a satisfactory criterion for agreement between the predicted specific heats and the actual specific heats would be that the Θ vs. T curves required by each be the same. This method also makes it easier to detect deviations from the Debye theory, especially in the region of very low temperatures.

Because of the great success of the Debye theory in giving a semi-quantitative description of the specific heats of simple solids, the more rigorous theory of Born and von Karman (Page xi) was neglected for many years. With the improved accuracy of later measurements, however, and with the increasing number of substances being studied, certain discrepancies of the Debye theory appeared, which suggested that a closer study of the Born-von Karman theory be made.

A closer analysis of the qualitative features of the frequency distribution of a simple cubic lattice was made by Blackman⁽¹⁾ in a series of papers starting in 1935. His results apply to crystals of the sodium chloride type; and his conclusion regarding certain low-temperature anomalies⁽¹³⁾ in the measured specific heat was that, to the degree of approximation attainable with the assumption of central, Hooke's-law-forces between nearest and next-nearest neighbors, the anomalies could not be explained by a difference in frequency spectrum between the Debye theory and the lattice theory. This question will be considered in detail in Section VI.

A short time after Blackman's work was published, Fine⁽¹⁰⁾ obtained a frequency spectrum for the body-centered element tungsten, by numerical integration. Fine's work represents a great step forward, for this was the first time anyone had considered a monatomic crystal of a type actually occurring in nature, all other investigators having considered only the sodium chloride lattice. Fine did not obtain his frequency spectrum in the form of three separate branches such that each could be studied individually, but rather worked with the entire distribution. Thus any sharp corners in the distribution that might have been introduced through the three branches extending over different ranges of frequency cannot be found in his result. This point may prove important in trying to fit a specific heat curve by using three Debye functions. The manner in which the secular determinant yields a number of separate branches will be studied in detail in connection with the solution of the secular determinant in Section II.

The sodium chloride lattice was considered also in a recent paper by Kellermann⁽¹⁴⁾, who approached the problem of lattice dynamics from a purely electromagnetic standpoint. He evaluated the forces acting upon an ion in terms of the retarded potentials due to all of the other ions, and not only arrived at a frequency spectrum (which differed markedly from that of Blackman), but also calculated the elastic constants of sodium chloride, the agreement with experimental elastic constants being within a few per cent.

The most recent development in the problem of lattice dynamics appeared in a series of papers by Montroll⁽¹⁶⁾ and his coworkers. Montroll made use of the fact that the trace of the matrix associated with the secular determinant is equal to the sum of the squares of all the frequencies appearing in the spectrum; and in general, the trace of the n th power of this matrix is equal

to the sum of the $2n$ th powers of all of the frequencies. By actually carrying out this summation for six or seven powers of the matrix, the first six or seven moments of the frequency distribution taken about the original were obtained. If the distribution function $N(\nu)$ were expanded in any set of polynomials which are orthogonal in an interval coinciding with that occupied by the function $N(\nu)$, the coefficient of the n th polynomial in the expansion would be a linear combination of the first n moments of the distribution. Montroll applied this method, using Legendre polynomials, to body-centered lattices having various ratios of next-nearest to nearest neighbor force constants, including the case of tungsten. His distribution was somewhat similar to Fine's for this case.

This ends the historical sketch of work in this field; the specific problems involved in finding the frequency spectrum of a monatomic crystal lattice will now be treated. The main purpose of the foregoing discussion has been to acquaint the reader with some of the developments in the theory of specific heats that bear upon the questions to be discussed in the present paper. Many of the topics will receive broader treatment in the text.

SECTION I

THE EQUATIONS OF MOTION OF A FACE-CENTERED CUBIC CRYSTAL LATTICE

1. Introduction

In the present section the equations of motion of a face-centered cubic crystal lattice will be derived, and the secular determinant governing its frequency spectrum will be obtained. The most direct approach to the equations of motion would be to write down the components of force acting on any atom in a lattice, and to equate these forces to the respective components of mass times acceleration for the particle. For later work, however, in which the quadratic form of the potential energy will simplify the evaluation of the atomic force constants, the use of Lagrange's equations is indicated. Expressions for the kinetic and potential energy of the vibrating lattice will thus be written, and after a coordinate transformation which amounts almost to a change to normal coordinates, the equations of motion will be obtained with the help of Lagrange's equations. The condition that the solutions of the Lagrangian equations be periodic in time with the same frequency and arbitrary amplitude will then yield a secular determinant for the lattice.

2. Notation

An orthogonal Cartesian coordinate system (X, Y, Z) oriented along the principal crystallographic axes of the crystal will be used. The crystal lattice will be defined in the customary manner by means of three primitive translation vectors $(\bar{A}_1, \bar{A}_2, \bar{A}_3)$ (not orthogonal to one another for the case treated here), such that any lattice site can be reached from the lattice site at the origin of the (X, Y, Z) system by means of a vector of the form $\bar{r}_{abc} = a\bar{A}_1 + b\bar{A}_2 + c\bar{A}_3$ where (a, b, c) are integers. The primitive triple

$(\bar{A}_1, \bar{A}_2, \bar{A}_3)$ may of course be written in terms of the set of unit vectors $(\bar{i}, \bar{j}, \bar{k})$ parallel to the three axes (X,Y,Z) respectively.

Figure 1a shows a face-centered cubic crystal lattice with the primitive translation vectors identified. To illustrate how each lattice site can be reached by a sum of the form given above, the Cartesian coordinates of some of the atoms are given in the short table below, together with the vector expression in terms of the primitive translation vectors.

Atom coordinates	\bar{A}_{123}	(a,b,c)
d, 0, 0	$-\bar{A}_1 + \bar{A}_2 + \bar{A}_3$	(-1,1,1)
d, d, 0	$2\bar{A}_3$	(0,0,2)
d, d, d	$\bar{A}_1 + \bar{A}_2 + \bar{A}_3$	(1,1,1)
d,d/2,d/2	$\bar{A}_2 + \bar{A}_3$	(0,1,1)
d/2,d,d/2	$\bar{A}_1 + \bar{A}_3$	(1,0,1)

To show that the point at the center of the cube cannot be reached by a vector of this form, it suffices to write down the vector from the origin to the center of the cube. It is just one-half of the vector from the origin to the farthest corner of a cube, namely, $\frac{1}{2}(\bar{A}_1 + \bar{A}_2 + \bar{A}_3)$, which corresponds to half-integral values of (a,b,c).

The shape of the crystal will be assumed to be a parallelepiped having three principal edges $N_1\bar{A}_1, N_2\bar{A}_2, N_3\bar{A}_3$. Thus all lattice sites inside the crystal can be reached by combinations (a,b,c) such that $0 < a < N_1, 0 < b < N_2$ and $0 < c < N_3$. The boundary of the crystal is shown in Figure 1b.

Corresponding to this crystal lattice, there is a reciprocal lattice⁽³⁾ whose primitive triple $(\bar{B}_1, \bar{B}_2, \bar{B}_3)$ may be expressed in terms of the vectors $(\bar{A}_1, \bar{A}_2, \bar{A}_3)$ by the relations

$$(1.1) \quad \bar{B}_1 = \frac{\bar{A}_2 \times \bar{A}_3}{\bar{A}_1 \cdot (\bar{A}_2 \times \bar{A}_3)}, \quad \bar{B}_2 = \frac{\bar{A}_3 \times \bar{A}_1}{\bar{A}_2 \cdot (\bar{A}_3 \times \bar{A}_1)}, \quad \bar{B}_3 = \frac{\bar{A}_1 \times \bar{A}_2}{\bar{A}_3 \cdot (\bar{A}_1 \times \bar{A}_2)}.$$

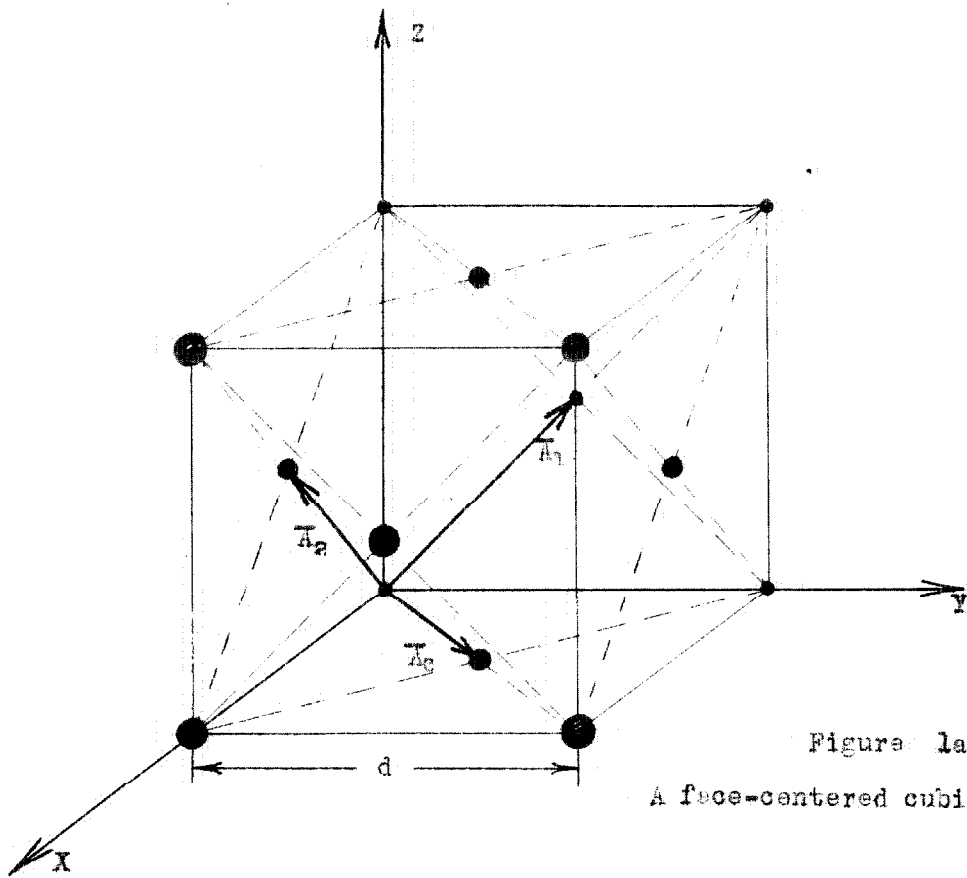


Figure 1a.
A face-centered cubic lattice.

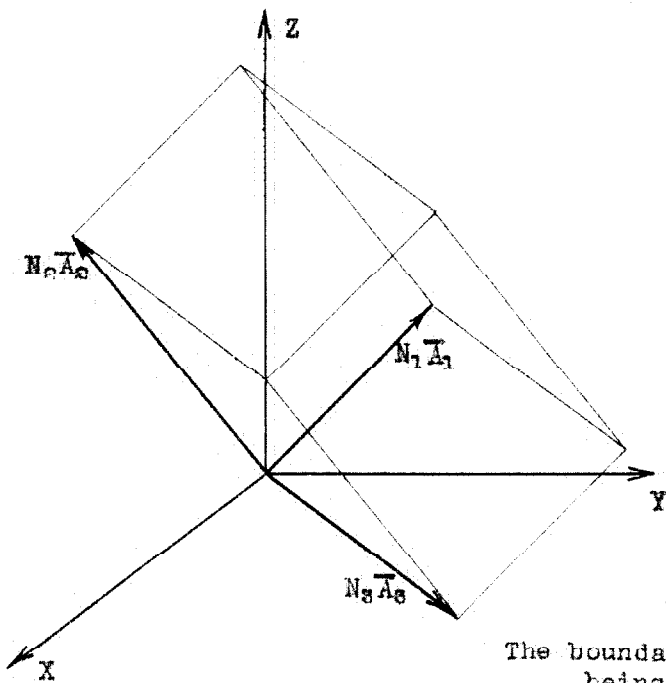


Figure 1b.
The boundary lines of the crystal
being treated.

The displacement (from its equilibrium position) of the mass-particle associated with the lattice site (abc) will have the components $(u_{abc}, v_{abc}, w_{abc})$ along the (X,Y,Z) axes, respectively.

The potential energy expression will contain relative displacements of the form $(u_{a+1bc} - u_{abc})$, etc. The subscripts in such an expression are quite cumbersome, so an abbreviation will be used which replaces (abc) by o , and $(a+1bc)$ by $(1oo)$, etc., with the (abc) subscript appearing outside the entire expression. Thus, the example given above would become $(u_{1oo} - u_o)_{abc}$.

Regarding the nature of the forces acting between the atoms, a central Hooke's-law force, with force constant α , will be assumed to act between nearest neighbors, and a central Hooke's-law force, with force constant γ , between next-nearest neighbors. Further remarks concerning these force constants will be reserved for a later time (Section V).

Other symbols will be required from time to time, but it would be more confusing to introduce them now than later. The Lagrangian function for the face-centered cubic lattice will now be written with the aid of the above definitions.

3. Kinetic Energy of the Face-Centered Cubic Lattice

In terms of the quantities defined in the previous paragraph, the kinetic energy of the face-centered cubic lattice may be written

$$T = \frac{1}{2} m \sum_{a=0}^{N_1} \sum_{b=0}^{N_2} \sum_{c=0}^{N_3} (\dot{u}_o^2 + \dot{v}_o^2 + \dot{w}_o^2)_{abc}$$

which may be abbreviated

$$(1.2) \quad T = \frac{1}{2} m \sum_{abc} (\dot{u}_o^2 + \dot{v}_o^2 + \dot{w}_o^2)_{abc}$$

where m is the mass of each particle, and the dot denotes differentiation with respect to the time.

4. Potential Energy of the Face-Centered Cubic Lattice

Using the notation defined in Paragraph 3, the potential energy of the face-centered lattice may be written in the form,

$$(1.3) \quad V = \frac{1}{2} \sum_{abc} \left\{ \alpha/2 \left[(v_{100} - v_0 + w_{100} - w_0)^2 + (w_{010} - w_0 + u_{010} - u_0)^2 \right. \right. \\ + (u_{001} - u_0 + v_{001} - v_0)^2 + (v_{1-10} - v_0 - u_{1-10} + u_0)^2 \\ + (w_{0-1-1} - w_0 - v_{0-1-1} + v_0)^2 + (u_{-101} - u_0 - w_{-101} + w_0)^2 \left. \right] \\ \left. + \gamma \left[(u_{-111} - u_0)^2 + (v_{1-11} - v_0)^2 + (w_{11-1} - w_0)^2 \right] \right\}_{abc}$$

where each of the terms represents the square of the change in distance between the two atoms defined by the subscripts, up to the second order in the relative displacements of the atoms, and multiplied by the appropriate force constant. The fact that those atoms on the boundary faces of the crystal will yield terms of different form from those in the interior is for the moment ignored. The expression given above would be strictly correct if the summation were restricted to exclude the boundary layers on three sides of the parallelepiped. In any case, the fractional error would be no larger than the ratio of the number of particles in the surface of the crystal to the number of particles inside it.

5. The Born - von Karman Boundary Condition

In order to obtain a complete solution for the motion of the crystal lattice, it is necessary to specify the constraints, or boundary condition, that it must satisfy. For example, it is necessary to know whether the boundary surfaces are fixed, perfectly free, or subject to outside forces, etc. The form of the solution will depend to a large extent upon the boundary condition, but the total number of normal modes of vibration will always be equal to the number of degrees of freedom that remain after the boundary condition is imposed. The constraints in this case will be applied only to the atoms lying on the surface

of the crystal, so that the number of degrees of freedom will still be of the order of 10^{24} for a mole of the substance. Thus, it may be expected that the exact form of the boundary condition will have only a minor effect upon the frequency distribution of the normal modes.

One boundary condition is that used by Born and von Karman⁽²⁾ in their original paper. This condition requires that the displacements of atoms in corresponding positions in opposite boundary faces of the crystal be the same. Currently it is known as the periodicity condition.

Expressed analytically, the cyclic character of the Born-von Karman boundary condition is satisfied by a Fourier expansion of the form

$$(1.4a) \quad u_{abc} = \sum_{lmn} U_{lmn} e^{2\pi i (\bar{A}_{abc} \cdot \bar{B}_{lmn})}$$

where the U_{lmn} are functions of the time. Here, $\bar{A}_{abc} = a\bar{A}_1 + b\bar{A}_2 + c\bar{A}_3$ is the position vector to the lattice site (abc) and $\bar{B}_{lmn} = l\bar{B}_1/N_1 + m\bar{B}_2/N_2 + n\bar{B}_3/N_3$ where (lmn) are integers, and $(\bar{B}_1, \bar{B}_2, \bar{B}_3)$ are the primitive vectors of the reciprocal lattice. The range of variation of (lmn) will be discussed in Section II. It suffices here to say that the total number of combinations of (lmn) will be equal to one-third the number of degrees of freedom of the crystal. The exponential factor may be written

$$e^{2\pi i (\bar{A}_{abc} \cdot \bar{B}_{lmn})} = e^{2\pi i (la/N_1 + mb/N_2 + nc/N_3)},$$

since $\bar{A}_i \cdot \bar{B}_j = \delta_{ij}$. This expression clearly has the required periodicity property, i.e.,

$$e^{2\pi i (la/N_1 + mb/N_2 + nc/N_3)} = e^{2\pi i (la/N_1 + mb/N_2 + n(c+N_3)/N_3)}$$

and similarly for a and b.

Similarly, the displacements among the remaining axes are written

$$(1.1b) \quad v_{abc} = \sum_{lmn} V_{lmn} e^{2\pi i(\bar{A}_{abc} \cdot \bar{B}_{lmn})}$$

$$(1.1c) \quad w_{abc} = \sum_{lmn} W_{lmn} e^{2\pi i(\bar{A}_{abc} \cdot \bar{B}_{lmn})}$$

Because of the complex nature of the (U, V, W) , the displacements (u, v, w) can be real only if

$$U_{lmn} = U_{-l-m-n}^*, \quad V_{lmn} = V_{-l-m-n}^*, \quad \text{and} \quad W_{lmn} = W_{-l-m-n}^*.$$

6. Lagrangian Function in Terms of the Normal Coordinates

When the transformations given above are substituted into the expressions for the kinetic and potential energy, the Lagrangian function takes the form

$$(1.6) \quad L = T - V = \frac{1}{2} \sum_{abc} \sum_{lmn} \sum_{l'm'n'} \left\{ m(\dot{U}_{lmn} \dot{U}_{l'm'n'} + \dot{V}_{lmn} \dot{V}_{l'm'n'} + \dot{W}_{lmn} \dot{W}_{l'm'n'}) \right. \\ - \alpha/2 \left[(V_{lmn} + W_{lmn})(V_{l'm'n'} + W_{l'm'n'}) (e^{2\pi i l/N_1} - 1) (e^{2\pi i l'/N_1} - 1) \right. \\ + (W_{lmn} + U_{lmn})(W_{l'm'n'} + U_{l'm'n'}) (e^{2\pi i m/N_2} - 1) (e^{2\pi i m'/N_2} - 1) \\ + (U_{lmn} + V_{lmn})(U_{l'm'n'} + V_{l'm'n'}) (e^{2\pi i n/N_3} - 1) (e^{2\pi i n'/N_3} - 1) \\ + (V_{lmn} - U_{lmn})(V_{l'm'n'} - U_{l'm'n'}) (e^{2\pi i (l/N_1 - m/N_2)} - 1) (e^{2\pi i (l'/N_1 - m'/N_2)} - 1) \\ + (W_{lmn} - V_{lmn})(W_{l'm'n'} - V_{l'm'n'}) (e^{2\pi i (m/N_2 - n/N_3)} - 1) (e^{2\pi i (m'/N_2 - n'/N_3)} - 1) \\ + (U_{lmn} - W_{lmn})(U_{l'm'n'} - W_{l'm'n'}) (e^{2\pi i (n/N_3 - l/N_1)} - 1) (e^{2\pi i (n'/N_3 - l'/N_1)} - 1) \left. \right] \\ - \gamma \left[U_{lmn} U_{l'm'n'} (e^{2\pi i (-l/N_1 + m/N_2 + n/N_3)} - 1) (e^{2\pi i (-l'/N_1 + m'/N_2 + n'/N_3)} - 1) \right. \\ + V_{lmn} V_{l'm'n'} (e^{2\pi i (l/N_1 - m/N_2 + n/N_3)} - 1) (e^{2\pi i (l'/N_1 - m'/N_2 + n'/N_3)} - 1) \\ + W_{lmn} W_{l'm'n'} (e^{2\pi i (l/N_1 + m/N_2 - n/N_3)} - 1) (e^{2\pi i (l'/N_1 + m'/N_2 - n'/N_3)} - 1) \left. \right] \left. \right\} \\ \times e^{2\pi i \bar{A}_{abc} \cdot (\bar{B}_{lmn} + \bar{B}_{l'm'n'})}$$

To illustrate the steps by which this expression was derived, the first term in the potential energy (1.3) is treated in detail:

$$\begin{aligned}
 V' &= \frac{1}{2} \sum_{abc} a/2 (v_{100} - v_0 + w_{100} - w)_{abc}^2 \\
 &= \frac{1}{2} \sum_{abc} a/2 (v_{a+1bc} - v_{abc} + w_{a+1bc} - w_{abc})^2 \\
 &= \frac{1}{2} \sum_{abc} \sum_{lmn} \sum_{l'm'n'} a/2 \left\{ v_{lmn} e^{2\pi i(l(a+1)/N_1 + mb/N_2 + nc/N_3)} \right. \\
 &\quad - v_{lmn} e^{2\pi i(la/N_1 + mb/N_2 + nc/N_3)} + v_{lmn} e^{2\pi i(l(a+1)/N_1 + mb/N_2 + nc/N_3)} \\
 &\quad - w_{lmn} e^{2\pi i(la/N_1 + mb/N_2 + nc/N_3)} \left. \right\} \left\{ v_{l'm'n'} e^{2\pi i(l'(a+1)/N_1 + m'b/N_2 + n'c/N_3)} \right. \\
 &\quad - v_{l'm'n'} e^{2\pi i(l'a/N_1 + m'b/N_2 + n'c/N_3)} + w_{l'm'n'} e^{2\pi i(l'(a+1)/N_1 + m'b/N_2 + n'c/N_3)} \\
 &\quad \left. - w_{l'm'n'} e^{2\pi i(l'a/N_1 + m'b/N_2 + n'c/N_3)} \right\}
 \end{aligned}$$

but

$$e^{2\pi i(l(a+1)/N_1 + mb/N_2 + nc/N_3)} = e^{2\pi il/N_1} e^{2\pi i(la/N_1 + mb/N_2 + nc/N_3)}$$

so that

$$\begin{aligned}
 V' &= \frac{1}{2} \sum_{abc} \sum_{lmn} \sum_{l'm'n'} a/2 (v_{lmn} + w_{lmn}) (v_{l'm'n'} + w_{l'm'n'}) \\
 &\quad \times (e^{2\pi il/N_1} - 1) (e^{2\pi il'/N_1} - 1) e^{2\pi i [(1+l')a/N_1 + (m+m')b/N_2 + (n+n')c/N_3]} \\
 &= \frac{1}{2} \sum_{abc} \sum_{lmn} \sum_{l'm'n'} a/2 (v_{lmn} + w_{lmn}) (v_{l'm'n'} + w_{l'm'n'}) \\
 &\quad \times (e^{2\pi il/N_1} - 1) (e^{2\pi il'/N_1} - 1) e^{2\pi i \bar{A}_{abc}} \cdot (\bar{B}_{lmn} + \bar{B}_{l'm'n'})
 \end{aligned}$$

as was asserted above.

Now it will be seen from an inspection of (1.6) that the only dependence of the expression upon the position indices (abc) is in the vector \bar{A}_{abc} ; this appears only in the exponential which is a factor of the remainder of the expression. Thus, if the summation over (abc) is carried out, there

results a remarkable simplification of the Lagrangian function. In the summation over a , one is always confronted with an expression of the form

$$S_e = K \sum_{a=0}^{N_1} e^{2\pi i(1+l')a/N_1}$$

where K is not dependent on a .

Geometrically, the summation represents the resultant vector obtained by adding together the sides of a polygon (or star-shaped figure, depending upon the value of l and l') over an integral number of complete cycles. The sum is thus equal to zero for all values of l and l' except when $l + l' = 0$. In the latter case, the value of the exponential is unity, so that $S_a = N_1 K$.

Applying this principle to the expression (1.6) and making use of (1.5), one obtains,

$$\begin{aligned}
 L = & \frac{1}{2} \sum_{lmn} \left\{ m(\dot{U}_{lmn} \dot{U}_{lmn}^* + \dot{V}_{lmn} \dot{V}_{lmn}^* + \dot{W}_{lmn} \dot{W}_{lmn}^*) \right. \\
 & + \alpha/2 \left[(V_{lmn} + W_{lmn})(V_{lmn}^* + W_{lmn}^*)(2 - 2 \cos 2\pi(l/N_1)) \right. \\
 & + (V_{lmn} + U_{lmn})(V_{lmn}^* + U_{lmn}^*)(2 - 2 \cos 2\pi(m/N_2)) \\
 & + (U_{lmn} + V_{lmn})(U_{lmn}^* + V_{lmn}^*)(2 - 2 \cos 2\pi(n/N_3)) \\
 & + (V_{lmn} - U_{lmn})(V_{lmn}^* - U_{lmn}^*)(2 - 2 \cos 2\pi(l/N_1 - m/N_2)) \\
 & + (W_{lmn} - V_{lmn})(W_{lmn}^* - V_{lmn}^*)(2 - 2 \cos 2\pi(m/N_2 - n/N_3)) \\
 & + (U_{lmn} - W_{lmn})(U_{lmn}^* - W_{lmn}^*)(2 - 2 \cos 2\pi(n/N_3 - l/N_1)) \left. \right] \\
 & + \gamma \left[(U_{lmn} U_{lmn}^* (2 - 2 \cos 2\pi(-l/N_1 + m/N_2 + n/N_3)) \right. \\
 & + V_{lmn} V_{lmn}^* (2 - 2 \cos 2\pi(l/N_1 - m/N_2 + n/N_3)) \\
 & + W_{lmn} W_{lmn}^* (2 - 2 \cos 2\pi(l/N_1 + m/N_2 - n/N_3)) \left. \right] .
 \end{aligned}
 \tag{1.7}$$

7. Lagrangian Equations of Motion

With the Lagrangian function (1,7) expressed in terms of the new coordinates (U,V,W), the Lagrangian equations of motion may be written in the form

$$(1.8) \quad d/dt(\partial L / \partial \dot{U}_{lmn}^*) - \partial L / \partial U_{lmn}^* = 0,$$

with similar equations for the V_{lmn}^* and W_{lmn}^* .

The U_{lmn}^* equation is as follows:

$$\begin{aligned} m\ddot{U}_{lmn} + \alpha \left[(W_{lmn} + U_{lmn}) (1 - \cos 2\pi m/N_2) \right. \\ + (U_{lmn} + V_{lmn}) (1 - \cos 2\pi n/N_3) \\ - (V_{lmn} - U_{lmn}) (1 - \cos 2\pi [1/N_1 - m/N_2]) \\ + (U_{lmn} - W_{lmn}) (1 - \cos 2\pi [n/N_3 - 1/N_1]) \left. \right] \\ + 2\gamma U_{lmn} (1 - \cos 2\pi [-1/N_1 + m/N_2 + n/N_3]) = 0. \end{aligned}$$

The V_{lmn}^* and W_{lmn}^* equations may be obtained from the above by cyclic permutation of (U,V,W) and (lmn).

8. The Propagation Vector

In the discussion of the properties of the frequency spectrum it is convenient to use a rectangular Cartesian coordinate system in reciprocal lattice space. Each allowable vector \bar{B}_{lmn} of the coordinate transformation (1.4) may be defined in terms of its $(\bar{I}, \bar{J}, \bar{K})$ components along the (x,y,z) axes, respectively, of the system; and conversely, a vector drawn from the origin to any point in the reciprocal lattice is an allowable vector \bar{B}_{lmn} . The direction of such a vector defines the direction of propagation of a plane wave traveling through the lattice, and its "length" is equal to the wave-number of the plane

wave. It will be found in Section II that there exist three different normal modes of vibration having the same wave-number vector, and that these normal modes of vibration in general have different frequencies. In order to define the (x, y, z) coordinates of a point of the reciprocal lattice in terms of its wave-number vector indices (lmn) , the primitive vectors $(\bar{B}_1, \bar{B}_2, \bar{B}_3)$ must be expressed in terms of the unit vectors $(\bar{i}, \bar{j}, \bar{k})$. To accomplish this the three primitive vectors $(\bar{A}_1, \bar{A}_2, \bar{A}_3)$ of the direct lattice must first be expressed in terms of $(\bar{i}, \bar{j}, \bar{k})$. Referring to Figure 1, one may express the primitive triple in terms of the cell dimension d , as follows:

$$(1.10) \quad \begin{aligned} \bar{A}_1 &= d/2 (\bar{j} + \bar{k}) \\ \bar{A}_2 &= d/2 (\bar{k} + \bar{i}) \\ \bar{A}_3 &= d/2 (\bar{i} + \bar{j}) \end{aligned}$$

and from (1.1), $(\bar{B}_1, \bar{B}_2, \bar{B}_3)$ are found to be

$$(1.11) \quad \begin{aligned} \bar{B}_1 &= 1/d (-\bar{i} + \bar{j} + \bar{k}) \\ \bar{B}_2 &= 1/d (\bar{i} - \bar{j} + \bar{k}) \\ \bar{B}_3 &= 1/d (\bar{i} + \bar{j} - \bar{k}) \end{aligned}$$

The vectors $(\bar{B}_1, \bar{B}_2, \bar{B}_3)$ define a body-centered lattice. In terms of these vectors, the vectors \bar{B}_{lmn} may be written

$$(1.12) \quad \begin{aligned} \bar{B}_{lmn} &= l \bar{B}_1/N_1 + m \bar{B}_2/N_2 + n \bar{B}_3/N_3 \\ &= 1/d \bar{i} (-l/N_1 + m/N_2 + n/N_3) \\ &\quad + \bar{j} (l/N_1 - m/N_2 + n/N_3) \\ &\quad + \bar{k} (l/N_1 + m/N_2 - n/N_3) . \end{aligned}$$

The coordinates of the point of the reciprocal lattice corresponding to \bar{E}_{lmn} will be defined as follows:

$$(1.13a) \quad \begin{aligned} x &= \pi(-l/N_1 + m/N_2 + n/N_3) \\ y &= \pi(l/N_1 - m/N_2 + n/N_3) \\ z &= \pi(l/N_1 + m/N_2 - n/N_3). \end{aligned}$$

Thus,

$$(1.13b) \quad \bar{E}_{lmn} = \bar{r}/nd, \text{ where } \bar{r} = x\bar{i} + y\bar{j} + z\bar{k}.$$

It will be noted that (x, y, z) are dimensionless. The vector \bar{r} is called the propagation vector of the plane wave defined by \bar{E}_{lmn} .

9. The Secular Determinant

In order to find those combinations of the $(U, V, W)_{lmn}$ which define the normal coordinates of the system, values of ω are sought, such that

$$(1.14) \quad \begin{aligned} U_{lmn} &= A_{lmn} e^{i\omega t} \\ V_{lmn} &= B_{lmn} e^{i\omega t} \\ W_{lmn} &= C_{lmn} e^{i\omega t} \end{aligned}$$

the A_{lmn} , B_{lmn} , and C_{lmn} being complex constants, not all zero.

When the above substitution, together with the substitution (1.13a), is made in the first Lagrangian equation (1.9), cancellation of the common factor $e^{i\omega t}$ and collection of terms result in,

$$(1.15) \quad \begin{aligned} &A_{lmn} \left[\alpha \left\{ 4 - \cos(z+x) - \cos(x+y) - \cos(x-y) - \cos(z-x) \right\} + 2\gamma (1 - \cos 2x) - m\omega^2 \right] \\ &+ B_{lmn} \alpha \left\{ \cos(x-y) - \cos(x+y) \right\} + C_{lmn} \alpha \left\{ \cos(z-x) - \cos(z+x) \right\} = 0. \end{aligned}$$

Combining the trigonometric terms, and dividing through by $2a$, there results

$$(1.16a) \quad \begin{aligned} & A_{lmn} \left\{ 2 - \cos x(\cos y + \cos z) + 2\gamma/a \sin^2 x - m\omega^2/2a \right\} \\ & + B_{lmn} \sin x \sin y + C_{lmn} \sin x \sin z = 0, \end{aligned}$$

The Lagrangian equations for V_{lmn}^* and W_{lmn}^* , similarly treated, yield

$$(1.16b) \quad \begin{aligned} & A_{lmn} \sin x \sin y \\ & B_{lmn} \left\{ 2 - \cos y(\cos z + \cos x) + 2\gamma/a \sin^2 y - m\omega^2/2a \right\} \\ & C_{lmn} \sin y \sin z = 0 \end{aligned}$$

$$(1.16c) \quad \begin{aligned} & A_{lmn} \sin x \sin z \\ & B_{lmn} \sin y \sin z \\ & C_{lmn} \left\{ 2 - \cos z(\cos x + \cos y) + 2\gamma/a \sin^2 z - m\omega^2/2a \right\} = 0. \end{aligned}$$

As is well known from the theory of linear equations, the only values of $(A,B,C)_{lmn}$ that will satisfy the set of equations (1.16) are $(0,0,0)$ unless the determinant of the coefficients is itself equal to zero. In the latter case one of the quantities can be chosen arbitrarily, and the three equations then are compatible and may be solved for the other two quantities. The determinant of the coefficients of $(A,B,C)_{lmn}$ is called the secular determinant.

It should be noted that the coordinate transformation of Born and von Karman has brought the Lagrangian equations into a particularly simple form. If the Lagrangian equations for the coordinates $(u,v,w)_{abc}$ had been written, each Lagrangian equation would have contained coordinates having indices other than (abc) . Thus, each normal coordinate would have been a linear combination of all of the coordinates $(u,v,w)_{abc}$ and the secular determinant would have been

of order equal to the number of degrees of freedom of the entire crystal. In our case, the entire secular determinant is still of the order, but it is factorsble into a product of third-order determinants, all of which are represented by the general secular determinant

$$(1.17) \begin{vmatrix} 2 + 2\gamma/a \sin^2 x & & \\ -\cos x(\cos y + \cos z) & \sin x \sin y & \sin x \sin z \\ -m\omega^2/2a & & \\ \sin x \sin y & 2 + 2\gamma/a \sin^2 y & \\ -\cos y(\cos z + \cos x) & -m\omega^2/2a & \sin y \sin z \\ \sin x \sin z & \sin y \sin z & 2 + 2\gamma/a \sin^2 z \\ -\cos z(\cos x + \cos y) & & -m\omega^2/2a \end{vmatrix} = 0$$

The complete secular determinant for the face-centered cubic lattice is that determinant formed by a diagonal array of all determinants of the form (1.17), each obtained by substituting into (1.17) one of the possible sets of values of (lmn) , and having zeros everywhere else.

SECTION II

GENERAL PROPERTIES OF THE SECULAR DETERMINANT

1. Introduction

The properties of the secular determinant derived in the preceding section will now be determined. The symmetry properties of its solutions in (x, y, z) space will first be considered, followed by a discussion of the periodicity properties of those solutions. In the course of this treatment, the range of variation of the indices (lmn) which define the propagation vector (see Paragraph 8, Section II) will be fixed.

It should be emphasized that the dynamical problem of the motion of a crystal lattice is actually solved when the secular determinant defining the normal coordinates is obtained. That is, any permissible set of integers (lmn) may be chosen at will, and with the help of the secular determinant the normal coordinates and frequencies associated with the corresponding propagation vector can be found. The complete solution of the problem therefore consists in solving the secular determinant for each of the finite number of such combinations (lmn) and in writing down the most general sum of all of the normal coordinates thus found, each multiplied by an arbitrary constant.

For the purpose of this discussion the normal coordinates themselves need not be known; however, a knowledge of the distribution of frequencies of the various normal vibrations is required, since the statistical treatment depends upon the distribution function $N(\nu)$. The remainder of this paper is largely devoted to the evaluation of the distribution function $N(\nu)$. The function $N(\nu)$ is regarded as being continuous, except possibly for a finite number of values of ν .

2. Definition of the Continuous Distribution Function $N(\nu)$

The solution of the secular determinant of the preceding section yields three values of ν^2 for each permissible set of coordinates (x,y,z) because the expansion of the determinant in polynomial form gives a cubic equation in ν^2 . The values of ν^2 defining the normal vibrations are discrete, but only because the values of (x,y,z) that may be inserted into the determinant are themselves discrete. It is clear that if any set of values of (x,y,z) were permissible, the roots of the determinant would be continuous functions of the continuous variables (x,y,z) . As a matter of fact, the successive permissible values of (x,y,z) are separated from one another by amounts that are practically infinitesimal in comparison with a complete period of any of the trigonometric functions appearing in the determinant. Therefore, the respective roots corresponding to two adjacent permissible points (x,y,z) would be expected to differ by physically infinitesimal amounts.

The actual frequency spectrum will consist of a large number of discrete frequencies. To find the number of frequencies lying in any range ν to $\nu + d\nu$, one could, in principle, actually tabulate the various discrete roots of the determinant in order of increasing frequency and count the roots lying between the prescribed frequency limits. A conceivable method of tabulation might consist in forming a three-dimensional array of points located in a one-to-one correspondence with the permissible points (x,y,z) of propagation vector space, and labeling each point with the three roots of the secular determinant corresponding to it. The operation of counting the frequencies lying between given limits would then consist, for each of the three roots of the determinant, in counting the number of frequencies lying between two surfaces, so placed that all frequencies within the range of interest, and no frequencies lying outside

the range, lie between them. However, for each of the three roots there is a one-to-one correspondence between permissible points (x,y,z) and frequencies, so that one actually would be counting the number of permissible points lying between the two surfaces. Finally, the permissible points are uniformly distributed in space, so that a definite volume of space (similar in shape to the unit cell of the reciprocal lattice) is associated with each point. The counting operation is therefore equivalent to the measurement of the volume of (x,y,z) space lying between the two surfaces.

The surfaces just described may be taken to be those surfaces obtained by inserting into the secular determinant the limits of the frequency range under consideration, for the surfaces thus obtained do indeed possess the required property that all those frequencies, and only those frequencies, which lie between the frequency limits, lie also between the surfaces.

Thus it appears that the actual discrete frequency spectrum may be closely approximated by the continuous function

$$(2.1) \quad N(\nu) = K \, dV/d\nu,$$

where K is the number of permissible points per unit volume of (x,y,z) space, and $V(\nu)$ is the volume in (x,y,z) space enclosed by the surface $\nu = \text{const.}$, V being regarded as a continuous function of the continuous variables (x,y,z) .

3. Symmetry Properties of the Secular Determinant

Physically, one is sure that there can be no difference in the properties of the crystal in directions that are symmetrically oriented with respect to the symmetry axes and planes of the crystal. Thus, it may be expected that the roots of the secular determinant would have the same symmetry properties as the cubic crystal. This is readily verified mathematically from the secular determinant itself, by merely observing that the roots of the determinant are invariant

to all the symmetry operations of the cubic system, i.e.,

substitution of x for $-x$, y for $-y$, or z for $-z$ (reflection in axial planes);

substitution of x for y , y for x , z for $-z$; y for z , z for y , x for $-x$;

or z for x , x for z , y for $-y$ (rotation about diagonal axes);

substitution of x for $\pm y$, y for $\pm z$, and z for $\pm x$ (rotation about trigonal axes);

substitution of x for y , y for $-x$, z for z ; y for z , z for $-y$, x for x ;

or z for x , x for $-z$, y for y (rotation about tetragonal axes).

The above considerations do not require that the constant-frequency surfaces themselves possess these symmetry properties individually, for it is conceivable that the surfaces could intersect one another in such a way that the set of surfaces would be invariant to symmetry operations, but each individual surface still not be invariant. If, however, one of the surfaces does not intersect either of the other two, each surface must individually possess the symmetry of the crystal.

In any case, the shapes of the constant frequency surfaces in all directions from the origin are known if their shapes can be determined inside the smallest solid angle bounded by the symmetry planes of the crystal that pass through the origin. For the cubic system, this solid angle amounts to $1/48$ of the total solid angle surrounding the origin; this may be taken to be that region lying in the positive octant, bounded by the planes $y = 0$, $x = y$, and $x = z$. This region is sketched in Figure 2.

4. Periodicity Properties of the Roots of the Secular Determinant

It is clear by inspection that the roots of the secular determinant are periodic in (x, y, z) with period 2π in each direction. This means that the solutions in the neighborhood of the points $(2k_1\pi, 2k_2\pi, 2k_3\pi)$, with (k_1, k_2, k_3)

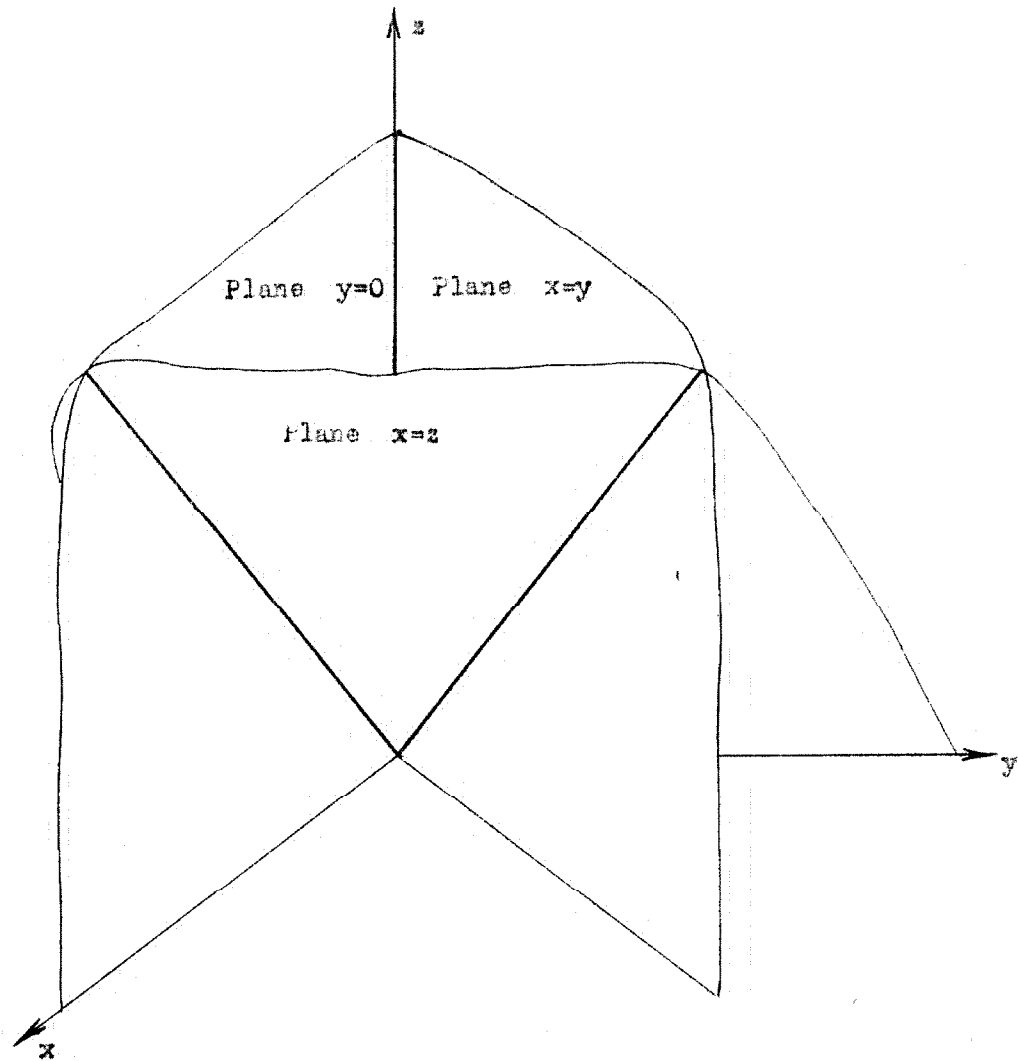


Figure 2.

The symmetry planes of the roots of the secular determinant.

integers, are the same as the solutions in the corresponding neighborhood of the origin.

Furthermore, substitution of $[x + (2k_1+1)\pi, y + (2k_2+1)\pi, z + (2k_3+1)\pi]$ respectively for (x,y,z) leaves the secular determinant unchanged. This indicates that the roots of the secular determinant are periodic in (x,y,z) space with the same periodicity as a body-centered lattice. That is, if a point is translated by an amount corresponding to an invariant translation of the body-centered lattice, it then coincides with a second point having the same roots as the first. Therefore, if the constant-frequency surfaces are known inside the unit cell of this body-centered lattice, they will be known at all other points in (x,y,z) space. This lattice will be called the periodicity lattice for the roots of the secular determinant.

5. Range of Variation of (l,m)

The results of the preceding two paragraphs may now be used to determine the range of permissible values of (l,m) (see Paragraph 5, Section I). The total number of possible combinations must of course be equal to $N_1N_2N_3$, the number of atoms in the lattice, and there remains merely the task of determining the locations in (x,y,z) space of the corresponding permissible points. The volume of (x,y,z) space occupied by these points will be $N_1N_2N_3V_0$ where V_0 is the "volume" of the unit cell of the lattice in (x,y,z) space upon which the permissible points lie. The primitive vectors for this lattice may be obtained, with the aid of equations (1.11) and (1.13b) as follows:

$$(2.2) \quad \bar{c}_1 = \pi d\bar{B}_1/N_1, \quad \bar{c}_2 = \pi d\bar{B}_2/N_2, \quad \bar{c}_3 = \pi d\bar{B}_3/N_3$$

The volume of the unit cell of this lattice is found, in the usual manner, to be

$$(2.3) \quad V_0 = \bar{C}_1 \cdot (\bar{C}_2 \times \bar{C}_3) = (\pi^3 d^3 / N_1 N_2 N_3) \bar{B}_1 \cdot (\bar{B}_2 \times \bar{B}_3).$$

Thus

$$(2.4) \quad V = N_1 N_2 N_3 V = \pi^3 d^3 / d^3 (-\bar{i} + \bar{j} + \bar{k}) \cdot (2\bar{k} + 2\bar{j}) = 4\pi^3$$

The volume in (x,y,z) space occupied by the permissible points is therefore equal to the volume of the unit cell of the periodicity lattice, and hence coincides with the minimum cycle of periodicity of the roots of the secular determinant.

There remains the problem of finding the shape of the boundary of the unit cell of the periodicity lattice. Here some criterion must be introduced by which one part of (x,y,z) space may be judged preferable to another part of (x,y,z) space for our purposes, since, up to this point, any volume which included each point of the cycle of periodicity once and only once, would suffice. This criterion is simply that the propagation vector drawn from the origin to any point inside our unit cell be shorter than any of the infinite number of other propagation vectors that could be drawn from the same origin to corresponding points in other periodicity cycles. Physically, all such vectors would describe the same displacements of the atoms, and the one being chosen is that which corresponds to the largest wave length (smallest wave number) for the elastic wave. That this criterion is reasonable can be seen quite readily from a consideration of the one-dimensional chain of mass particles shown in Figure 3.

It is clear that the physical displacements of the atoms could be represented as well mathematically by sine waves of many different wave lengths; two of these are shown. It is also clear that no physical significance can be attached to wave lengths shorter than the distance between points in

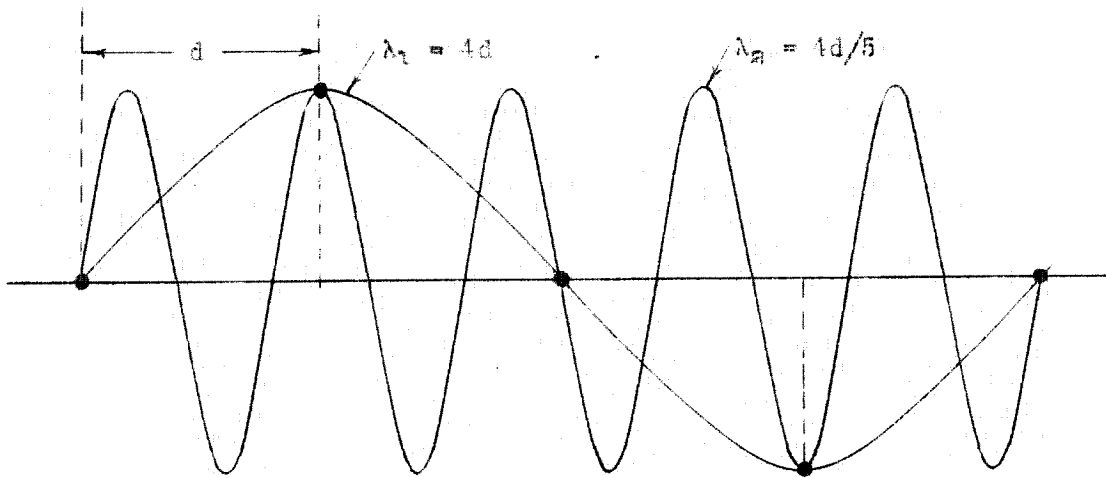


Figure 3. Sino-wave displacements of a chain of mass particles.

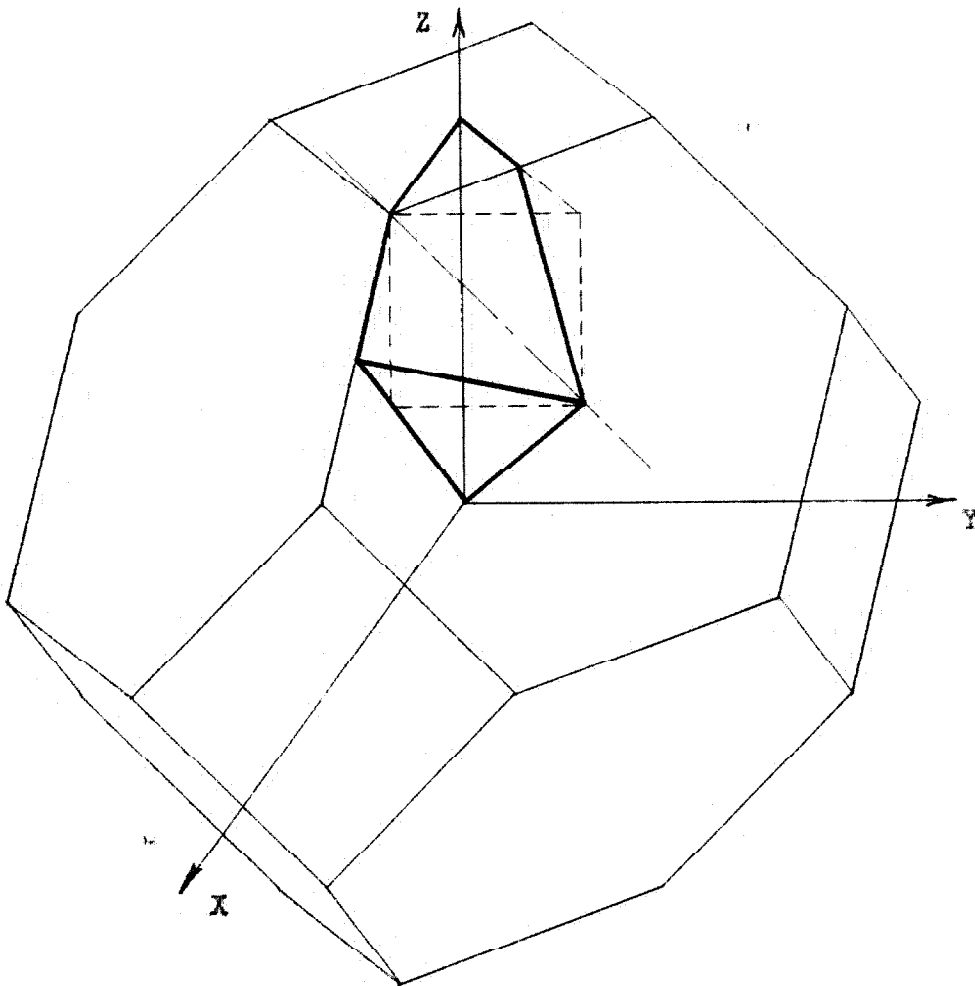


Figure 4. The first Brillouin Zone of a face-centered cubic crystal lattice.

the chain. The above condition follows, since there is only one sine wave with wave length greater than the distance between adjacent points.

With this criterion, the region in which the permissible points of (x,y,z) space lie, will be seen to have the shape of the first Brillouin zone⁽³⁾ of the crystal lattice in question. The range of variation of (lmn) is, therefore, such that the corresponding permissible points (x,y,z) lie inside this zone.

The first Brillouin zone of the face-centered cubic crystal lattice is shown in Figure 1. The intersections of the three symmetry planes, described in Paragraph 3 above, with the surface of the zone, are outlined by heavy lines. A knowledge of the shapes of the frequency surfaces inside the zone, and enclosed by those planes, is sufficient to determine the frequency distribution, $N(\nu)$. We shall call the (x,y,z) space enclosed by these boundaries the fundamental region of the secular determinant.

6. Special Solutions of the Secular Determinant

It has been pointed out in Section I that the secular determinant may be factored into third-order determinants of the form

$$(2.5) \quad \begin{vmatrix} 2 + 2\gamma/a \sin^2 x & & & \\ -\cos x(\cos y + \cos z) & \sin x \sin y & & \sin x \sin z \\ -\lambda^2 & & & \\ \sin x \sin y & 2 + 2\gamma/a \sin^2 y & & \\ -\cos y(\cos z + \cos x) & -\lambda^2 & & \sin y \sin z \\ \sin x \sin z & \sin y \sin z & 2 + 2\gamma/a \sin^2 z & \\ & & -\cos z(\cos x + \cos y) & \\ & & -\lambda^2 & \end{vmatrix} = 0$$

where λ^2 has been written for $m^2/2a$ in equation (1.17). The quantity λ is a dimensionless parameter, but for convenience it will be referred to as the

frequency, since it is linearly related to the true frequency, ν (or $\omega/2\pi$).

The expansion of this determinant leads to a cubic equation in λ^2 which cannot be solved conveniently. In the symmetry planes of the periodicity lattice, and in the plane $z = \pi$, however, the secular determinant may be factored, giving three solutions which may be written in a convenient form. It will be found that the solutions in the plane $y = 0$ may be matched with the solutions in the planes $x = y$, $x = z$, and $x = \pi$ in such a way that three distinct surfaces are obtained for each value of λ^2 . The three families of surfaces will be called the three branches of the roots of the secular determinant, and for convenience they will be identified by the arbitrary labels, I, II, III.

As an example of the solution of the secular determinant in a special plane, consider the plane $x = y$. In this plane, the secular determinant becomes

$$(2.6) \quad \begin{vmatrix} 2 + 2\gamma/a \sin^2 x & & & \\ -\cos^2 x - \cos x \cos z & \sin^2 x & & \sin x \sin z \\ -\lambda^2 & & & \\ \sin^2 x & & & \\ & 2 + 2\gamma/a \sin^2 x & & \\ & -\cos^2 x - \cos x \cos z & & \sin x \sin z \\ & -\lambda^2 & & \\ \sin x \sin z & & & \\ & \sin x \sin z & & \\ & & 2 + 2\gamma/a \sin^2 z & \\ & & -2 \cos x \cos z & \\ & & -\lambda^2 & \end{vmatrix} = 0$$

One of the roots of the determinant may be written down immediately:

If

$$2 + 2\gamma/a \sin^2 x - \cos^2 x - \cos x \cos z - \lambda^2 = \sin^2 x,$$

the first two rows (or columns) of the determinant will be equal. Hence, one root is

$$(2.7) \quad \lambda^2 = 1 - \cos x \cos z + 2\gamma/a \sin^2 x.$$

The remaining two roots (as well as the one given above) may be obtained by manipulation of the rows and columns of (2.6). The determinant is of the form

$$(2.8) \quad D = \begin{vmatrix} A - \lambda^2 & B & C \\ B & A - \lambda^2 & C \\ C & C & E - \lambda^2 \end{vmatrix} = 0$$

The determinant may be transformed through a series of simple steps as follows:

$$(2.9) \quad D = \begin{vmatrix} A-B-\lambda^2 & B & C \\ B-A+\lambda^2 & A-\lambda^2 & C \\ 0 & C & E-\lambda^2 \end{vmatrix} = \begin{vmatrix} A-B-\lambda^2 & B & C \\ 0 & A+B-\lambda^2 & 2C \\ 0 & C & E-\lambda^2 \end{vmatrix} = (A-B-\lambda^2) \begin{vmatrix} A+B-\lambda^2 & 2C \\ C & E-\lambda^2 \end{vmatrix}$$

The determinant D clearly has the roots

$$(2.10) \quad \begin{aligned} \lambda^2 &= A-B, \\ \lambda^2 &= (A+B+E)/2 \pm \frac{1}{2} \sqrt{(A+B-E)^2 + 8C^2}. \end{aligned}$$

When the above process of solving the determinant in the three planes of symmetry is carried out, and the solutions are matched along their common lines, one obtains for the three branches the following set of solutions:

Branch I

$$(2.11a) \quad \begin{aligned} \text{Plane } y = 0: \lambda_1^2 &= 2 - \frac{1}{2} \cos x - \frac{1}{2} \cos z - \cos x \cos z + 2\gamma/a \sin^2 x + \gamma/a \sin^2 z \\ &- \sqrt{(\gamma/a \sin^2 x - \gamma/a \sin^2 z - \frac{1}{2} \cos x + \frac{1}{2} \cos z)^2 + \sin^2 x \sin^2 z} \end{aligned}$$

$$\text{Plane } x = y: \lambda_1^2 = 1 - \cos x \cos z + 2\gamma/a \sin^2 x$$

Branch II

Plane $y = 0$: $\lambda_{\frac{y}{a}}^2 = 2 - \cos x - \cos z$
(2.11b)

Plane $x = y$: $\lambda_{\frac{x}{a}}^2 = \frac{2}{a^2}(1 - \cos x \cos z) + (1 + \gamma/a) \sin^2 x \sin^2 z$
 $- \frac{1}{a^2} \sqrt{(1 - \cos x \cos z - (2 + 2\gamma/a) \sin^2 x + 2\gamma/a \sin^2 z)^2 + 8 \sin^2 x \sin^2 z}$

Branch III

Plane $y = 0$: $\lambda_{\frac{y}{a}}^2 = 2 - \frac{1}{2a^2} \cos x - \frac{1}{2a^2} \cos z - \cos x \cos z - \gamma/a \sin^2 x - \gamma/a \sin^2 z$
 $+ \sqrt{(\gamma/a \sin^2 x - \gamma/a \sin^2 z - \frac{1}{2a^2} \cos x + \frac{1}{2a^2} \cos z)^2 + \sin^2 x \sin^2 z}$
(2.11c)

Plane $x = y$: $\lambda_{\frac{x}{a}}^2 = \frac{2}{a^2}(1 - \cos x \cos z) + (1 + \gamma/a) \sin^2 x + \gamma/a \sin^2 z$
 $+ \frac{1}{2a^2} \sqrt{[1 - \cos x \cos z - (2 + 2\gamma/a) \sin^2 x + 2\gamma/a \sin^2 z]^2 + 8 \sin^2 x \sin^2 z}$

The solution for the plane $x = z$ is obtained, in each case, by substituting z for y in the solution for the plane $x = y$, and the solution for the plane $x = \pi$ is obtained by substituting $\pi - x$ for x and $\pi - z$ for y in the solution for the plane $y = 0$.

This identification of the three branches is not unique, and indeed it will be necessary to study the matter more carefully when the contours of the constant frequency are plotted (Section III).

7. Orthogonality of Surfaces and Symmetry Planes

It is clear, from the fact that a symmetry plane divides each surface into two halves which are mirror images, that the surfaces of constant frequency either meet the planes at right angles, or have sharp edges coinciding with the planes. If the second derivative of λ^2 , with respect to a coordinate in a direction perpendicular to a symmetry plane, is finite, it follows that the corresponding principal radius of curvature of the surface is not zero, and hence that the surface

meets the plane normally,

To show that this is the case for the plane $y = 0$, the second derivative of the secular determinant with respect to y will be written, y set equal to zero, and the determinant solved for $\partial^2 D / \partial y^2$. This process will be made more compact with the introduction of the notation

$$(2.12) \quad D = \begin{vmatrix} D_1 & D_2 & D_3 \end{vmatrix} = 0$$

where D_1 represents, symbolically, the elements of the first column of D , and similarly for D_2 and D_3 ; furthermore, if

$$(2.13) \quad \frac{n}{Dy} = \left(\frac{n}{D_1y}, \frac{n}{D_2y}, \frac{n}{D_3y} \right)$$

is defined to be an array, each element of which is the n th derivative, with respect to y , of the corresponding element of D , one may write, symbolically, using the rule for differentiation of determinants

$$(2.14) \quad \partial D / \partial y = \begin{vmatrix} D_1^1y & D_2 & D_3 \end{vmatrix} + \begin{vmatrix} D_1 & D_2^1y & D_3 \end{vmatrix} + \begin{vmatrix} D_1 & D_2 & D_3^1y \end{vmatrix} = 0$$

(The first determinant, for example, is made up of the first column of D_1^1y , and the second and third columns of D .) Similarly,

$$(2.15) \quad \begin{aligned} \partial^2 D / \partial y^2 &= \begin{vmatrix} D_1^2y & D_2 & D_3 \end{vmatrix} + \begin{vmatrix} D_1^1y & D_2^1y & D_3 \end{vmatrix} + \begin{vmatrix} D_1^1y & D_2 & D_3^1y \end{vmatrix} \\ &+ \begin{vmatrix} D_1^1y & D_2^1y & D_3 \end{vmatrix} + \begin{vmatrix} D_1 & D_2^2y & D_3 \end{vmatrix} + \begin{vmatrix} D_1^1 & D_2^1y & D_3^1y \end{vmatrix} \\ &+ \begin{vmatrix} D_1^1y & D_2 & D_3^1y \end{vmatrix} + \begin{vmatrix} D_1 & D_2^1y & D_3^1y \end{vmatrix} + \begin{vmatrix} D_1 & D_2 & D_3^2y \end{vmatrix} \\ &= \begin{vmatrix} D_2^2y & D_2 & D_3 \end{vmatrix} + \begin{vmatrix} D_1 & D_2^2y & D_3 \end{vmatrix} + \begin{vmatrix} D_1 & D_2 & D_3^2y \end{vmatrix} \\ &+ 2 \begin{vmatrix} D_1^1y & D_2^1y & D_3 \end{vmatrix} + 2 \begin{vmatrix} D_1^1y & D_2 & D_3^1y \end{vmatrix} + 2 \begin{vmatrix} D_1 & D_2^1y & D_3^1y \end{vmatrix} \\ &= 0. \end{aligned}$$

In the case of the secular determinant for the face-centered crystal lattice,

$$(2.16) \quad D_y^1 = \begin{vmatrix} \cos x \sin y & \sin x \cos y & 0 \\ -\partial \lambda^2 / \partial y & & \\ \sin x \cos y & 4\gamma/a \sin y \cos y + \sin y (\cos z + \cos x) - \partial \lambda^2 / \partial y & \sin z \cos y \\ 0 & \sin z \cos y & \cos z \sin y - \partial \lambda^2 / \partial y \end{vmatrix}$$

and

$$(2.17) \quad D_y^2 = \begin{vmatrix} \cos x \cos y & -\sin x \sin y & 0 \\ -\partial^2 \lambda^2 / \partial y^2 & & \\ -\sin x \sin y & 4\gamma/a \cos 2y - \partial^2 \lambda^2 / \partial y^2 - \cos y (\cos z + \cos x) & -\sin z \sin y \\ 0 & -\sin z \sin y & \cos z \cos y - \partial^2 \lambda^2 / \partial y^2 \end{vmatrix}$$

Thus,

$$(2.18) \quad \left. \frac{\partial D}{\partial y} \right|_{y=0} = \begin{vmatrix} -\partial \lambda^2 / \partial y & 0 & \sin x \sin z \\ \sin x & 2 - \cos x - \cos z - \lambda^2 & 0 \\ 0 & 0 & 2 + 2\gamma/a \sin^2 z - \cos z - \cos x \cos z - \lambda^2 \end{vmatrix}$$

$$(2.18 \text{ cont'd}) \quad + \begin{vmatrix} 2 + 2\gamma/a \sin^2 x & \sin x & \sin x \sin z \\ -\cos x - \cos x \cos z & & \\ -\lambda^2 & & \\ 0 & -\partial \lambda^2 / \partial y & 0 \\ \sin x \sin z & \sin z & 2 + 2\gamma/a \sin z \\ & & -\cos z - \cos x \cos z \\ & & -\lambda^2 \end{vmatrix}$$

$$+ \begin{vmatrix} 2 + 2\gamma/a \sin^2 x & 0 & 0 \\ -\cos x - \cos x \cos z & & \\ -\lambda^2 & & \\ 0 & 2 - \cos x & \sin z \\ & -\cos z - \lambda^2 & \\ \sin x \sin z & 0 & -\partial \lambda^2 / \partial y \end{vmatrix} = 0$$

Solving for $\partial \lambda^2 / \partial y$,

$$(2.19) \quad -\partial \lambda^2 / \partial y \left[(\lambda_2^2 - \lambda^2) (\lambda_8^2 + \lambda_1^2 - 2\lambda^2) + (\lambda_8^2 - \lambda^2) (\lambda_1^2 - \lambda^2) \right] = 0.$$

The expression in the brackets vanishes only at points where two of the branches coincide, so that $\partial \lambda^2 / \partial y$ is zero except possibly at such points. Similarly,

$$(2.20) \quad \left. \frac{\partial^2 D}{\partial y^2} \right|_{y=0} = \begin{vmatrix} \cos x & & \sin x \sin z \\ -\partial^2 \lambda^2 / \partial y^2 & 0 & \\ 0 & 2 - \cos x & 0 \\ & -\cos z - \lambda^2 & \\ 0 & 0 & 2 + 2\gamma/a \sin^2 z \\ & & -\cos z - \cos x \cos z \\ & & \lambda^2 \end{vmatrix}$$

$$\begin{array}{c}
 \left| \begin{array}{ccc}
 2 + 2\gamma/a \sin^2 x & & \\
 -\cos x - \cos x \cos z & 0 & \sin x \sin z \\
 -\lambda^2 & & \\
 \end{array} \right. \\
 + \left| \begin{array}{ccc}
 0 & -4\gamma/a - \partial^2 \lambda^2 / \partial y^2 & \\
 & + \cos y (\cos z + \cos x) & 0 \\
 \sin x \sin z & 0 & 2 + 2\gamma/a \sin^2 z \\
 & & -\cos x - \cos x \cos z \\
 & & -\lambda^2
 \end{array} \right.
 \end{array}$$

$$\begin{array}{c}
 \left| \begin{array}{ccc}
 2 + 2\gamma/a \sin^2 x & & \\
 -\cos x - \cos x \cos z & 0 & 0 \\
 \lambda^2 & & \\
 \end{array} \right. \\
 + \left| \begin{array}{ccc}
 0 & 2 - \lambda^2 & \\
 & -\cos x - \cos z & 0 \\
 \sin x \sin z & 0 & \cos z \\
 & & -\partial^2 \lambda^2 / \partial y^2
 \end{array} \right.
 \end{array}$$

(2.20
cont'd)

$$\begin{array}{c}
 \left| \begin{array}{ccc}
 -\partial \lambda^2 / \partial y & \sin x & \sin x \sin z \\
 \sin x & -\partial \lambda^2 / \partial y & 0 \\
 0 & \sin z & 2 + 2\gamma/a \sin^2 x \\
 & & -\cos x - \cos x \cos z \\
 & & -\lambda^2
 \end{array} \right.
 \end{array}$$

$$\begin{array}{c}
 \left| \begin{array}{ccc}
 -\partial \lambda^2 / \partial y & 0 & 0 \\
 \sin x & 2 - \lambda^2 & \\
 & -\cos x - \cos z & \sin z \\
 0 & 0 & -\partial \lambda^2 / \partial y
 \end{array} \right.
 \end{array}$$

$$\begin{array}{c}
 \left| \begin{array}{ccc}
 2 + 2\gamma/a \sin^2 x & & \\
 -\cos x - \cos z \cos x & \sin x & 0 \\
 -\lambda^2 & & \\
 \end{array} \right. \\
 + 2 \left| \begin{array}{ccc}
 0 & -\partial \lambda^2 / \partial y & \sin z \\
 \sin x \sin z & \sin z & -\partial \lambda^2 / \partial y
 \end{array} \right. = 0
 \end{array}$$

Collection of terms and utilization of the expressions (2.11) will result in

$$(2.21) \quad -\partial^2 \lambda^2 / \partial y^2 \left[(\lambda_2^2 - \lambda^2) (\lambda_3^2 + \lambda_4^2 - 2\lambda^2) + (\lambda_3^2 - \lambda^2) (\lambda_4^2 - \lambda^2) \right] + R = 0$$

where R denotes the remainder of the terms. It is clear that $\partial^2 \lambda^2 / \partial y^2$ can be infinite only where the expression in the brackets vanishes, since R is always finite. For the three branches this expression is

Branch I

$$(\lambda_2^2 - \lambda_1^2) (\lambda_3^2 - \lambda_1^2)$$

Branch II

$$(2.22) \quad (\lambda_1^2 - \lambda_2^2) (\lambda_3^2 - \lambda_2^2)$$

Branch III

$$(\lambda_1^2 - \lambda_3^2) (\lambda_2^2 - \lambda_3^2)$$

so that the derivative $\partial^2 \lambda^2 / \partial y^2$ can become infinite only where the constant frequency contours of two branches intersect. We shall see in Section III that this occurs for a given value of λ^2 only at isolated points or along isolated lines whose significance will then be clear. The situation is exactly the same in the other symmetry planes of the secular determinant. The general conclusion is that except at a few points the constant frequency surfaces meet the symmetry planes orthogonally.

SECTION III

THE SURFACES OF CONSTANT FREQUENCY

1. Introduction

In the present section, the three branches of the roots of the secular determinant, defined in the symmetry planes by Equation (2.11), will be studied in detail, and the contours of constant frequency will be plotted in the symmetry planes. In anticipation of a result of Section V, that the parameter γ/a will have a value near -0.1 for crystals of interest, the family of contours for each branch will be drawn for two values of this parameter: 0.0 and -0.1 .

The contours for these two cases are similar in shape and position, so that in the interest of simplicity only the case of γ/a equal to zero will be treated at length. The other case will then be treated as a small perturbation of this case.

2. Fundamental Region of Symmetry and Periodicity

As has been pointed out in Paragraphs 3 and 5 of Section II, the symmetry and periodicity properties of the secular determinant are such that a knowledge of the frequency surfaces inside a certain "fundamental region" is sufficient to define the frequency spectrum of the lattice. This fundamental region is bounded by the planes $y = 0$, $x = y$, $x = z$, $z = \pi$, and $x + y + z = 3\pi/2$.

As long as no physical significance is attached to the indices (lmn) , however, the Brillouin zone need not be taken as the shape of the outer boundary of the region, but any other boundary that encloses the same frequencies may be used. In preparation for the application of these frequency contours to the calculation of the frequency distribution in Section IV, one minor change will be made in the shape of the fundamental region in order to simplify the measurement of the volume enclosed by each surface. This change is the substitution of the plane $x = \pi/2$ for the plane $x + y + z = 3\pi/2$ as one of the outer boundaries of the fundamental

region. The new region so defined is indicated by the dotted lines in Figure 4.

3. Contours for $\gamma/a = 0$

In the case that γ/a is equal to zero, the solutions (2,11) of the secular determinant take on the specially simple forms

Branch I

$$\begin{aligned} \text{plane } y = 0: \lambda_1^2 &= 2 - \frac{1}{2} \cos x - \frac{1}{2} \cos z - \cos x \cos z \\ &\quad - \sqrt{\left(\frac{1}{2} \cos x - \frac{1}{2} \cos z\right)^2 + \sin^2 x \sin^2 z} \\ \text{plane } x = y: \lambda_1^2 &= 1 - \cos x \cos z \end{aligned}$$

Branch II

$$\begin{aligned} \text{plane } y = 0: \lambda_2^2 &= 2 - \cos x - \cos z \\ \text{plane } x = y: \lambda_2^2 &= \frac{1}{2} (1 - \cos x \cos z) + \sin^2 x \\ &\quad - \frac{1}{2} \sqrt{(1 - \cos x \cos z - 2 \sin^2 x)^2 + 8 \sin^2 x \sin^2 z} \end{aligned}$$

Branch III

$$\begin{aligned} \text{plane } y = 0: \lambda_3^2 &= 2 - \frac{1}{2} \cos x - \frac{1}{2} \cos x - \frac{1}{2} \cos z - \cos x \cos z \\ &\quad + \sqrt{\left(\frac{1}{2} \cos x - \frac{1}{2} \cos z\right)^2 + \sin^2 x \sin^2 z} \\ \text{plane } x = y: \lambda_3^2 &= \frac{1}{2} (1 - \cos x \cos z) + \sin^2 x \\ &\quad + \frac{1}{2} \sqrt{(1 - \cos x \cos z - 2 \sin^2 x)^2 + 8 \sin^2 x \sin^2 z}. \end{aligned}$$

The solutions in the planes $x = z$ and $z = \pi$ are to be found in the same manner as in Equation (2,11).

Eventually the contours must be known for prescribed values of λ . The process by which these contours were found is as follows: Those of the above equations that involve square roots (Ia, IIb, IIIa,b) were solved for λ at intervals of $\pi/12$ in x and z . The values of x and z for which λ takes on the desired values were then determined from these results by graphical interpolation.

The remaining two equations (Ib, IIIa) were solved directly for z in terms of λ and x , and hence presented no problem.

The values of λ obtained by substituting the various values of x and z into Equations (3.1) are given in the following tables. For convenience, values x and z are given in degrees.

TABLE 1

Root of the Secular Determinant for Branch I, Plane $y = 0$

z deg.	x deg.						
	0	15	30	45	60	75	90
0	.000	.185	.366	.541	.707	.861	1.000
15	.165	.187	.351	.507	.678	.840	.984
30	.366	.381	.367	.489	.642	.802	.949
45	.541	.507	.489	.542	.649	.784	.925
60	.707	.678	.642	.649	.707	.803	.921
75	.861	.840	.802	.784	.803	.861	.945
90	1.000	.984	.949	.925	.921	.945	1.000
105	1.121	1.111	1.075	1.059	1.043	1.048	1.072
120	1.213	1.219	1.200	1.178	1.161	1.152	1.161
135	1.307	1.300	1.292	1.278	1.263	1.252	1.250
150	1.336	1.363	1.358	1.351	1.344	1.337	1.328
165	1.402	1.401	1.400	1.398	1.395	1.388	1.390
180	1.414	1.414	1.414	1.414	1.414	1.414	1.414

TABLE 2

Root of the Secular Determinant for Branch I, Plane $z = \pi$

y deg.	x deg.						
	0	15	30	45	60	75	90
0	1.414	1.414	1.414	1.414	1.414	1.414	1.414
15	1.414	1.402	1.392	1.388	1.388	1.388	1.390
30	1.414	1.392	1.367	1.346	1.333	1.329	1.330
45	1.414	1.388	1.346	1.306	1.276	1.258	1.250
60	1.414	1.388	1.333	1.276	1.223	1.185	1.161
75	1.414	1.388	1.329	1.258	1.185	1.122	1.075
90	1.414	1.390	1.330	1.250	1.161	1.075	1.000

TABLE 3

Root of the Secular Determinant for Branch II, Planes $x = y$, $x = z$

z (or y) deg.	x deg.						
	0	15	30	45	60	75	90
0	.000	.261	.517	.765	1.000	1.219	1.414
15	.185	.260	.497	.742	.970	1.182	1.371
30	.366	.353	.500	.703	.914	1.107	1.278
45	.541	.519	.573	.707	.868	1.028	1.176
60	.707	.687	.697	.765	.866	.974	1.084
75	.861	.851	.846	.869	.913	.966	1.023
90	1.000	1.000	1.000	1.000	1.000	1.000	1.000
105	1.121	1.132	1.145	1.142	1.116	1.072	1.023
120	1.223	1.243	1.278	1.282	1.246	1.173	1.084
135	1.306	1.331	1.382	1.414	1.381	1.298	1.176
150	1.368	1.396	1.469	1.528	1.511	1.419	1.278
165	1.402	1.435	1.521	1.610	1.630	1.530	1.371
180	1.414	1.448	1.538	1.643	1.752	1.588	1.414

TABLE 4

Root of the Secular Determinant for Branch III, Plane $y = 0$

z deg.	x deg.						
	0	15	30	45	60	75	90
0	.000	.261	.517	.765	1.000	1.218	1.414
15	.261	.411	.622	.840	1.051	1.252	1.436
30	.517	.622	.796	.982	1.163	1.336	1.494
45	.765	.840	.982	1.137	1.289	1.431	1.559
60	1.000	1.051	1.163	1.289	1.414	1.528	1.628
75	1.218	1.252	1.336	1.431	1.528	1.613	1.679
90	1.414	1.436	1.494	1.559	1.628	1.679	1.732
105	1.586	1.599	1.630	1.670	1.710	1.741	1.761
120	1.732	1.736	1.748	1.761	1.775	1.779	1.774
135	1.848	1.846	1.841	1.833	1.819	1.798	1.772
150	1.932	1.925	1.910	1.885	1.849	1.805	1.761
165	1.983	1.972	1.950	1.914	1.867	1.808	1.740
180	2.000	1.990	1.965	1.925	1.870	1.804	1.732

TABLE 5

Root of the Secular Determinant for Branch III, Planes $x = y$, $x = z$

z (or y) deg.	x deg.						
	0	15	30	45	60	75	90
0	.000	.410	.796	1.137	1.414	1.613	1.732
15	.261	.518	.862	1.188	1.451	1.648	1.785
30	.518	.710	1.000	1.291	1.537	1.722	1.832
45	.765	.904	1.154	1.414	1.638	1.805	1.901
60	1.000	1.100	1.308	1.533	1.732	1.878	1.954
75	1.218	1.288	1.452	1.640	1.810	1.930	1.988
90	1.414	1.460	1.580	1.732	1.870	1.965	2.000
105	1.567	1.611	1.690	1.800	1.908	1.976	1.988
120	1.731	1.740	1.778	1.847	1.920	1.968	1.954
135	1.846	1.844	1.848	1.870	1.909	1.931	1.901
150	1.932	1.921	1.892	1.871	1.875	1.876	1.832
165	1.982	1.967	1.921	1.856	1.812	1.809	1.785
180	2.000	1.981	1.930	1.848	1.732	1.768	1.732

TABLE 6

Root of the Secular Determinant for Branch III, Plane $z = \pi$

y deg.	x deg.						
	0	15	30	45	60	75	90
0	1.414	1.426	1.460	1.513	1.580	1.655	1.732
15	1.426	1.449	1.488	1.541	1.602	1.671	1.739
30	1.460	1.488	1.538	1.592	1.649	1.705	1.758
45	1.513	1.541	1.592	1.643	1.693	1.736	1.722
60	1.580	1.602	1.649	1.693	1.732	1.758	1.777
75	1.655	1.671	1.705	1.736	1.758	1.765	1.761
90	1.732	1.739	1.758	1.772	1.777	1.761	1.732

From the data in the foregoing tables, the curves of z as a function of λ , for fixed values of x , were drawn and values of z corresponding to certain values of λ were read from the curves. A similar treatment with fixed values of z yielded values of x corresponding to these same values of λ .

The results of this graphical interpolation, together with the results of direct computation are given in the following tables for Branch I, planes $x = y$

and $x = z$, and Branch III, planes $y = 0$ and $z = \pi$. In addition to these tabular data, values of z vs. λ , x vs. λ , or y vs. λ , are given along various special lines for each branch. These lines are the ones along which the roots of the secular determinant may be written in specially simple form. The equation connecting x , y , or z with λ will be given for each case. Finally, there are also given the values of r vs. λ along the line $x = z/2$, $y = z/4$. This line is not one of the simple lines mentioned above, but is, on the contrary, almost as complicated as any other; in the next section it will be found that information concerning the variation of λ along this line is useful in the mechanical determination of the frequency spectrum, because it makes almost equal angles with the three symmetry planes. The secular determinant was solved for several points equally spaced along this line, and the information given below was obtained from these solutions by graphical interpolation.

TABLE 7

x (or z) as a Function of λ and z (or x) in the Plane $y = 0$ (Branch I)

λ	x (or z) deg.						
	0	15	30	45	60	75	90
0.5	41.4	44.2	46.2	16.5/34.7	----	----	----
0.6	50.2	53.1	56.0	53.5	----	----	----
0.7	59.3	62.1	65.2	65.8	6.5/58.5	----	----
0.8	68.9	71.4	74.8	76.6	74.8	32.2/57.8	----
0.9	79.0	81.2	84.6	87.1	87.5	82.3	----
1.0	90.0	91.8	95.3	98.2	99.4	98.2	90.0
1.1	102.1	103.5	106.8	110.3	111.7	112.5	109.2
1.2	116.1	117.2	120.0	123.2	125.1	126.4	126.5
1.3	133.6	134.4	136.7	139.3	141.2	142.6	143.8
1.4	163.7	164.5	165.0	116.5	166.5	169.0	168.3

Line $y = 0$, $x = z$: same as for $x = 0$ in Table 7.

Line $y = 0$, $x = \pi - z$: $\lambda^2 = 1 - \cos z$

λ	1.0	1.1	1.2	1.3	1.4
z	90.0	67.5	55.1	41.4	16.4

TABLE 8

x as a Function of λ and z in the Plane $y = 0$ (Branch I)

λ	x deg.				
	105	120	135	150	165
1.1	19.5	----	----	----	----
1.2	----	30.0	----	----	----
1.3	----	----	20.0	----	----
1.4	----	----	----	----	30.0

TABLE 9

x as a Function of λ and z in the Plane $x = y$ (Branch I)

λ	x deg.						
	0	15	30	45	60	75	90
0.5	41.5	39.1	30.0	-----	-----	-----	-----
0.6	50.2	48.6	42.4	25.2	-----	-----	-----
0.7	59.4	58.2	53.9	43.9	-----	-----	-----
0.8	68.9	68.1	65.4	59.4	44.0	-----	-----
0.9	79.1	78.7	77.3	74.4	67.7	42.8	-----
1.0	90.0	90.0	90.0	90.0	90.0	90.0	90.0
1.1	102.1	102.5	104.0	107.3	114.8	144.2	-----
1.2	116.1	117.1	120.5	128.4	151.7	-----	-----
1.3	133.6	135.5	142.8	167.0	-----	-----	-----
1.4	163.4	-----	-----	-----	-----	-----	-----

Line $x = y = z$: $\lambda^2 = \sin^2 z$

λ	0.5	0.6	0.7	0.8	0.9	1.0
z	30.0	36.9	44.4	53.1	64.1	90.0

Line $x = y = \pi - z$: $\lambda^2 = 1 + \cos^2 z$

λ	1.1	1.2	1.3	1.4
x	62.8	48.5	33.9	11.9

TABLE 12

x as a Function of λ and z in the Plane $y = 0$ (Branch II)

λ	z deg.					
	105	120	135	150	165	180
1.2	35.1	----	----	----	----	----
1.3	55.4	36.0	----	----	----	----
1.4	72.6	57.3	41.7	25.1	----	----
1.5	89.5	75.5	62.8	52.0	44.3	41.5
1.6	----	----	81.6	72.2	66.1	63.9
1.7	----	----	----	----	85.6	83.7

Line $y = 0$, $x = z$; $\lambda^2 = 2 - 2 \cos z$

λ	0.5	0.6	0.7	0.8	0.9	1.0	1.1	1.2	1.3	1.4
x	28.9	34.9	41.0	47.2	53.5	60.0	66.7	73.7	81.1	88.8

TABLE 13

z as a Function of λ and x in the Plane $x = y$ (Branch II)

λ	x deg.						
	0	15	30	45	60	75	90
0.5	41.4	43.6	12.4/30.0	----	----	----	----
0.6	50.2	52.4	48.4	----	----	----	----
0.7	59.3	61.2	60.3	32.0/41.6	----	----	----
0.8	68.9	70.2	70.6	65.8	----	----	----
0.9	79.0	79.6	80.3	78.8	32.9/72.0	----	----
1.0	90.0	90.0	90.0	90.0	0.0/90.0	51.8/90.0	90.0
1.1	102.1	101.3	100.2	100.6	103.1	30.9/109.3	57.1
1.2	116.1	113.8	111.3	111.0	114.9	10.8/123.2	41.3
1.3	133.7	129.2	123.3	121.8	125.9	135.4	26.7
1.4	163.7	151.8	137.5	133.4	136.8	147.6	8.3
1.5	----	----	157.9	146.4	148.5	160.7	----
1.6	----	----	----	162.8	161.1	----	----
1.7	----	----	----	----	175.0	----	----

TABLE 14

x as a Function of λ and z in the Plane $x = y$ (Branch II)

λ	z deg.						
	0	15	30	45	60	75	90
0.5	28.9	30.0	30.0	----	----	----	----
0.6	34.9	36.4	37.5	33.5	----	----	----
0.7	41.0	42.7	44.6	44.5	7.6/31.8	----	----
0.8	47.2	49.1	51.9	54.0	40.6	----	----
0.9	53.5	55.5	59.0	62.8	64.6	56.6	----
1.0	60.0	62.0	66.4	72.1	76.6	82.9	All x
1.1	66.7	68.8	74.4	81.9	92.6	113.8	----
1.2	73.7	76.2	82.8	92.4	109.5	----	----
1.3	81.1	84.0	92.1	105.3	----	----	----
1.4	88.8	92.5	102.8/163.8	126.1/144.6	----	----	----
1.5	97.2/155.7	102.0/153.1	117.8/143.7	----	----	----	----
1.6	106.2/141.3	113.5/137.4	----	----	----	----	----
1.7	116.4/126.3	----	----	----	----	----	----

Line $x = y = z$: $\sin x = \lambda$

λ	0.5	0.6	0.7	0.8	0.9	1.0
x	30.0	36.8	44.4	53.1	64.1	90.0

TABLE 15

x (or y) as a Function of λ and y (or x) in the Plane $z = \pi$ (Branch II)

λ	y (or x) deg.						
	0	15	30	45	60	75	90
1.5	----	33.8	18.7	----	----	90.5	75.5
1.6	----	59.2	47.5	32.0	13.0/86.6	72.5	55.9
1.7	----	81.4	73.5/88.6	62.3/79.4	7.3/67.1	23.5/51.1	27.2
3	90.0	88.0	82.3	73.0	60.0	42.2	0

Line $z = \pi$, $x = y$: $\lambda^2 = 1 + \cos x + 2 \sin^2 x$ ($x < 60$), $\lambda^2 = 2(1 + \cos x)$ ($x > 60$)

λ	1.5	1.6	1.7	1.7	1.6	1.5
x	24.5	38.7	53.7	63.6	73.8	82.8

TABLE 19

x as a Function of λ and z in the Plane $x = y$ (Branch III)

λ	z deg.						
	0	15	30	45	60	75	90
0.5	18.6	14.3	-----	-----	-----	-----	-----
0.6	22.0	18.5	8.2	-----	-----	-----	-----
0.7	26.1	22.8	14.3	-----	-----	-----	-----
0.8	30.4	27.1	20.0	6.9	-----	-----	-----
0.9	34.5	31.5	25.1	14.5	-----	-----	-----
1.0	38.8	36.1	30.0	21.1	0.0	-----	-----
1.1	43.2	40.9	34.8	27.1	14.8	-----	-----
1.2	48.2	45.9	39.9	32.6	22.3	-----	-----
1.3	53.4	51.1	45.3	38.2	29.2	16.0	-----
1.4	59.2	56.8	51.2	44.1	36.0	25.2	-----
1.5	65.8	63.1	57.6	54.4	42.8	33.6	20.7
1.6	73.6	70.6	64.5	57.2	49.7	41.8/169.5	31.9
1.7	84.7	80.5	72.9	64.9	57.3	49.9/148.4	41.8
1.8	128.3	99.0	84.5	74.4	65.9/143.8	59.0/135.1	51.9
1.85	135.2	133.6	94.2	80.5/148.5	70.8/133.9	64.4/128.6	57.4
1.9	143.6	144.2	153.5	89.6/122.9	77.1/124.5	70.9/121.5	63.8
1.95	154.2	158.8	-----	-----	88.5/112.0	79.0/112.0	71.6
2.0	180.0	-----	-----	-----	-----	-----	90.0

Line $x = y = z$: $\lambda = 2 \sin z$

λ	0.5	0.6	0.7	0.8	0.9	1.0	1.1	1.2	1.3
z	14.5	17.4	20.4	23.6	26.7	30.0	33.3	36.8	40.5

λ	1.4	1.5	1.6	1.7	1.8	1.85	1.9	1.95	2.0
z	44.4	48.5	53.1	58.2	64.0	67.7	71.8	77.2	90.0

Line $x = y = \pi - z$: $8 \sin^2 x = \lambda^2 + 17\lambda - 96 \lambda^2 + 128$

λ	2.0	1.95	1.9	1.9	1.95	2.0
x	0	18.9	28.5	55.1	66.8	90.0

TABLE 20

y or x as a Function of λ and x or y in the Plane $z = \pi$ (Branch III)

λ	x, y deg.						
	0	15	30	45	60	75	90
1.8	76.1	74.1	68.0	57.8	42.3	11.1	----
1.85	65.0	62.9	56.2	44.3	22.9	----	----
1.9	52.4	49.9	41.9	25.5	----	----	----
1.95	36.6	33.3	20.5	----	----	----	----

Line $x = \pi/2$, $x = \pi - y$: $8 \sin^2 y = (2\lambda^2 - 5)^2 - 1$

λ	1.8	1.85	1.9	1.95	2.0
y	22.6	33.2	44.5	58.3	90.0

Line $x = z/2$, $y = z/4$:

λ	0.5	0.6	0.7	0.8	0.9	1.0	1.1	1.2	1.3
r	26.6	32.2	37.8	43.5	49.4	55.3	61.8	68.5	75.5

λ	1.4	1.5	1.6	1.7	1.8	1.85	1.85	1.8
r	83.0	91.1	101.0	112.0	128.0	146.5	172.8	197.6

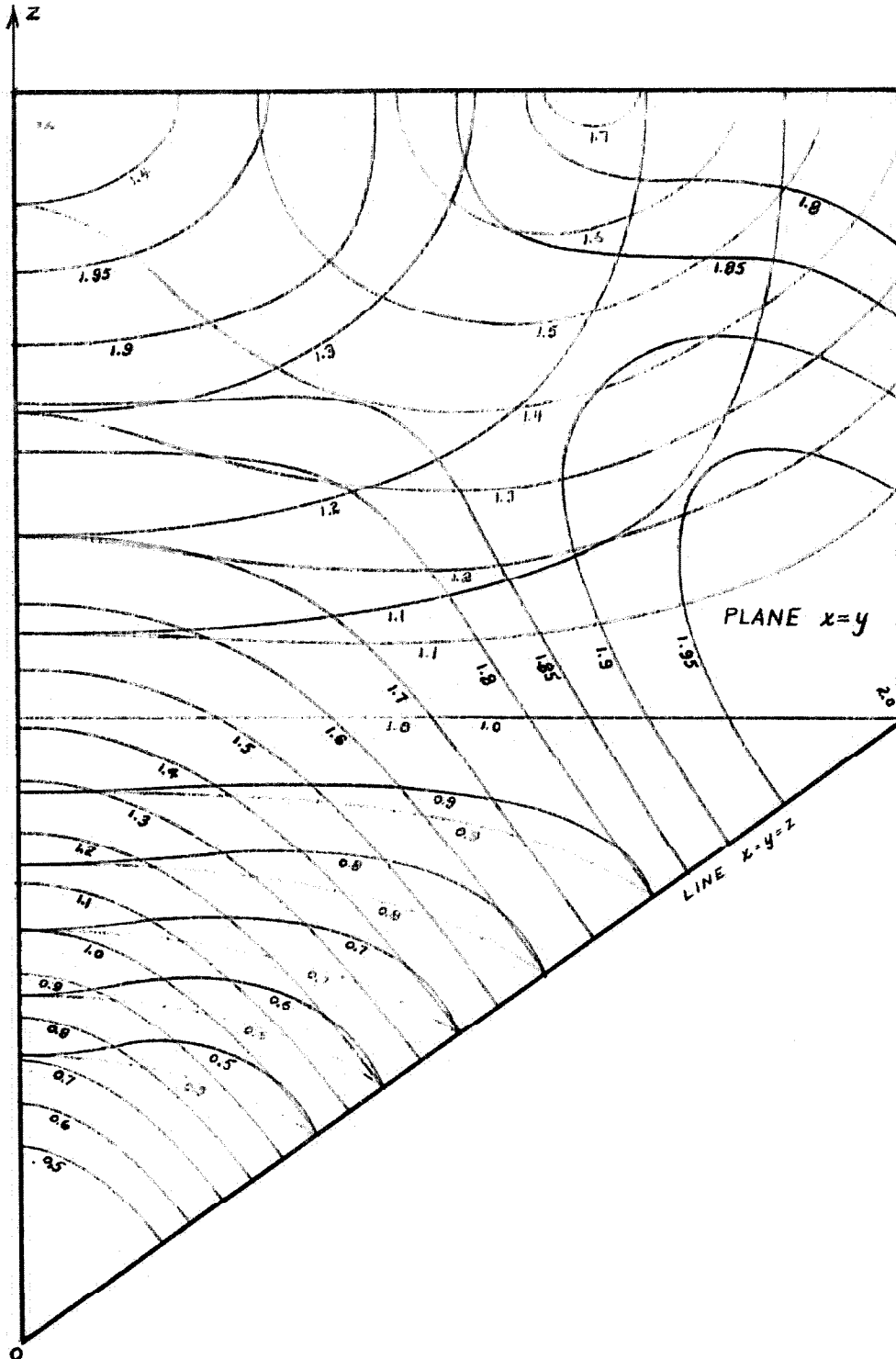
Figure 5 is a three-dimensional plot of the data given in the foregoing tables. The transparent sheets of the figure are labeled to correspond with the planes they represent, and when folded up and joined together they illustrate in a pseudo-three-dimensional manner the nature of the constant-frequency surfaces in (x,y,z) space.

4. Complete Identification of the Branches

With the aid of Figure 5 it is easy to see that the identification of the three branches in the various planes, as given by Equations (2.11), is substantially correct. There are, however, two exceptions to this identification; these exceptions will now be discussed.

First, it is necessary to interchange the solutions for Branches II

FIGURE 5. A THREE-DIMENSIONAL PLOT OF THE CONTOURS OF CONSTANT FREQUENCY.



and III, in the plane $z = \pi$, when $\lambda^2 = 3$. Thus, all the contours of Branch III in the plane $x = \pi$ and lying between the dashed curve $\lambda^2 = 3$ and the z axis, are defined by the equation given for Branch II, and vice versa. This interchange clearly makes the solutions in that plane match the solutions in the adjoining planes along their common boundaries.

The second interchange of solutions is less easily visualized than the above one, for it is not a question of matching the contours along boundaries. It will be noted from Figure 5 that the contours for Branches I and II coincide at all points along the z axis and along the line $x = y = z$, and that the two contours for $\lambda = 1, 0$ coincide everywhere in the plane $x = y$. Since the contours coincide along these two boundary lines the question is raised as to which set of contours goes with which branch of the secular determinant. Depending upon the answer to this question, there will exist one or the other of two situations. First, if the contours for each branch in the plane $x = z$ have the same equation (with y replacing z) as the contours in the plane $x = y$ (i.e., if the identification of the branches is correctly given by Equations (3.1)), the contours in the plane $x = z$ can be obtained from the contours in the plane $x = y$ by rotating the part of this plane nearest the z plane, about the line $x = y = z$, until it coincides with the plane $x = z$. (This process can be visualized easily with the aid of Figure 5.) In this case, since the contours do not intersect the line $x = y = z$ orthogonally, the surfaces will be sharply wrinkled near this line, as shown in Figure 6.

The point of view in Figure 6 is from the interior of the fundamental region, with the $x = y$ and $x = z$ planes located to one's left and right, respectively.

The surfaces for the two branches will clearly intersect one another along some line lying in the interior of the region; by symmetry this line

will be in the plane $x - y/2 - z/2 = 0$ (for points lying near the line $x = y = z$), and will intersect the line $x = y = z$ orthogonally, provided that the angles between each family of contours and the line $x = y = z$ are equal. That these angles are equal is easily shown by evaluating the slopes of the constant frequency curves of the two branches where they cross the line $x = y = z$. This is done by implicit differentiation of the Equations (3.1) with the result that, for Branch I, $(1/\sqrt{2}) dz/dx = \tan A = -1/\sqrt{2}$; for Branch II, $(1/\sqrt{2}) dz/dx = \tan B = -5/\sqrt{2}$; and the slope of the line $x = y = z$ in the plane $x = y$ is $\tan C = 1/\sqrt{2}$. Thus, $\tan(A-C) = \tan(C-B)$. This is shown in Figure 7.

On the other hand, if the equations for the contours of each branch are not those given in Equation (3.1), but are instead interchanged in the plane $x = y$ for $\lambda \neq 1, 0$, the situation near the line $x = y = z$ will be that shown in Figure 8.

In this case, the surfaces for the two branches will not intersect one another, except at the cusps of the conical sections, and the intersections of the surfaces with the plane $x = y/2 - z/2 = 0$ will be along two separate lines which intersect the line $x = y = z$ at the same angle as do the lines in the symmetry planes.

The method by which this question can be answered is now clear. If the secular determinant is solved for one point, on the line perpendicular to $x = y = z$ and lying in the plane $x - y/2 - z/2 = 0$, such that this point is near enough to the line $x = y = z$, one of two results will be obtained: either two of the roots will be equal (or very nearly so), or all of the roots will be distinct, and the difference between the nearest two will be consistent with the shapes and spacing of the successive surfaces, i.e., their values will be nearly given by the first two terms of a three-dimensional Taylor expansion.

Proceeding according to this plan, one finds that the line which lies

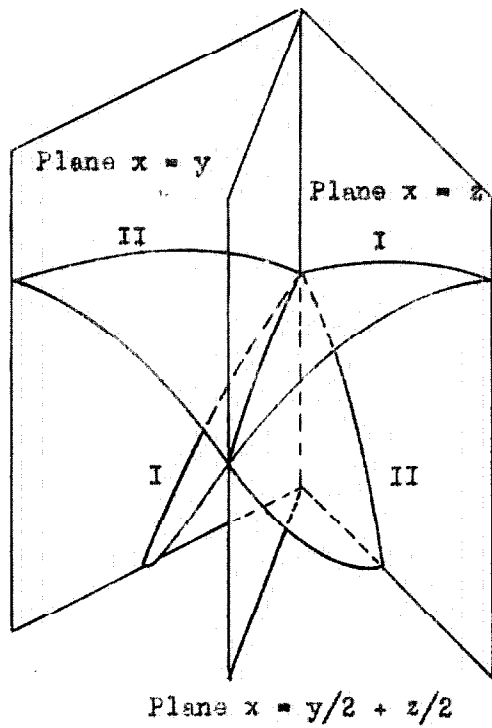


Figure 6. Surfaces near the line $x=y=z$ for one possible correlation of solutions.

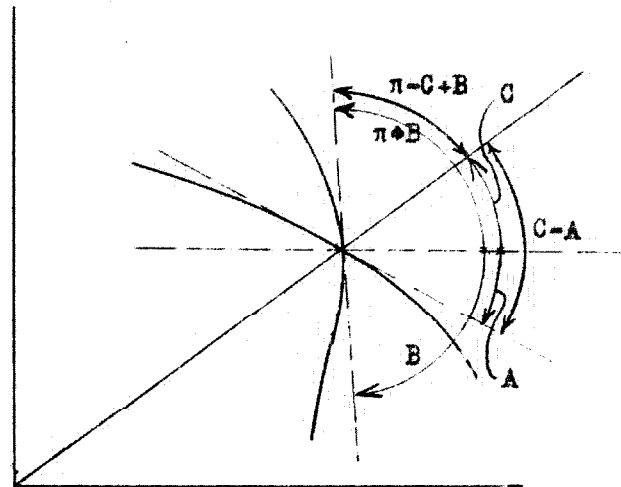


Figure 7. Branches I and II make equal angles with the line $x=y=z$.

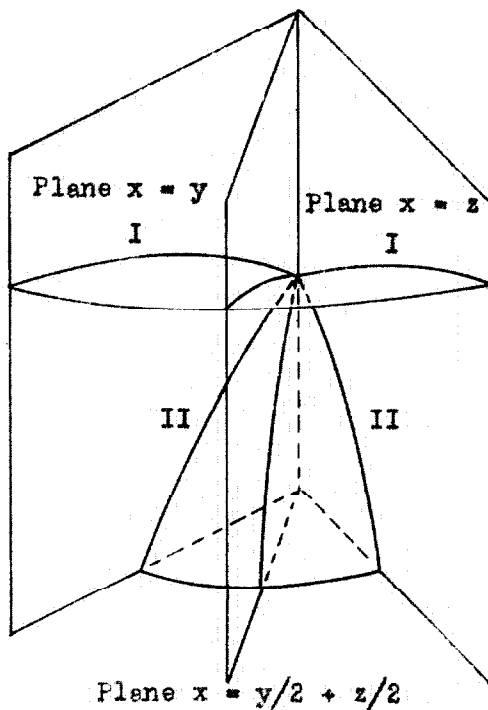


Figure 8. Surfaces near the line $x=y=z$ for the other possible correlation of solutions.

in the plane $x - y/2 = 0$ and is perpendicular to the line $x = y = z$ has the equation $(y + z = 2k, x = k)$. The neighborhood of the point $x = y = z = 30^\circ$, where λ has the value of 0.5 for both Branches I and II, will now be considered.

Taking for simplicity the point $(30^\circ, 25^\circ, 35^\circ)$, one may expand the determinant into the cubic equation

$$\lambda^3 - 1.52660 \lambda^2 + .58974 \lambda - .06735 = 0,$$

which has the roots

$$\lambda_1 = \pm .4875,$$

$$\lambda_2 = \pm .5304,$$

$$\text{and } \lambda_3 = \pm 1.00384.$$

Since the roots are distinct and the first two lie on opposite sides of 0.5, it is immediately suspected that the second situation mentioned above is the actual case; however, a somewhat more certain test may be made. If it is assumed that the directional derivative of λ along a radial line passing through the point $(30^\circ, 25^\circ, 35^\circ)$ is the same as along the line $x = y = z$, approximate distances of the surfaces from the point may be evaluated. For these two branches,

$$\lambda = \sin z = \sin (r/\sqrt{3})$$

$$d\lambda/dr = (1/\sqrt{3}) \cos (r/\sqrt{3}) = (1/\sqrt{3}) \cos 30^\circ = \frac{1}{2} \text{ per radian} \approx .01 \text{ per degree.}$$

Hence

$$r = \lambda/(d\lambda/dr) = .0304/.01 = 3^\circ \text{ for } \lambda_2$$

and

$$r = -.0125/.01 = -1.3^\circ \text{ for } \lambda_1.$$

Figure 9 shows graphically the degree of approximation to which the

above results correspond to the contours given in Figure 5.

The above considerations have shown that the nature of the surfaces is as shown in Figure 8, which corresponds to an interchange of the equations (3.1) for Branch I and Branch II in the plane $x = y$ for $\lambda < 1.0$. This interchange has been taken into account in Figure 5.

5. Contours for $\gamma/a = -0.1$

The contours for the case $\gamma/a = 0$ have been investigated in the previous paragraph, and the information contained in the tabular data is roughly represented by Figure 5. The contours for this case will now be given more accurately, and the contours for the case $\gamma/a = -0.1$ will be found. Instead of repeating for the latter case all of the operations that were used in the previous paragraph for the basic case, one may solve the secular determinant along the lines where the roots have especially simple form. Then, with the assumption that the new contours have nearly the same shape as the contours for the case $\gamma/a = 0$, the curves may be drawn.

Equations (2.11) for the solutions of the secular determinant in the symmetry planes yield the following expressions for the three branches of the constant-frequency surfaces:

Branch I

$$\text{Line } y = 0, x = 0: \lambda^2 = 1 - \cos z$$

$$\text{Line } y = 0, x = z: \lambda^2 = 1 - \cos z + 2\gamma/a \sin^2 z$$

$$\begin{aligned} \text{Line } y = 0, x = \pi/2: \quad & 1 - 4\gamma^2/a^2 + 2(\lambda^2 - 2)\gamma/a \cos^2 z + (\lambda^2 - 2) - 2\gamma/a \cos z \\ & + (\lambda^2 - 2)^2 - 4(\lambda^2 - 2)\gamma/a + 4\gamma^2/a^2 - 1 = 0 \end{aligned}$$

$$\text{Line } y = 0, z = \pi: \lambda^2 = 2 + 2\gamma/a \sin^2 x$$

$$\begin{aligned} \text{Line } y = 0, x = \pi - z: \quad & 4\gamma^2/a^2 - 4\gamma/a \sin^2 z + 2(\lambda^2 - 3)(1 - 2\gamma/a) + 1 \sin z \\ & + (\lambda^2 - 3)^2 - 1 = 0 \end{aligned}$$

$$\text{Line } x = y = z: \lambda^2 = 1 + 2\gamma/a \sin^2 x$$

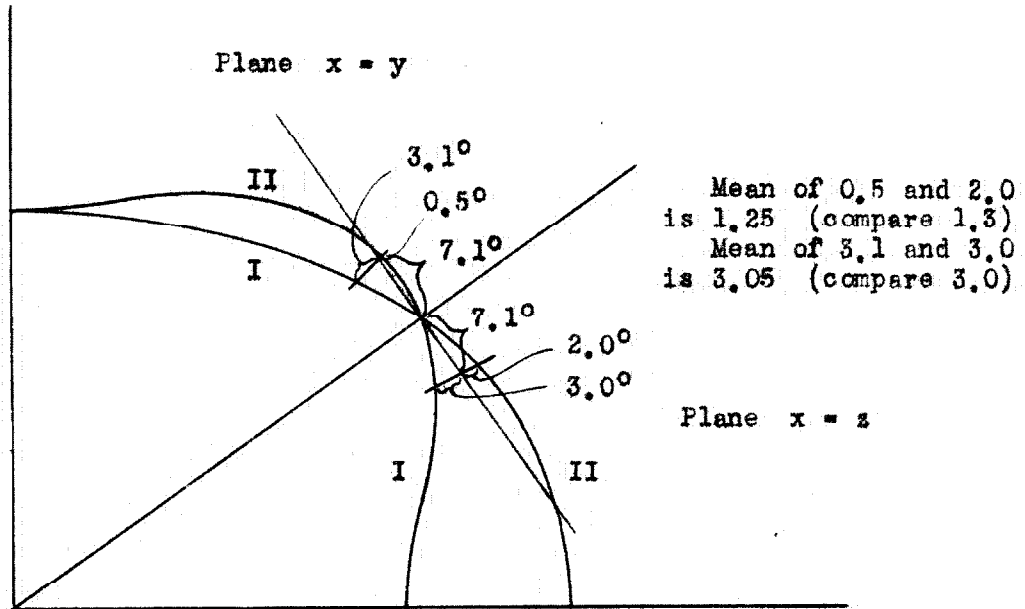


Figure 9. Illustration of the degree of approximation to which the results of the analysis in the text corresponds to the contours given in Figure 5. The point (30, 25, 35) is 7.1° from the point (30, 30, 30), and the distance of each contour from a point in the plane of the contours and lying 7.1° from the latter of the above points is therefore shown. If the curves in the plane $x = y/2 + z/2$ are about halfway between the (rotated) curves in the planes $x = y$ and $x = z$, the graphical results agree quite well with the analytical results of the text.

$$\text{Line } x = y = \pi - z: \lambda^2 = 2(1 - 2\gamma/a) \sin^2 z$$

$$\text{Line } x = y, z = \pi/2: \lambda^2 = 1 + 2\gamma/a \sin^2 x$$

$$\text{Line } x = y = \pi/2: \lambda^2 = 1 + 2\gamma/a$$

$$\text{Line } x = y, x = \pi: \lambda^2 = 1 + \cos x + 2\gamma/a \sin^2 x$$

$$\text{Line } x = y, x = 0: \lambda^2 = 1 - \cos x + 2\gamma/a \sin^2 x$$

$$\text{Line } x = \pi/2, y = \pi - z: \sin^2 x: (\lambda^2 - 2 - 2\gamma/a)(\lambda^2 - 3) / (2 + 2\lambda^2\gamma/a - 4\lambda^2/a^2)$$

Branch II

$$\text{Plane } y = 0: \lambda^2 = 2 - \cos x - \cos z$$

$$\text{Line } x = y = z: \lambda^2 = (1 + 2\gamma/a) \sin^2 z$$

$$\text{Line } x = y = \pi/2: \sin^2 z = (\lambda^2 - 2)(\lambda^2 - 3 - 2\gamma/a) / (2 + 2\lambda^2\gamma/a - 6\gamma/a + 4\gamma^2/a^2)$$

$$\text{Line } x = \pi/2, y = \pi - z: \sin^2 z = (3 - \lambda^2) / (2 - 2\gamma/a)$$

Branch III

$$\text{Line } y = 0, x = 0: \lambda^2 = 2 - 2 \cos z + 2\gamma/a \sin^2 z$$

$$\text{Line } y = 0, x = z: \lambda^2 = 1 - \cos z + (2 + 2\gamma/a) \sin^2 z$$

$$\begin{aligned} \text{Line } y = 0, y = \pi/2: \quad & 1 - 4\gamma^2/a^2 + 2(\lambda^2 - 2)\gamma/a \cos^2 z + (\lambda^2 - 2) - 2\gamma/a \cos z \\ & + (\lambda^2 - 2)^2 - 4(\lambda^2 - 2)\gamma/a + 4\lambda^2/a^2 - 1 = 0 \end{aligned}$$

$$\text{Line } y = 0, z = \pi: \lambda^2 = 3 + \cos x$$

$$\begin{aligned} \text{Line } y = 0, x = \pi - z: \quad & (4\gamma^2/a^2 - 4\gamma/a) \sin^2 z + 2(\lambda^2 - 3)(1 - 2\gamma/a) + 1 \sin z \\ & + (\lambda^2 - 3)^2 - 1 = 0 \end{aligned}$$

$$\text{Line } x = y = z: \lambda^2 = (4 + 2\gamma/a) \sin^2 z$$

$$\text{Line } x = y = \pi - z: \lambda_0^2 + 2\gamma/a \sin^2 z \text{ (Where } \lambda_0^2 \text{ is solutions for } \gamma/a = 0)$$

$$\text{Line } x = y, z = \pi/2: \sin^2 x = (\lambda^2 - 2)(\lambda^2 - 1 - 2\gamma/a) / 2\lambda^2(1 + \gamma/a) - 2 - 8\gamma/a - 4\gamma^2/a^2$$

$$\text{Line } x = y = \pi/2: \sin^2 z = (\lambda^2 - 2)(\lambda^2 - 3 - 2\gamma/a) / (2 + 2\lambda^2\gamma/a - 6\gamma^2/a^2)$$

$$\text{Line } x = \pi/2, y = \pi - z: \sin^2 z = (\lambda^2 - 2 - 2\gamma/a)(\lambda^2 - 3) / (2 + 2\lambda^2\gamma/a - 4\gamma/a - 4\gamma^2/a^2)$$

Figures 10 to 15 were drawn with the aid of the tabular data given for the basic case $\gamma/a = 0$ as well as the numerical values obtained from the preceding expressions for the case $\gamma/a = -0.1$. Each contour for the latter case was drawn through its known intercepts with the various lines, and was then made to go smoothly from one intercept to another along a path that resembled a nearby contour for the basic case. In most instances the corresponding contours for the basic case and the other case are quite close together, so that no difficulty was encountered in this procedure.

6. Nature of the Contours Near the Origin

It can easily be shown from the secular determinant that the frequency spectrum resembles a Debye distribution in the region of low frequencies. It is important for the work of Section IV that the contours be determined for this case. The low frequencies are found near the origin in (x, y, z) space, so that the approximations $\sin x = x$ and $\cos x = 1 - x^2/2$ are valid. With these and similar expressions for y and z , the secular determinant (2.5) becomes

$$(3.2) \quad \begin{vmatrix} (1 + 2\gamma/a)x^2 + y^2/2 + z^2/2 - \lambda^2 & x y & x z \\ x y & (1 + 2\gamma/a)y^2 + x^2/2 + z^2/2 - \lambda^2 & y z \\ x z & y z & (1 + 2\gamma/a)z^2 + x^2/2 + y^2/2 - \lambda^2 \end{vmatrix} = 0$$

Transformation to spherical polar coordinates and division of the secular determinant by r^6 yields

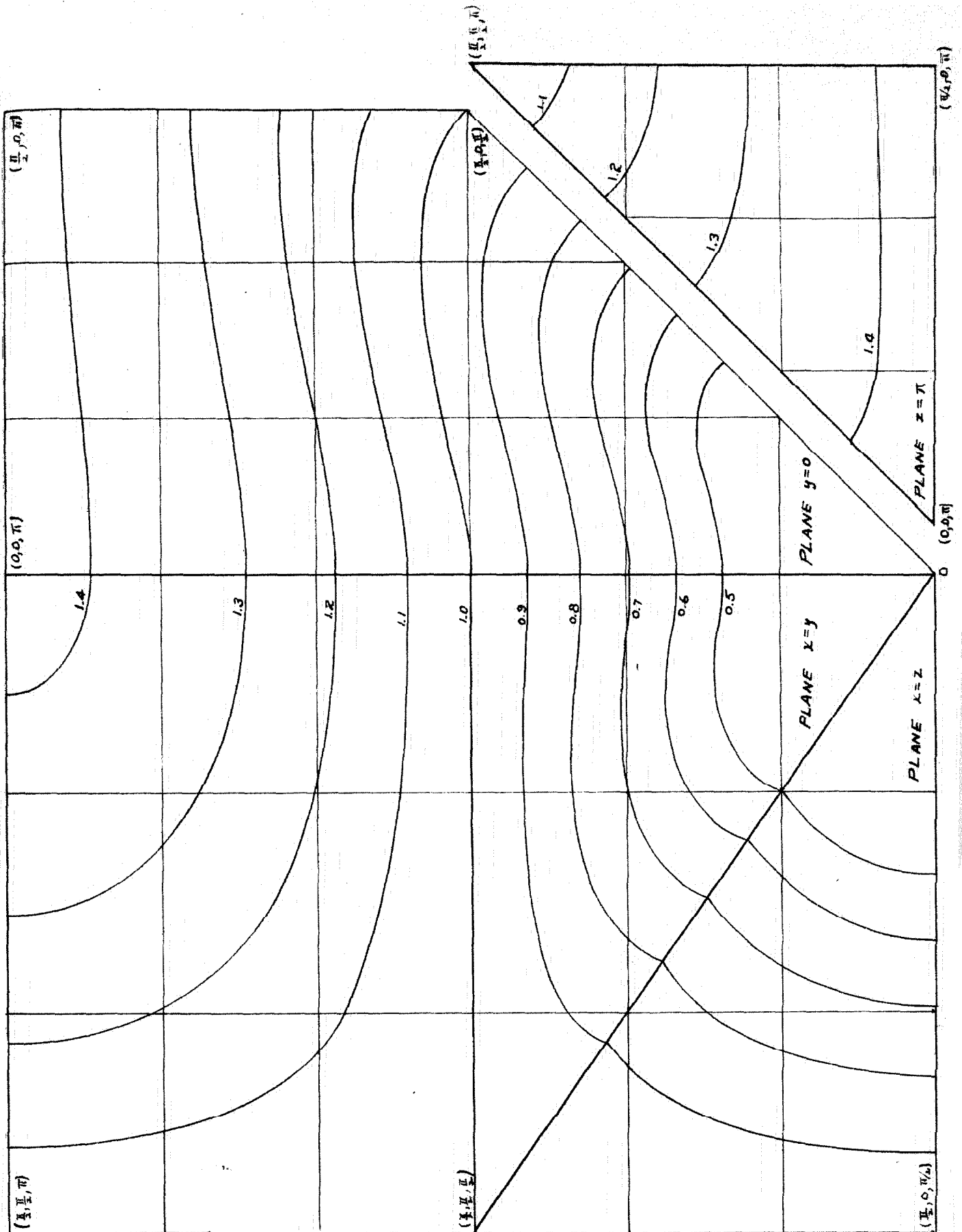


Figure 10. Contours of constant frequency for $\gamma/a = 0$.
(BRANCH I)

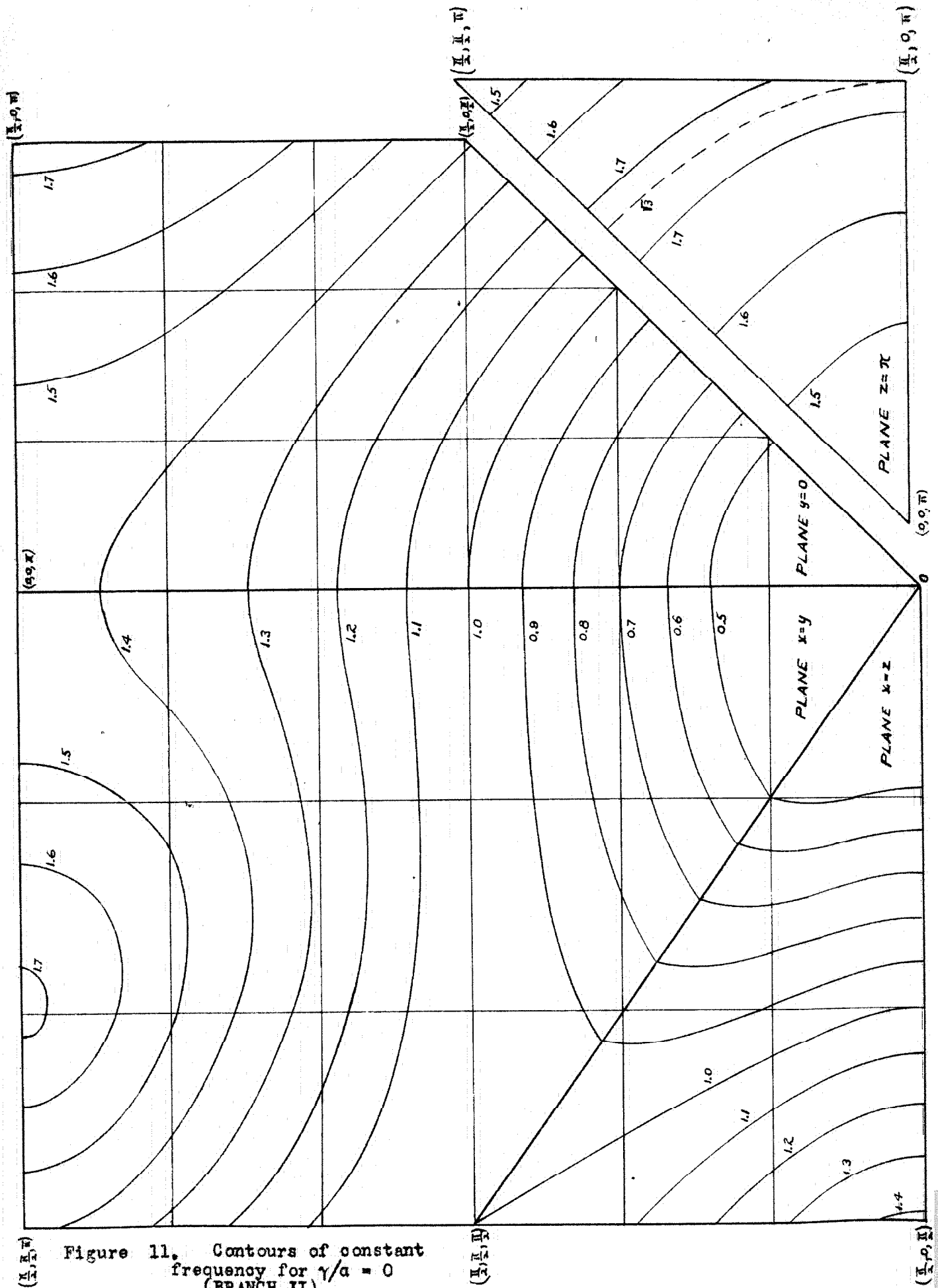


Figure 11. Contours of constant frequency for $\gamma/a = 0$ (BRANCH II)

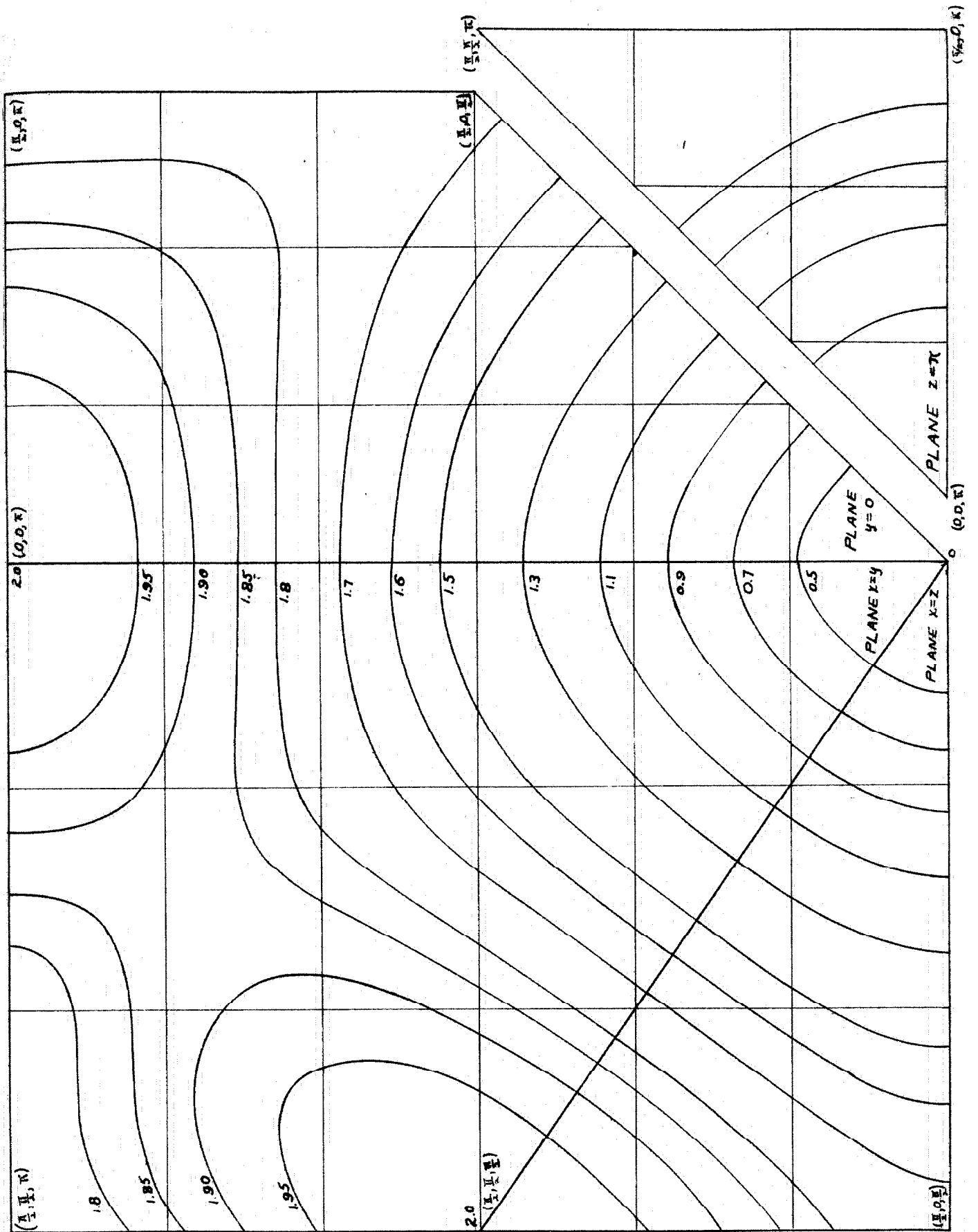


Figure 12. Contours of constant frequency for $\gamma/a = 0$
(BRANCH III)

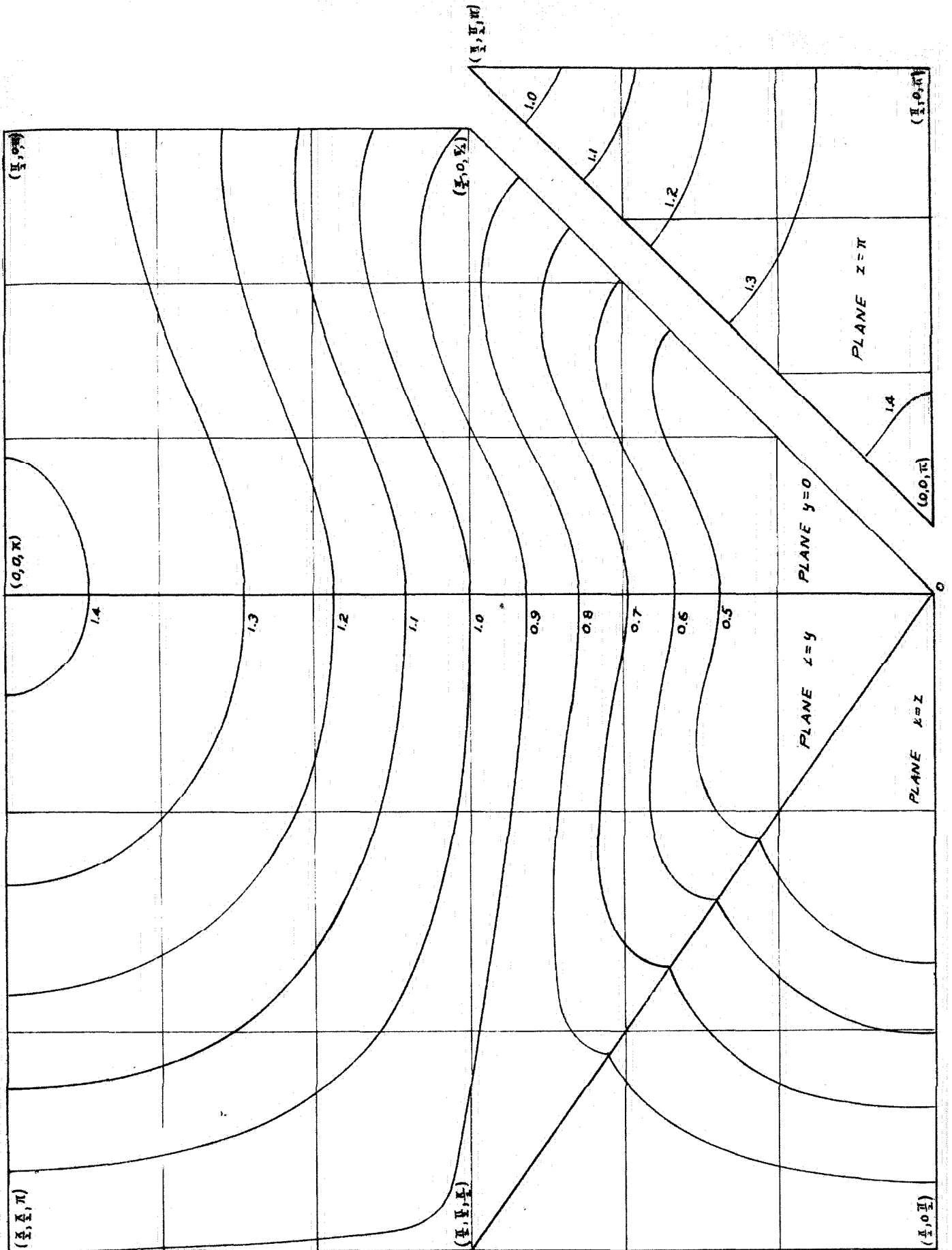


Figure 13. Constant-frequency contours for $\gamma/a = -0.1$
(BRANCH I)

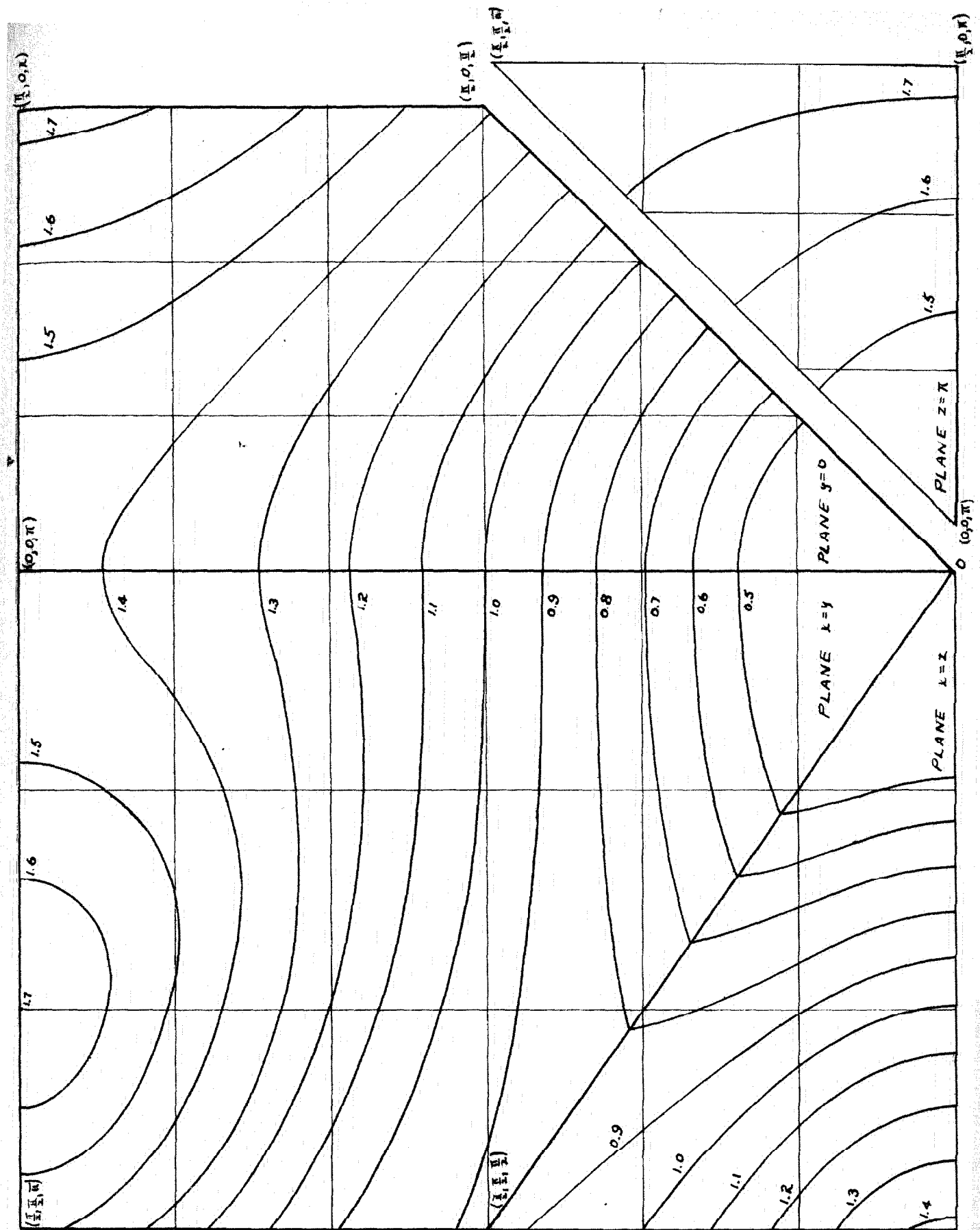


Figure 14. Constant-frequency contours for $\gamma/a = -0.1$
(BRANCH II)

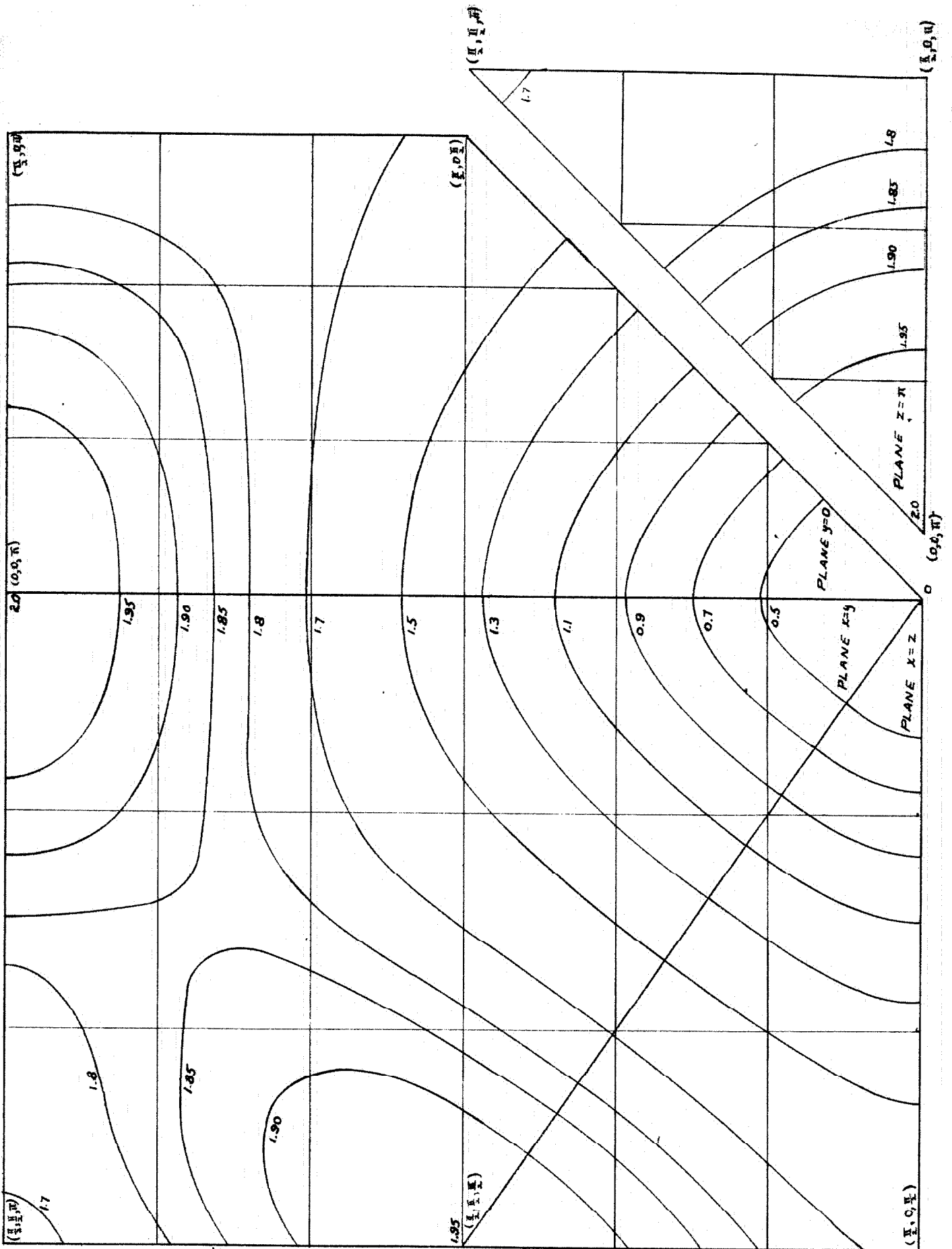


Figure 15. Constant-frequency contours for $\gamma/a = -0.1$
(BRANCH III)

$$(3.3) \quad \begin{vmatrix} \left(\frac{1}{2} + 2\gamma/a \right) \sin^2 \theta \cos^2 \phi + \frac{1}{2} - \lambda^2/r^2 & \sin^2 \theta \sin \phi \cos \phi & \sin \theta \cos \theta \cos \phi \\ \sin^2 \theta \sin \phi \cos \phi & \left(\frac{1}{2} + 2\gamma/a \right) \sin^2 \phi \sin^2 \theta + \frac{1}{2} - \lambda^2/r^2 & \sin \theta \cos \theta \sin \phi \\ \sin \theta \cos \theta \cos \phi & \sin \theta \cos \theta \sin \phi & \left(\frac{1}{2} + 2\gamma/a \right) \cos^2 \theta + \frac{1}{2} - \lambda^2/r^2 \end{vmatrix} = 0$$

It is clear that this determinant will have solutions of the form $r^2 = \lambda^2 F(\theta, \phi)$ so that the volume enclosed by each constant-frequency surface will be proportional to λ^3 . Thus, the distribution function, which is proportional to the derivative of the volume with respect to λ , will have the form $N(\lambda) = A \lambda^2$, for small enough values of λ . The constant A will be determined in Section IV.

To find the contours in the three symmetry planes, the determinant (3.3) can be solved in the planes $\phi = 0$ and $\phi = \pi/4$, with the following results:

Branch I

$$\text{Plane } y = 0: \lambda_1^2/r^2 = 3/4 + \gamma/a - \frac{1}{2} \sqrt{\left(\frac{1}{2} + 2\gamma/a \right)^2 + (3/4 - 2\gamma/a - 4\gamma^2/a^2) \sin^2 2\theta}$$

$$\text{Plane } x = y: \lambda_2^2/r^2 = \frac{1}{2} - (1/4 - \gamma/a) \sin^2 \theta$$

Branch II

$$\text{Plane } y = 0: \lambda_2^2/r^2 = \frac{1}{2}$$

$$\text{Plane } x = y: \lambda_2^2/r^2 = 3/4 + \gamma/a + (1/8 - \gamma/2a) \sin^2 \theta$$

$$- \frac{1}{2} \sqrt{\left[\left(\frac{1}{2} + 2\gamma/a \right) - (5/4 + 3\gamma/a) \sin^2 \theta \right]^2 + \sin^2 2\theta}$$

Branch III

$$\text{Plane } y = 0: \lambda_3^2/r^2 = 3/4 + \gamma/a + \frac{1}{2} \sqrt{\left(\frac{1}{2} + 2\gamma/a \right)^2 + (3/4 - 2\gamma/a - 4\gamma^2/a^2) \sin^2 2\theta}$$

$$\text{Plane } x = y: \lambda_3^2/r^2 = 3/4 + \gamma/a + (1/8 - \gamma/2a) \sin^2 \theta$$

$$+ \frac{1}{2} \sqrt{\left[\left(\frac{1}{2} + 2\gamma/a \right) - (5/4 + 3\gamma/a) \sin^2 \theta \right]^2 + \sin^2 2\theta}$$

The contours of constant frequency for $\gamma/a = 0$ and $\gamma/a = -0.1$ are drawn in Figure 16. The scale of this figure and the value of λ were chosen to agree with Figures 10 to 15 for later applications.

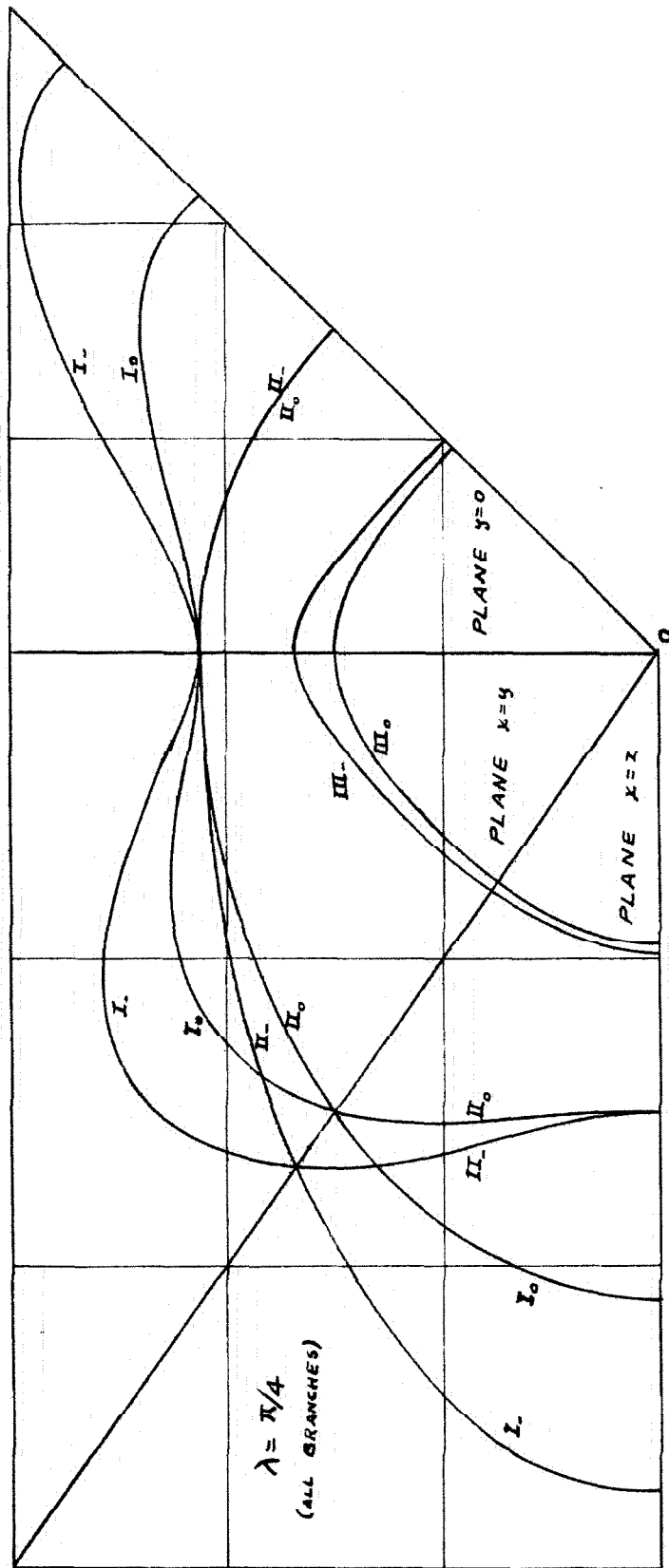


Figure 16. Constant-frequency contours for $\gamma/a = 0$ and $\gamma/a = -0.1$, neglecting higher order terms in the series expansions of the trigonometric terms of the secular determinant.

SECTION IV

THE FREQUENCY SPECTRUM OF A FACE-CENTERED CUBIC CRYSTAL LATTICE

1. Introduction

The final step in the solution of the dynamical problem of the vibrational motion of a face-centered cubic crystal lattice is the actual numerical calculation of the frequency spectrum, using the data of Section III. There are many different ways in which such a computation could be made; the method used here has been chosen for its inherent simplicity, and because results that are correct to within a few percent are obtainable more quickly and with less chance of computational error than by other methods. This method consists in actually modeling the constant-frequency surfaces in three dimensions, and then measuring the volumes enclosed by these surfaces with the help of Archimedes' principle.

2. Construction of the Constant-Frequency Surfaces

Plaster of Paris is an excellent material for modeling the surfaces, for it can be cast so as to reproduce the smallest detail of a mold without shrinkage or expansion; it can be machined (sawed, sanded, carved); it is rigid, so that it maintains its shape; it is inexpensive; it is convenient to use because it requires only cold water in mixing, and the proportions are not critical.

A mold was constructed of 1/8-inch sheet brass, having the shape and size of the boundary planes of Figure 5, with the boundary plane $x = y$ omitted. The mold was machined so that a flat sheet of material, placed upon the open face of the mold, coincided with the plane $x = y$. A small hole was drilled in the center of one edge of the mold, so that a wire stretched from the origin through this hole corresponded to the line $(x = z/2, y = z/4)$. (This is a line along which the secular determinant was solved in the preceding section.)

Using this mold, nine blocks of plaster were cast in the shape of Figure 5. Section III in the following manner: the mold was greased with Petrolatum, and

then a straight piece of 1/16-inch drill rod was laid in it to define the line described above. The plaster was mixed with a slight amount of Le Page's glue to retard setting. After the plaster was placed in the mold it was agitated to make air bubbles rise. Most of the excess plaster was then scraped off and the remainder was forced out by a slab of 1/4-inch plate glass, pressed down on the open face of the mold. After the plaster had set it was removed from the mold by forcing a small stream of compressed air from a soft rubber tube between the slightly flexible brass mold and the plaster block. The blocks were then allowed to dry for a few days.

A number of reference lines were scratched on the exposed edges of the mold and on the exposed faces of the plaster blocks. This was done to facilitate the later replacement of the plaster pieces in their proper positions in the mold. Contours corresponding to Figures 10 - 15 of Section III were carefully drawn upon three sheets of coordinate paper which had been cut out so that they could be folded up into the shape of Figure 5, Section III. The contours on these sheets were then transferred to the surfaces of the plaster blocks by wrapping a sheet around a block and pricking through the paper with a pin along each contour, and later drawing the curves in pencil. In this way a pair of duplicate sets was drawn for each branch for the basic case, and one set was drawn for each branch for the other value of γ/α .

Each block was cut into a number of pieces by sawing between alternate pairs of contours, and the surfaces were carved. Actually, this process was carried out by sawing off one piece at a time, starting with the piece farthest from the origin; this method permitted the intercept of each surface with the line ($x = z/2$, $y = z/4$) to be laid off accurately by placing the block in the mold and measuring from the origin (in the mold) to the surface of the block with a wire of the proper length. This procedure was necessary because the plaster always broke near the origin when the drill rod, which defined the

above line, was removed from the block. The duplicate sets of surfaces for each branch of the basic case ($\nu/a = 0$) were not carved in exactly the same way; for one set of a pair, the saw cuts were half way between the saw cuts for the other set, so that each surface was carved once from its convex side and once from its concave side. In this way it was possible to minimize the psychological errors in estimating whether the surfaces were orthogonal to the boundary planes.

The above process thus yielded a number of pieces, each bounded by one or two of the constant-frequency surfaces and the boundary planes. To obtain the alternate pieces of each set (the ones that were destroyed by the saw-cuts and the carving process) the carved pieces were greased and placed into the mold, and a thin mixture of plaster was poured into the spaces between them. After this plaster had set, the pieces were removed from the mold and were separated by applying gentle but firm pressure with the fingers; all of the pieces were then boiled in paraffin to reduce their tendency to absorb water.

3. Measurement of Volumes

The volumes enclosed by successive surfaces were next measured by weighing the amount of water displaced by the corresponding pieces of plaster. This was done by weighing each piece of each set twice - first while it was submerged (after it had ceased to absorb water), and then in air (after all water drops had been wiped off). The difference between these two weights in grams is then equal to the volume of the piece in cubic centimeters, within the limits of accuracy of the measurements. Tables 21 to 26 (inclusive) give the results of weighing the nine sets of surfaces that were carved. The total volume occupied by all of the pieces of a set should theoretically be 486.0 c.c.

TABLE 21

Volume of Plaster Models of Constant-frequency Surfaces
Branch I, $\gamma/a = 0$

Interval		Set A			Set B		
λ_1	to λ_2	$W_{H_2O}(g.)$	$W_{air}(g.)$	$V(c.c.)$	$W_{H_2O}(g.)$	$W_{air}(g.)$	$V(c.c.)$
0.0	0.5	7.33	20.17	12.70	6.25	18.43	12.18
0.5	0.6	4.77	14.07	9.30	6.87	17.16	10.29
0.6	0.7	9.56	25.07	15.50	6.53	20.19	13.86
0.7	0.8	8.89	23.91	20.02	15.47	38.84	23.37
0.8	0.9	18.5	52.1	33.6	14.8	43.4	28.6
0.9	1.0	21.9	57.5	45.6	31.8	83.4	51.6
1.0	1.1	49.6	137.5	37.9	33.2	111.8	78.6
1.1	1.2	37.0	121.0	84.0	51.2	139.6	88.4
1.2	1.3	51.2	139.4	88.2	40.5	121.0	83.5
1.3	1.4	39.6	122.4	82.8	41.5	127.7	86.2
1.4	$\sqrt{2}$	7.3	18.7	11.4	5.0	15.8	10.8
Total Volume, V_0 :				491.1	Total Volume, V_0 : 487.5		

TABLE 22

Volume of Plaster Models of Constant-frequency Surfaces
Branch III, $\gamma/a = 0$

Interval		Set A			Set B		
λ_1	to λ_2	$W_{H_2O}(g.)$	$W_{air}(g.)$	$V(c.c.)$	$W_{H_2O}(g.)$	$W_{air}(g.)$	$V(c.c.)$
0.0	0.5	3.93	11.50	7.51	3.46	11.02	7.56
0.5	0.6	2.03	8.03	6.00	2.22	7.95	5.73
0.6	0.7	3.78	12.05	8.27	4.50	13.27	5.77
0.7	0.8	5.05	17.61	12.56	4.86	17.50	15.84
0.8	0.9	8.5	27.9	19.4	10.1	29.7	19.6
0.9	1.0	11.7	41.4	29.7	10.3	38.0	27.7
1.0	1.1	19.0	61.1	42.1	22.0	67.7	45.7
1.1	1.2	17.0	66.1	49.1	19.1	62.0	42.9
1.2	1.3	21.0	73.5	52.5	29.2	89.0	59.8
1.3	1.4	26.2	91.9	65.7	20.6	78.5	57.9
1.4	1.5	27.0	100.3	73.3	44.5	126.3	81.8
1.5	1.6	25.4	99.1	73.7	21.0	86.1	63.1
1.6	1.7	13.6	56.1	42.5	21.0	69.2	48.2
1.7	$\sqrt{3}$	2.21	8.50	5.29	2.37	7.77	4.80
Total volume, V_0 :				487.6	Total volume, V_0 : 488.4		

TABLE 23

Volume of Plaster Models of Constant-frequency Surfaces
Branch III, $\gamma/a = 0$

Interval		Set A			Set B		
λ_1	to λ_2	$W_{H_2O}(g.)$	$W_{air}(g.)$	$V(c.c.)$	$W_{H_2O}(g.)$	$W_{air}(g.)$	$V(c.c.)$
0.0	0.5	.97	2.70	1.73	1.12	2.86	1.74
0.5	0.7	2.06	5.15	3.09	1.48	4.66	3.18
0.7	0.9	2.41	8.14	5.73	3.58	9.47	5.89
0.9	1.1	3.67	16.84	10.17	4.45	14.91	10.46
1.1	1.3	6.5	23.8	17.3	10.8	28.2	17.4
1.3	1.5	19.0	48.3	29.3	9.0	38.0	29.0
1.5	1.7	23.4	80.9	57.5	30.1	90.1	60.0
1.7	1.8	57.4	150.2	92.8	39.0	125.9	86.9
1.8	1.85	41.0	139.9	98.9	66.0	178.2	112.2
1.85	1.9	49.5	141.6	92.1	27.9	112.0	84.1
1.9	1.95	21.0	75.2	54.2	32.7	88.8	56.1
1.95	2.0	14.5	40.7	26.2	7.7	31.9	24.2
Total Volume, V_0				489.1	Total Volume, V_0 491.2		

TABLE 24

Volume of Plaster Models of Constant-frequency Surfaces
Branch I $\gamma/a = -0.1$

Interval		$W_{H_2O}(g.)$	$W_{air}(g.)$	$V(c.c.)$
λ_1	to λ_2			
0.0	0.5	10.21	28.82	18.61
0.5	0.6	9.70	24.75	15.05
0.6	0.7	10.65	30.25	19.60
0.7	0.8	21.0	53.7	32.7
0.8	0.9	21.6	61.1	39.5
0.9	1.0	44.0	117.6	73.6
1.0	1.1	37.9	108.7	70.8
1.1	1.2	46.8	125.5	78.7
1.2	1.3	41.1	120.9	79.8
1.3	1.4	34.1	91.6	57.5
1.4	$\sqrt{2}$	1.4	3.7	2.3
Total volume, V_0		488.2		

TABLE 25

Volume of Plaster Models of Constant-frequency Surfaces
Branch II, $\gamma/a = -0.1$

Interval		$W_{H_2O}(g.)$	$W_{air}(g.)$	$V(c.c.)$
λ_1	to λ_2			
0.0	0.5	4.20	11.96	7.76
0.5	0.6	4.36	10.98	6.62
0.6	0.7	4.90	14.19	9.29
0.7	0.8	10.6	26.7	16.1
0.8	0.9	11.5	34.5	23.0
0.9	1.0	24.7	63.4	38.7
1.0	1.1	20.5	60.1	39.6
1.1	1.2	32.6	83.6	51.0
1.2	1.3	22.7	68.8	46.1
1.3	1.4	44.1	111.4	67.3
1.4	1.5	33.0	101.3	68.3
1.5	1.6	46.3	117.5	71.2
1.6	1.7	18.0	58.9	40.9
1.7	$\sqrt{3}$	2.0	4.9	2.9
Total Volume, V_0				488.8

TABLE 26

Volume of Plaster Models of Constant-frequency Surfaces
Branch III, $\gamma/a = -0.1$

Interval		$W_{H_2O}(g.)$	$W_{air}(g.)$	$V(c.c.)$
λ_1	to λ_2			
0.0	0.5	1.25	3.27	2.02
0.5	0.7	1.87	5.17	3.30
0.7	0.8	4.20	11.27	7.07
0.9	1.1	6.23	17.70	11.47
1.1	1.3	11.6	31.6	20.0
1.3	1.5	11.5	44.4	32.9
1.5	1.7	43.1	118.8	75.7
1.7	1.8	46.1	153.5	107.4
1.8	1.85	64.0	177.4	113.4
1.85	1.9	30.6	100.9	73.3
1.9	1.95	22.2	61.0	38.8
1.95	2.0	4.5	13.2	8.7
Total volume, V_0				491.1

In addition to the nine complete sets of surfaces, there were also carved six individual pieces, corresponding to the contours of Figure 16. The results of weighing these individual blocks are given in Table 27.

TABLE 27

Volume of Individual Constant-frequency Surfaces
Frequency Interval 0.0 to $\pi/4$

γ/a	Branch	$W_{H_2O}(g.)$	$W_{air}(g.)$	$V(c.c.)$
0.0	I	25.8	70.1	44.3
0.0	II	14.1	39.3	25.2
0.0	III	4.0	9.9	5.9
-0.1	I	41.3	114.9	73.6
-0.1	II	15.4	42.6	27.2
-0.1	III	3.9	10.5	6.4

4. The Frequency Spectrum

The data given in the above tables will now be used to evaluate a quantity which is proportional to the distribution function $N(\nu)$. Three dimensionless functions $G_i(\lambda)$ of the dimensionless parameter λ may be defined as follows:

$$(4.1) \quad G_i(\lambda) = (2/3V_0) dV_i / d\lambda$$

where V_i is the volume of propagation vector space enclosed by the surface $\lambda = \text{const.}$ for the branch i ($i = I, II, \text{ or } III$), and V_0 is the total volume of propagation vector space included in the unit cell of the periodicity lattice. Clearly, the functions $G_i(\lambda)$ are independent of the units in which volume is measured. Further, the function $G(\lambda)$ defined as

$$(4.2) \quad G(\lambda) = G_I(\lambda) + G_{II}(\lambda) + G_{III}(\lambda)$$

is closely associated with the distribution function $N(\nu)$. For, recalling the discussion of Paragraph 2 of Section II, one may write, using the notation of Equations (2.1) and (4.1):

$$(4.3) \quad \int_0^{\nu_m} N(\nu) d\nu = K \int_0^{\nu_m} (dV/d\nu) d\nu = K V_0 = 3N_0$$

(since the total number of normal modes of a crystal made up of N_0 atoms is $3N_0$) and

$$(4.4) \quad \int_0^{\nu_m} G(\lambda) d\lambda = 2/3V \int_0^{\nu_m} (dV_I/d\lambda + dV_{II}/d\lambda + dV_{III}/d\lambda) d\lambda = 2.$$

Inasmuch as λ and ν are linearly related (see Equation (2.5)), one of the above expressions may be divided by the other to obtain

$$(4.5) \quad \frac{\int_0^{\nu_m} N(\nu) d\nu}{\int_0^{\nu_m} G(\lambda) d\lambda} = \frac{N(\nu) d\nu}{G(\lambda) d\lambda} = 3N_0/2.$$

Whence,

$$(4.6) \quad N(\nu) = (3N_0/2) G(\lambda) d\lambda/d\nu = 3\pi N_0 \sqrt{m/2a} G(\lambda).$$

Thus the function $G(\lambda)$ is proportional to the distribution function $N(\nu)$.

Table 8 contains the values of $(2/3V_0) dV_I/d\lambda$ tabulated against the upper limits of the intervals $\Delta\lambda$. These intervals are the same as for the corresponding ΔV_i in Tables 21 - 26.

Figure 17. The distribution Functions $G(\lambda)$ and $G_x(\lambda)$

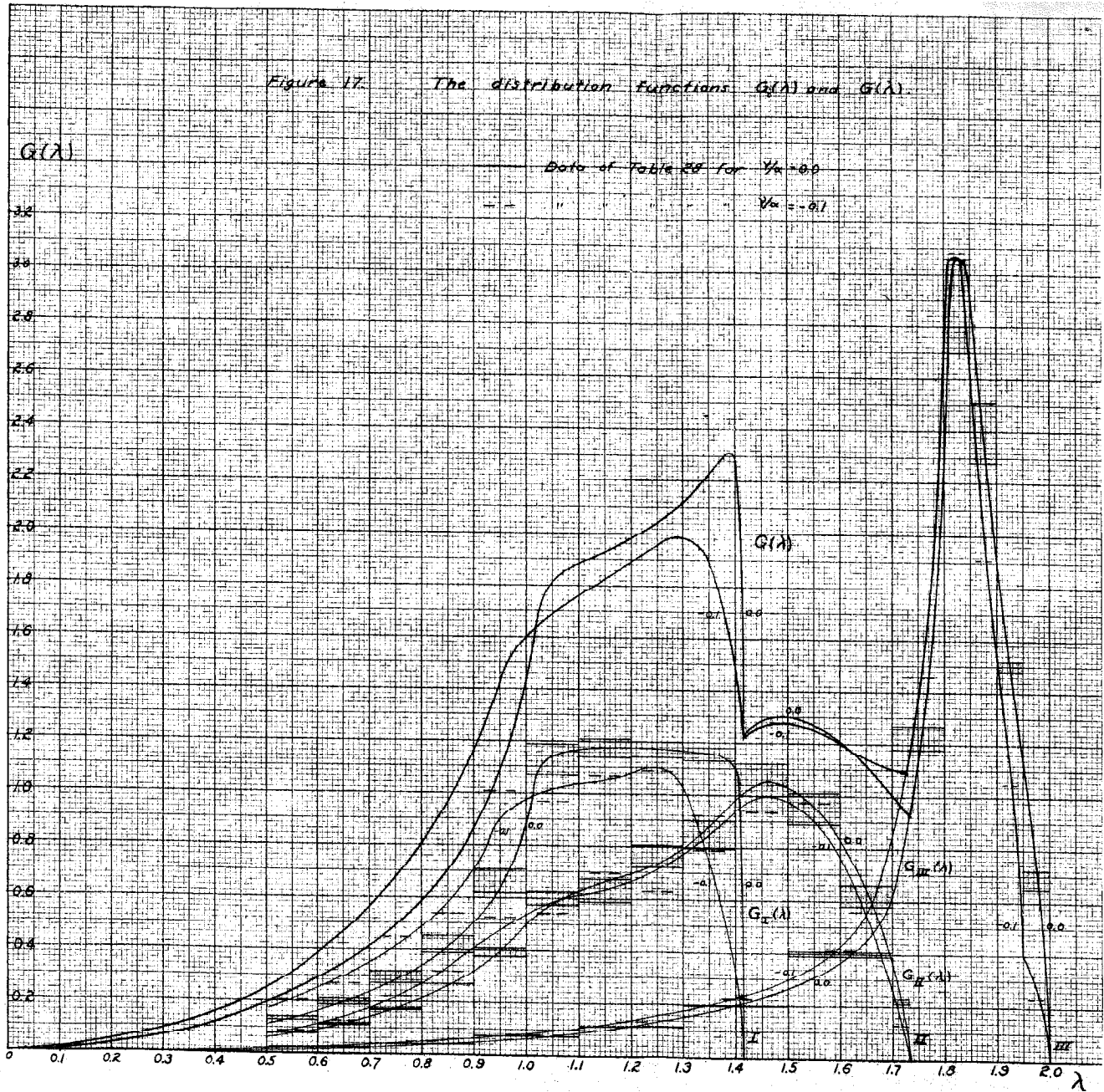


TABLE 28

Values of $(2/3V_0)\Delta V_i/\Delta\lambda$ for Plaster Models of Constant-frequency Surfaces

λ	Branch: Set: γ/a								
	I:A:0.0	I:B:0.0	I:-:-0.1	II:A:0	II:B:0	II:-:-0.1	III:A:0	III:B:0	III:-:-0.1
0.6	.127	.141	.206	.082	.078	.090	-----	-----	-----
0.7	.211	.189	.268	.113	.120	.127	.021	.022	.022
0.8	.272	.319	.447	.171	.175	.220	-----	-----	-----
0.9	.456	.392	.540	.266	.268	.318	.039	.040	.048
1.0	.620	.707	1.01	.405	.378	.529	-----	-----	-----
1.1	1.19	1.07	.97	.575	.623	.541	.070	.071	.078
1.2	1.14	1.21	1.07	.674	.586	.697	-----	-----	-----
1.3	1.20	1.14	1.09	.720	.808	.630	.117	.117	.136
1.4	1.13	1.18	.79	.900	.794	.920	-----	-----	-----
$\sqrt{2}$	1.09	1.05	.24	-----	-----	-----	-----	-----	-----
1.5	-----	-----	-----	1.00	1.12	.935	.200	.197	.223
1.6	-----	-----	-----	1.01	.89	.976	-----	-----	-----
1.7	-----	-----	-----	.58	.66	.560	.394	.407	.512
$\sqrt{3}$	-----	-----	-----	.23	.21	.13	-----	-----	-----
1.8	-----	-----	-----	-----	-----	-----	1.27	1.18	1.46
1.85	-----	-----	-----	-----	-----	-----	2.70	3.06	3.08
1.9	-----	-----	-----	-----	-----	-----	2.51	2.28	1.91
1.95	-----	-----	-----	-----	-----	-----	1.48	1.52	1.05
2.0	-----	-----	-----	-----	-----	-----	.72	.65	.24

Figure 17 shows the curves $G_i(\lambda)$ for the basic case ($\gamma/a = 0$) and for the case $\gamma/a = -0.1$. These were drawn so that the area under each curve is approximately equal to the area under the corresponding stepwise plot of the data of Table 28. The $G_i(\lambda)$ curves are added together for each case to form the corresponding $G(\lambda)$ curve.

5. Frequency Spectrum for Low Frequencies

The curves of Figure 17 are defined by the data of Table 28 only from $\lambda = 0.5$ to $\lambda = 2.0$. The interval from $\lambda = 0$ to $\lambda = 0.5$ is also important, however, as it is this part of the spectrum that governs the specific heat at low temperatures. It is possible to evaluate graphically the first two or three terms in a power series expansion in the neighborhood of the origin, by expressing the fractional volume occupied by all frequencies less than λ ,

for each branch, in the form

$$(4.7) \quad 2V_i(\lambda) / 3V_0 = k_i \lambda^6 \quad (i = I, II, III)$$

where $k_i = k_{0i} + k_{2i}\lambda^2 + k_{4i}\lambda^4 + \dots$. Odd powers of λ do not appear in the expression for k because $G_i(\lambda)$ must be a function of λ^2 .

Table 29 gives values of k computed from the data of Tables 21-27. These values are plotted in Figure 18. The values of k for $\lambda = 0$ were obtained from the data of Table 27, which represents the volume that would be enclosed by the surfaces $\lambda = \pi/4$ if all the surfaces were of the same shape as those for very small values of λ . (In this case, $G(\lambda)$ would be essentially a Debye distribution.)

Smooth curves were drawn through the points defining the upper and lower limits of the measured values, and a mean curve was drawn midway between these extremes. It should be noted that the successive points for each set generally fall alternately above and below the corresponding points for the duplicate set. This indicates that there was a tendency to carve away too little material from each surface.

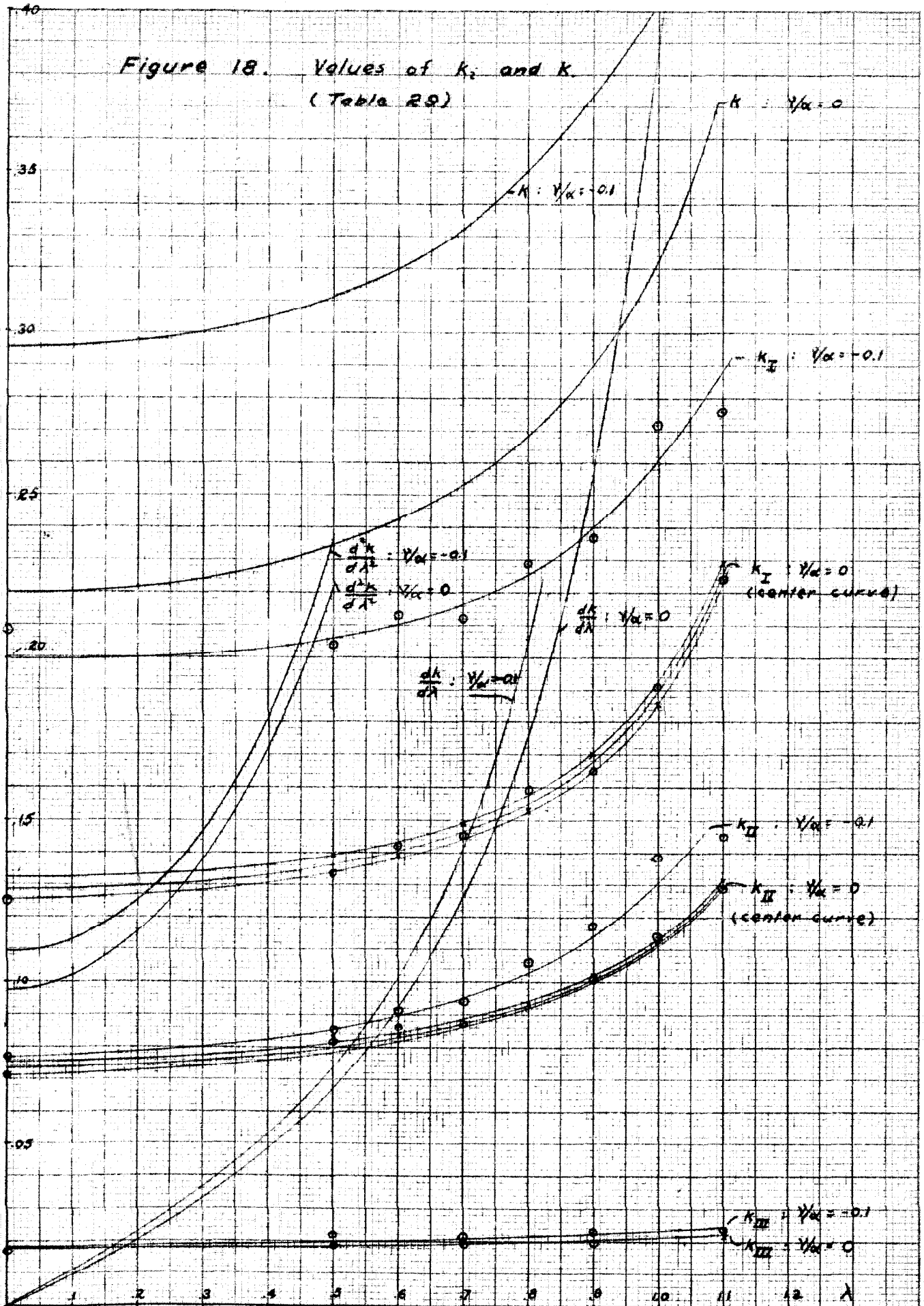
TABLE 29

Values of k_i for Plaster Models of Constant-frequency Surfaces

$$k_i = 2V_i(\lambda) / 3\lambda^6 V_0$$

λ	$\gamma/a = 0$						$\gamma/a = -0.1$		
	k_{IA}	k_{IB}	k_{IIIA}	k_{IIIB}	k_{IIIA}	k_{IIIB}	k_I	k_{II}	k_{III}
0	.125	---	----	.071	.017	----	.208	.077	.018
.5	.139	.133	.083	.082	.0187	.0187	.204	.085	.022
.6	.139	.142	.084	.085	----	----	.213	.091	----
.7	.149	.145	.088	.087	.0196	.0194	.212	.094	.021
.8	.153	.159	.093	.091	----	----	.229	.106	----
.9	.170	.165	.102	.101	.0197	.0201	.237	.117	.023
1.0	.186	.191	.112	.114	----	----	.272	.130	----
1.1	.229	.224	.131	.129	.0212	.0217	.276	.145	.024

Figure 18. Values of k_i and k
(Table 29)



The mean curves for the three branches were added together to produce a curve of k vs. λ where

$$(4.8) \quad k = 2V(\lambda)/3\lambda^2V_0 = k_0 + k_2\lambda^2 + k_4\lambda^4 + \dots$$

$$V(\lambda) = V_I(\lambda) + V_{II}(\lambda) + V_{III}(\lambda)$$

These two curves of k vs. λ (one for each of the two values of γ/a) were differentiated graphically three times. The latter curves are also shown in Figure 18.

The values of k_0 , k_2 , and k_4 were determined from the intercepts and slopes of these curves at $\lambda = 0$, with the following results:

TABLE 30

Values of k_0 , k_2 , and k_4 of Equation (4.8)			
γ/a	k_0	k_2	k_4
0.0	.22	.046	.040
-0.1	.30	.055	.035

The distribution function $G(\lambda)$ may be obtained from (4.8) as follows:

$$(4.9) \quad G(\lambda) = 2/3V_0 dV(\lambda) / d\lambda = d/d\lambda (k_0\lambda^3 + k_2\lambda^5 + k_4\lambda^7 + \dots)$$

$$= 3k_0\lambda^2 + 5k_2\lambda^4 + 7k_4\lambda^6 + \dots$$

Thus, for $\gamma/a = 0$,

$$(4.10) \quad G(\lambda) = 0.66\lambda^2 + 0.23\lambda^4 + 0.28\lambda^6 + \dots$$

and for $\gamma/a = -0.1$,

$$(4.11) \quad G(\lambda) = 0.88\lambda^2 + 0.27\lambda^4 + 0.24\lambda^6 + \dots$$

The coefficients of the λ^2 terms are of course known more accurately than those of the higher order terms, but for the computation of specific heats these expressions are sufficiently accurate.

The distribution functions $G(\lambda)$ are thus defined by the expressions (4.10) and (4.11) from $\lambda = 0$ to $\lambda = 0.5$, and by the curves of Figure 17 for other values of λ .

SECTION V

ATOMIC FORCE CONSTANTS

1. Introduction

In the preceding sections, the equations of motion of the face-centered cubic crystal lattice have been solved, and the frequency distributions have been obtained for certain relative values of the two atomic force constants. It is the purpose of this section to consider the nature of the elastic properties of actual crystals, and to correlate the force constants with the large-scale elastic properties. It is clear that an additional assumption must necessarily be made, before the two atomic force constants, α and γ , can be evaluated in terms of the observed elastic properties of a given crystalline solid; for a cubic crystal has, in general, three independent elastic constants. This assumption will involve the contribution of conduction electrons to the elastic constants of metals.

Finally, numerical values will be obtained for the atomic force constants of several elements. This will make it possible, in the next section, to evaluate numerically the specific heat curves of these elements, and to compare the results with experimental specific heats and with the Debye theory.

2. Outline of the Properties of the Elastic Constants

The elastic constants of a crystalline body are defined by the Generalized Hooke's Law Equation, which relates the components of stress and strain experienced by an element of volume of an elastic medium:

$$(5.1) \quad T_{ij} = c_{ijkl} e_{kl} ,$$

the summation convention being used.

In this tensor equation T_{ij} stands for the component along the i -axis of the force acting on a unit area perpendicular to the j -axis, and e_{kl} stands for the first-order unit strain defined by the relation

$$(5.2) \quad e_{kl} = \frac{1}{2} (\partial u_k / \partial x_l + \partial u_l / \partial x_k)$$

where u_k is the k -component of the displacement of a point, in the strained medium, from its position in the unstrained medium. The c_{ijkl} form a Cartesian tensor of the fourth rank. The stress T_{ij} is conventionally understood to be the force acting on that portion of the medium lying in the direction of smaller values of the coordinates x_j . The x_j are rectangular Cartesian coordinates.

Considerations of the static equilibrium of an arbitrary element of the medium require that

$$(5.3) \quad T_{ij} = T_{ji}$$

while the definition of the unit strains ensures that

$$(5.4) \quad e_{kl} = e_{lk}.$$

These two relations then require that

$$(5.5) \quad c_{ijkl} = c_{jikl} = c_{ijlk} = c_{jilk}.$$

The deformation energy per unit volume of the medium may be written by contraction of (5.1) with the strains e_{ij} :

$$(5.6) \quad 2\phi = T_{ij}e_{ij} = c_{ijkl}e_{ij}e_{kl}.$$

which requires that

$$(5.7) \quad c_{ijkl} = c_{klij}.$$

The above relations reduce the number of independent components of the elastic constant tensor from 81 to 21. Thus, the most general crystalline body would possess 21 independent elastic constants, but special properties of the crystal, such as symmetry, will reduce this number. The cubic system, having the highest degree of symmetry, retains only three independent elastic constants.

The relations (5.5) and (5.7) permit the use of a less cumbersome notation, in which the subscripts are reduced from four to two. If the old subscripts are identified with new ones according to the rule,

$$(5.8) \quad \begin{array}{l} \text{Old subscripts} \\ \hline \text{New subscripts} \end{array} \quad \begin{array}{cccccc} 11 & 22 & 33 & 23,32 & 13,31 & 12,21 \\ 1 & 2 & 3 & 4 & 5 & 6 \end{array}$$

the relations (5.5) are satisfied automatically, while the condition (5.7) reduces to

$$(5.9) \quad c_{ij} = c_{ji}$$

in the new notation.

The three elastic constants required for the cubic system are c_{11} , c_{12} , c_{44} ; in terms of these constants, the potential energy per unit volume of a deformed cubic crystal is

$$(5.10) \quad 2\phi = c_{11}(e_{11}^2 + e_{22}^2 + e_{33}^2) + 2c_{12}(e_{11}e_{22} + e_{22}e_{33} + e_{33}e_{11}) \\ + 4c_{44}(e_{12}^2 + e_{23}^2 + e_{31}^2).$$

The notation for the elastic constants used in this brief outline is the same as that used by Wooster⁽¹⁸⁾.

3. Elastic Constants of the Monovalent, Cubic Metals

No mention has yet been made of the substances to which the results of the previous sections are to be applied. A survey of the elements shows that, at ordinary temperatures, the only monatomic crystals having face-centered cubic lattices are metals; in particular, the noble metals and aluminum are of this class. The question is therefore raised as to what possible effects the conduction electrons of these metals might have upon the elastic properties and upon the frequency spectrum.

The elastic constants of some typical monovalent, cubic metals have been calculated by Fuchs⁽¹¹⁾, who obtained good agreement with experiment in all cases by regarding the conduction electrons as a gas of perfectly free noninteracting Fermi particles. The energy of such a gas depends only upon its volume, so that the conduction electrons contribute to the deformation energy only if the volume of the crystal changes. By considering two types of deformation that leave the volume of the crystal unchanged, Fuchs found that the quantities $(c_{11} - c_{12})$ and c_{44} should be independent of the properties of the Fermi gas.

Fuchs' result will be used in the evaluation of the atomic force constants α and γ , but it must first be shown that the compressibility of the Fermi gas will not affect the frequency spectrum of the lattice. Clearly, the Born-von Karman boundary condition (Section I) requires that the volume of the crystal, and hence the energy of the Fermi gas, remain constant, so that the conduction electrons can have no effect upon the motion of the lattice, and will therefore not affect the frequency spectrum.

4. Evaluation of α and γ

The atomic force constants, α and γ , will now be evaluated for the lattice considered in Section I. The procedure to be followed is to express

the potential energy of the lattice, for a state of homogeneous deformation, in terms of α and γ by means of Equation (1.3) and then to identify the coefficients of e_{11}^2 , $e_{11}e_{22}$, and e_{23}^2 respectively, in this form with the elastic constants c_{11} , c_{12} , and c_{44} of Equation (5.10). In carrying out this process, the expression (5.2) for the unit strains will be used, along with the expression

$$(5.11) \quad \omega_{k1} = \frac{1}{2d} (\partial u_k / \partial x_1 - \partial u_1 / \partial x_k),$$

which defines the components of rotation of the crystal. (ω_{12} is the component of the rotation about the z axis.)

Thus,

$$(5.12) \quad \partial u_k / \partial x_1 = e_{k1} + \omega_{k1} = e_{1k} - \omega_{1k}.$$

If the crystal is in a state of homogeneous deformation, the quantities $\partial u / \partial x$ are constants, so that the relative displacements of adjacent atoms which appear in Equation (1.3) may be treated as follows:

$$(5.13) \quad \begin{aligned} v_{100} - v_0 &= (\partial v / \partial x) \Delta x + (\partial v / \partial y) \Delta y + (\partial v / \partial z) \Delta z \\ &= \frac{1}{2d} d (\partial v / \partial y + \partial v / \partial z) \\ &= \frac{1}{2d} d (e_{22} + e_{23} + \omega_{23}). \end{aligned}$$

The first form of writing of the above equation utilizes the fact that the deformation is homogeneous, so that the higher terms in the Taylor expansion disappear; the second form results from the insertion of Δx , Δy , and Δz into the first form (refer to Figure 1, Section I); the third form follows from the identification of u_1 , u_2 , and u_3 in the elasticity notation of the present section with u , v , and w respectively of Equation (1.3), and a further substitution of the unit strains and rotations for the partial derivatives, in accordance with Equation (5.12).

If the rest of the terms of the Equation (1.3) are treated in a similar manner, the energy of deformation becomes

$$\begin{aligned}
 2V = \sum_{abc} & \left[ad^3/8 \left\{ (e_{22} + e_{33} + \omega_{23} + e_{33} + e_{32} + \omega_{32})^2 \right. \right. \\
 (5.14) & + (e_{33} + e_{31} + \omega_{31} + e_{11} + e_{13} + \omega_{13})^2 + (e_{11} + e_{12} + \omega_{12} + e_{22} + e_{21} + \omega_{21})^2 \\
 & + (e_{11} - e_{12} - \omega_{12} + e_{22} - e_{21} - \omega_{21})^2 + (e_{22} - e_{23} - \omega_{23} + e_{33} - e_{32} - \omega_{32})^2 \\
 & \left. \left. + (e_{33} - e_{31} - \omega_{31} + e_{11} - e_{13} - \omega_{13})^2 \right\} + \gamma d^3 (e_{11}^2 + e_{22}^2 + e_{33}^2) \right]
 \end{aligned}$$

Observing from (5.2) and (5.11) that $e_{kl} = e_{lk}$ and $\omega_{kl} = -\omega_{lk}$, and carrying out the summations over (abc),

$$\begin{aligned}
 2V = N_1 N_2 N_3 & \left[(ad^3/8) \left\{ 2(e_{22} + e_{33})^2 + 8d_{23}^2 + 2(e_{33} + e_{11})^2 + 8e_{31}^2 \right. \right. \\
 & \left. \left. + 2(e_{11} + e_{22})^2 + 8e_{12}^2 \right\} + \gamma d^3 (e_{11}^2 + e_{22}^2 + e_{33}^2) \right] \\
 (5.15) & = N_1 N_2 N_3 \left[(ad^3/8) \left\{ 4e_{11}^2 + 4e_{22}^2 + 4e_{33}^2 + 4e_{11}e_{22} + 4e_{22}e_{33} + 4e_{33}e_{11} \right. \right. \\
 & \left. \left. + 8e_{23}^2 + 8e_{31}^2 + 8e_{12}^2 \right\} + \gamma d^3 (e_{11}^2 + e_{22}^2 + e_{33}^2) \right] \\
 & = N_1 N_2 N_3 d^3 \left[(a/2 + \gamma) (e_{11}^2 + e_{22}^2 + e_{33}^2) \right. \\
 & \left. + 2(a/4) (e_{11}e_{22} + e_{22}e_{33} + e_{33}e_{11}) + 4(a/4) (e_{12}^2 + e_{23}^2 + e_{31}^2) \right] ,
 \end{aligned}$$

where the first equality follows from the fact that all terms of the sum over (abc) are the same for a homogeneous deformation, and the total number of different values assumed by the indices (abc) is equal to the number of atoms of the crystal: the second and third forms then follow by simple steps.

For comparison with (5.10), the energy per unit volume must be used; this is obtained from (5.15) by dividing both sides by the volume of the crystal, $N_1 N_2 N_3 d^3/4$:

$$\begin{aligned}
 2\phi = 8V/N_1 N_2 N_3 d^3 & = (1/d)(2a + 4\gamma)(e_{11}^2 + e_{22}^2 + e_{33}^2) \\
 (5.16) & + 2(a/d)(e_{11}e_{22} + e_{22}e_{33} + e_{33}e_{11}) + 4(a/d) (e_{12}^2 + e_{23}^2 + e_{31}^2) .
 \end{aligned}$$

Comparison of the right-hand sides of Equations (5.10) and (5.16) yields

$$(5.17) \quad \begin{aligned} c'_{11} &= (2a + 4\gamma)/d, \\ c'_{12} &= a/d, \\ c'_{44} &= a/d. \end{aligned}$$

The primes indicate that these are the contributions of the lattice ions to the elastic constants, exclusive of the compressibility of the electron gas.

To evaluate a and γ , Fuchs' result is taken into account by writing

$$(5.18) \quad c'_{11} - c'_{12} = c_{11} - c_{12} = (a + 4\gamma) / d$$

and

$$c'_{44} = c_{44} = a/d,$$

where the actual numerical values for the elastic constants of a face-centered cubic crystal may now be used.

In Table 31 are given the elastic constants at room temperature, together with the values of a and γ/a , computed from Equation (5.18) for some typical face-centered elements.

TABLE 31

Elastic Constants (9), Atomic Force Constants, and Cell Dimensions of some Face-centered Metals. (c_{11}, c_{12} , and c_{44} in units of 10^{11} dynes/cm².)

Metal	$d(\text{\AA})$	c_{11}	c_{12}	c_{44}	$c_{11} - c_{12}$	$a \times 10^{-8}$	γ/a
Cu	3.61	17.0	12.3	7.5	4.7	27.1	-0.09
Ag	4.08	12.2	9.1	4.4	3.1	18.0	-0.08
Au	4.07	18.7	15.7	4.4	3.0	17.9	-0.08
Al	4.04	11.9	6.2	2.9	5.7	11.7	+0.25

The case of silver will be treated numerically in the next section. It is in the region of absolute zero that the predictions of the theory will be

compared with experiment, so that the atomic force constants at absolute zero must be used. Eucken⁽⁸⁾ in 1913 used a value for the shear modulus of silver at absolute zero that was derived from Grüneisen's theory. This value also agreed with the experimental data existing at that time. The ratio of the shear modulus at absolute zero to the same at room temperature (for a poly-crystalline sample) is assumed to be the same as the corresponding ratio of the values of e_{44} , upon which the basic constant α depends. Thus, at absolute zero, the constant α for silver would have the value

$$\begin{aligned}
 \alpha_0 &= (\mu_0/\mu_{R.T.}) \alpha_{R.T.} \\
 (5.19) \quad &= 3500/2960 \times 18.0 \times 10^8 = 1.18 \times 18 \times 10^8 \\
 &= 21.3 \times 10^8 .
 \end{aligned}$$

The change in the cell dimension d due to thermal expansion is negligible over this temperature range.

SECTION VI

SPECIFIC HEATS OF FACE-CENTERED CUBIC ELEMENTS

1. Introduction

The frequency distributions of the normal modes of vibration of a face-centered cubic crystal, which were obtained in Section IV, will be applied in the present section to the computation of the specific heats of elements having this crystal structure. It is possible to evaluate the specific heats without using the numerical data of Section V, and this will be done. In order to compare these theoretical results with experimental observations, however, the numerical values of the atomic force constants must be used.

The course of the treatment is as follows: first, the specific heat integral (0.4) will be written in terms of the dimensionless parameter λ . Next, the specific heat will be evaluated for a number of values of a second parameter, T/β , where T is the absolute temperature and β is a constant characteristic of the element being studied and having the dimensions of temperature. These values of the specific heat will then be compared with a table of Debye specific heats, and the values of Θ/T corresponding to the chosen values of T/β will be found. Θ is the so-called Debye characteristic temperature (refer to p.xii of the Introduction). Finally, the values of Θ/T will be multiplied by the corresponding values of T/β to obtain Θ/β as a function of T/β . This function then yields a curve of Θ vs. T for any given element for which the value of β can be calculated.

Values of Θ/β as a function of T/β will be obtained for very small values of T/β by a method which utilizes the series expressions (4.10) and (4.11) for the distribution function $G(\lambda)$. Finally, these results will be compared numerically with the experimental values for the case of silver, for which specific heat data and elastic data are available.

2. The Specific Heat Integral

The specific heat integral was derived in the Introduction for a general

solid body characterized by the frequency distribution $N(\nu)$. This integral is

$$(6.1) \quad C_V = h^3/kT^3 \int_0^{\nu_m} \frac{\nu^3 e^{h\nu/kT}}{(e^{h\nu/kT} - 1)^2} N(\nu) d\nu.$$

The frequency distribution for a face-centered cubic lattice has been obtained in the form of a dimensionless function $G(\lambda)$ of the dimensionless parameter λ . The above integral will therefore be in a more convenient form if it is rewritten in terms of the parameter λ .

According to the definition of λ in connection with Equation (2.5)

$$(6.2) \quad \lambda = \frac{2\pi\nu}{a} = 2\pi\nu \frac{m}{2a},$$

and from Equation (4.4)

$$(6.3) \quad N(\nu)d\nu = (3N_0/2) G(\lambda)d\lambda$$

where N_0 will now be taken as Avogadro's number.

Using (6.2) one may write

$$(6.4) \quad h\nu/kT = \beta\lambda/T,$$

where

$$\beta^3 = h^3 a^3 / 2\pi^3 mk.$$

Thus (6.1) takes the form

$$(6.5) \quad \begin{aligned} C_V &= \frac{3}{2} N_0 k \int_0^{\lambda_m} \frac{(\beta\lambda/T)^3 e^{\beta\lambda/T}}{(e^{\beta\lambda/T} - 1)^2} G(\lambda) d\lambda \\ &= \frac{3}{2} R \int_0^{\lambda_m} \frac{(\beta\lambda/T)^3 e^{\beta\lambda/T}}{(e^{\beta\lambda/T} - 1)^2} G(\lambda) d\lambda, \end{aligned}$$

since $N_0 k = R$, the gas constant per mole, and $\lambda_m = 2.0$.

3. Specific Heats of Face-centered Cubic Elements

The expression (6.5) will now be used to evaluate the specific heats of face-centered cubic elements. The quantities appearing in the integrand must first be evaluated numerically.

Table 32 contains values of $(\beta\lambda/T)^2 e^{\beta\lambda/T} / (e^{\beta\lambda/T} - 1)^2$ as a function of T/β and λ .

TABLE 32

The Function $f(\beta\lambda/T) = (\beta\lambda/T)^2 / (e^{\beta\lambda/T} - 1)^2$

λ	T/β								
	0.10	0.15	0.20	0.25	0.30	0.35	0.40	0.50	1.00
0.0	1.000	1.000	1.000	1.000	1.000	1.000	1.000	1.000	1.000
0.1	.922	.964	.980	.987	.990	.993	.998	.998	1.000
0.2	.723	.864	.922	.950	.964	.974	.980	.987	.998
0.3	.495	.723	.831	.889	.922	.942	.955	.972	.993
0.4	.304	.569	.723	.812	.864	.898	.922	.950	.987
0.5	.171	.423	.607	.723	.798	.843	.878	.922	.980
0.6	.090	.304	.495	.629	.723	.786	.832	.889	.972
0.7	.045	.207	.392	.539	.648	.723	.779	.852	.961
0.8	.021	.137	.304	.454	.569	.657	.723	.812	.950
0.9	.010	.090	.228	.374	.495	.590	.666	.769	.935
1.0	.004	.056	.171	.304	.423	.525	.608	.723	.922
1.1	.002	.035	.125	.242	.357	.463	.550	.677	.904
1.2	.001	.021	.090	.193	.304	.405	.495	.629	.889
1.3	.000	.013	.064	.150	.250	.350	.442	.585	.871
1.4	.000	.006	.045	.118	.207	.302	.392	.539	.852
1.5	.000	.004	.031	.089	.171	.259	.346	.495	.831
1.6	.000	.003	.021	.067	.137	.222	.304	.454	.812
1.7	.000	.002	.015	.050	.110	.186	.263	.413	.790
1.8	.000	.001	.010	.037	.090	.155	.228	.374	.769
1.9	.000	.000	.008	.028	.070	.130	.196	.338	.746
2.0	.000	.000	.004	.020	.056	.108	.171	.304	.723

The values given by the above table are to be multiplied by the corresponding average values of $G(\lambda)\Delta\lambda$ and summed over the range of λ . The following values of $G(\lambda)$ were obtained from Figure 17 and Equations (4.10) and (4.11). These values do not correspond to the ordinates of the distribution function, but rather to averages over the intervals of width $\Delta\lambda = 0.1$ centered about the given values of λ .

TABLE 33

Values of $G(\lambda)$ for $\gamma/a = 0.0$ and $\gamma/a = -0.1$

λ	$G(\lambda)$	
	$\gamma/a = 0.0$	$\gamma/a = -0.1$
0.0	.000	.000
0.1	.007	.009
0.2	.026	.035
0.3	.061	.081
0.4	.113	.149
0.5	.19	.26
0.6	.28	.39
0.7	.41	.56
0.8	.59	.80
0.9	.86	1.17
1.0	1.46	1.58
1.1	1.87	1.76
1.2	1.98	1.89
1.3	2.12	1.96
1.4	1.83	1.48
1.5	1.28	1.27
1.6	1.20	1.20
1.7	1.02	1.13
1.8	2.28	2.44
1.9	1.95	1.58
2.0	0.35	0.12

The process of multiplying corresponding ordinates and summing was carried out on a calculating machine; when these results were multiplied by $(3/2) R$, the following values were obtained for C_V .

TABLE 34

 C_V in cal./mole deg. for Face-centered Cubic Elements

T/β	C_V (Cal./mol. deg.)	
	$\gamma/a = 0.0$	$\gamma/a = -0.1$
0.10	.0594	.0792
0.15	.236	.294
0.20	.585	.681
0.25	1.050	1.170
0.30	1.565	1.692
0.35	2.075	2.200
0.40	2.548	2.670
0.50	2.335	3.438
1.00	5.07	5.11

The specific heats obtained by the above process were then compared with a table of Debye specific heats⁽¹⁵⁾. The values of the Debye parameter Θ/T which yield specific heats equal to those in Table 33 were determined. These values of Θ/T , when multiplied by T/β , yielded the values of Θ/β that appear in Table 35.

TABLE 35

Θ/β as a Function of T/β for Face-centered Cubic Elements

T/β	Θ/β	
	$\gamma/a = 0.0$	$\gamma/a = -0.1$
0.10	1.935	1.805
0.15	1.875	1.741
0.20	1.824	1.722
0.25	1.812	1.728
0.30	1.810	1.741
0.35	1.813	1.750
0.40	1.812	1.751
0.50	1.814	1.760
1.00	1.825	1.780

4. Θ/β vs. T/β Curves for Very Low Temperatures

The integral (6.5) is not in a convenient form for the evaluation of specific heats and characteristic temperatures at very low temperatures. In the range of temperature where $T/\beta < 0.05$, the function given in Table 31 has an appreciable value only inside the range where (4.10) and (4.11) hold. Because of this fact, it is possible to make use of these series expansions to obtain a simple expression for (Θ/β) in the low-temperature range.

Inasmuch as the function of Table 31 decreases exponentially for large values of $\beta\lambda/T$, and is negligible outside the range of validity of the series expressions (4.10) and (4.11), no appreciable error will be made if the integral (6.5) is evaluated from $\lambda = 0$ to $\lambda = \infty$, using these series expressions for $G(\lambda)$ over this entire infinite range. Thus (6.5) would become, using the notation of (4.6):

$$\begin{aligned}
 (6.6) \quad C_v &= \frac{6}{5} R \int_0^\infty \frac{\beta^3 e^{\beta\lambda/T}}{T^3 (e^{\beta\lambda/T} - 1)^2} (3k_0\lambda^4 + 5k_2\lambda^6 + 7k_4\lambda^8 + \dots) d\lambda \\
 &= \frac{6}{5} R \left[3k_0(T/\beta)^3 D(4) + 5k_2(T/\beta)^5 D(6) + 7k_4(T/\beta)^7 D(8) + \dots \right]
 \end{aligned}$$

where

$$(6.6a) \quad D(n) = \int_0^\infty \frac{x^n e^x dx}{(e^x - 1)^2}.$$

In the range of very low temperatures that is now being discussed, the Debye specific heat given by Equation (0.7) takes the form

$$(6.7) \quad C = 9R (T/\theta)^3 D(4)$$

To find the Debye characteristic temperature, θ , as a function of T/β , the expressions (6.6) and (6.7) may be equated, with the result

$$\begin{aligned}
 (6.8) \quad 9R (T/\theta)^3 D(4) &= \frac{6}{5} R (T/\beta)^3 D(4) \left[3k_0 + 5k_2 T^2/\beta^2 D(6)/D(4) \right. \\
 &\quad \left. + 7k_4 T^4/\beta^4 D(8)/D(4) + \dots \right]
 \end{aligned}$$

This equation may now be solved for θ/β :

$$(6.9) \quad \theta/\beta = \left[\frac{6}{3k_0 + 5k_2 T^2/\beta^2 D(6)/D(4) + 7k_4 T^4/\beta^4 D(8)/D(4) + \dots} \right]^{\frac{1}{3}}$$

To evaluate the $D(n)$ function appearing in (6.9), integration of (6.6a) by parts and subsequent expansion of the denominator in a series yields

$$\begin{aligned}
 (6.10) \quad D(n) &= \int_0^\infty \frac{x^n e^x dx}{(e^x - 1)^2} = n \int_0^\infty \frac{x^{n-1} dx}{(e^x - 1)} = n \int_0^\infty \frac{x^{n-1} e^{-x} dx}{1 - e^{-x}} \\
 &= n \sum_{r=0}^{\infty} \int_0^\infty x^{n-1} e^{-x} e^{-rx} dx = n \sum_{r=0}^{\infty} \frac{(n-1)!}{(r+1)^n} \\
 &= n! \sum_{s=1}^{\infty} 1/s^n = (2\pi)^n / 2 B_{n/2} \quad (n \text{ even}).
 \end{aligned}$$

where $B_{n/2}$ is the $n/2$ th Bernoulli Number, as tabulated by Dwight (5). Dwight gives

$$B_2 = 1/30, B_3 = 1/42, B_4 = 1/30$$

so that

$$D(4) = 4\pi^4/15, D(6) = 16 \pi^6/21, D(8) = 64\pi^8/15$$

and hence

$$(6.11) \quad D(6) / D(4) = 20 \pi^2/7 \text{ and } D(8)/ D(4) = 16 \pi^4.$$

Insertion of (6.11) into (6.9) yields

$$(6.12) \quad \theta/\beta = \left[\frac{6}{3k_6 + 100 k_2 \pi^2 T^2 / 7\beta^2 + 112 k_4 \pi^4 T^4 / \beta^4 + \dots} \right]^{1/3}$$

Table 36 contains values of θ/β calculated from Equation (6.12) and Table 30.

TABLE 36

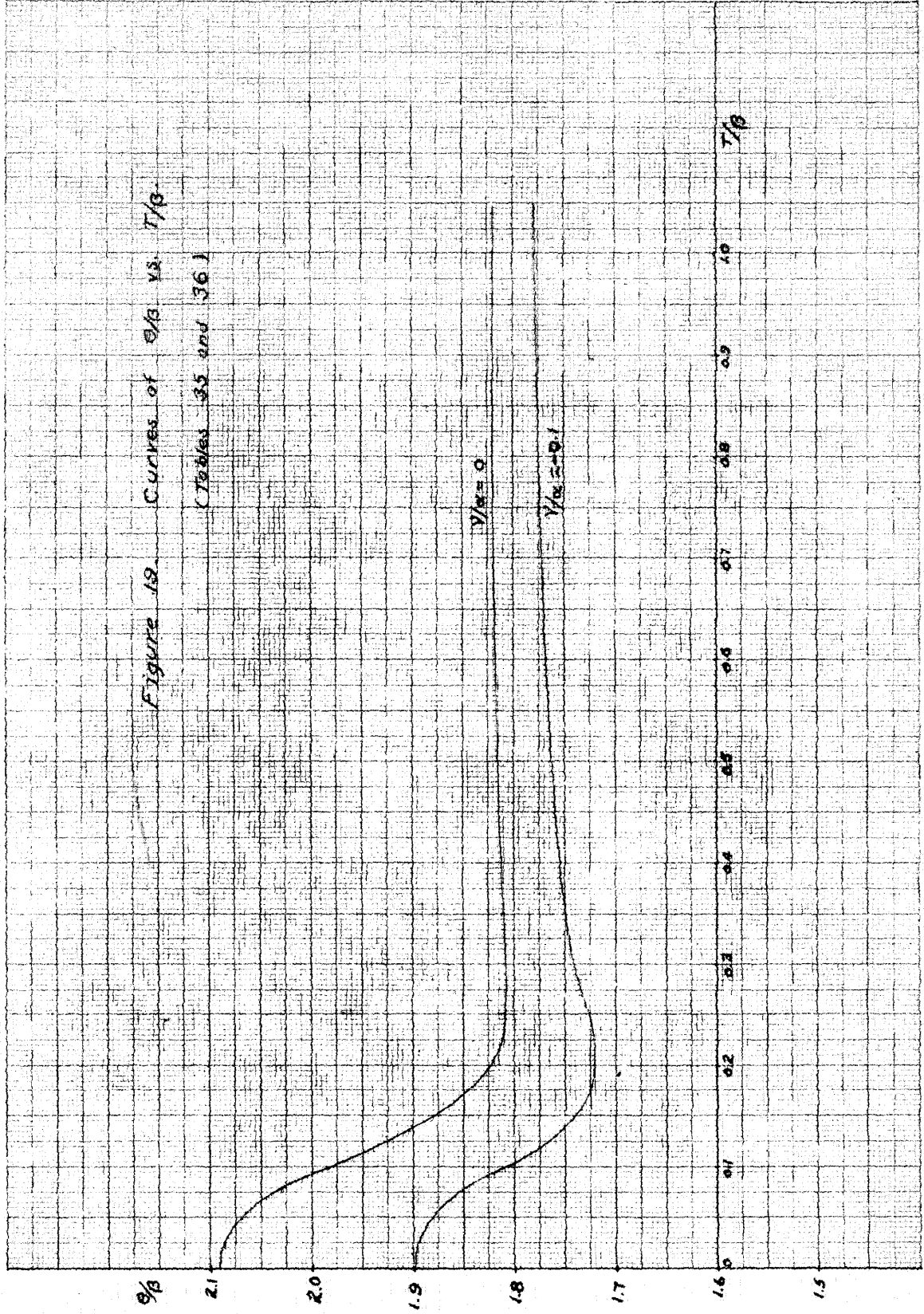
Values of θ/β Calculated from Equation (6.12) and Table 30.

T/ β	θ/β	
	$\gamma/a = 0.0$	$\gamma/a = -0.1$
0.00	2.090	1.898
0.02	2.083	1.895
0.04	2.076	1.888
0.06	2.056	1.872
0.08	2.025	1.850
0.10	1.985	1.805

5. Curves of θ/β vs. T/ β and Discussion of Results

The data of Tables 35 and 36 are shown in Figure 19. For the basic case (central forces between nearest neighbors only), the characteristic temperature drops abruptly from its value at absolute zero, to a value approximately

Figure 19. Curves of θ/θ_0 vs. T/θ_0
(Tables 35 and 36)



fifteen percent below the initial value, where it remains sensibly constant over a large temperature range. In the case of weak coupling between next-nearest neighbors of the type that is apparently characteristic of the noble metals, the characteristic temperature falls abruptly as for the basic case, but instead of remaining nearly constant, it passes through a definite minimum, and at the higher temperatures seems to be approaching the curve for the basic case. The difference between the maximum and minimum values of the characteristic temperature is in this case only about ten percent.

It is true that the atomic model used in this discussion is not refined enough to reveal small details in the characteristic temperature curve, because of the neglect of the effects of the more distant neighbors, the neglect of higher order terms in the potential energy expression (1.3), and the assumption that the conduction electrons are perfectly free. It seems safe to assert, however, that the important terms are included, and hence that the rise of the characteristic temperature with decreasing absolute temperature near absolute zero is a property of real crystals. It may also be reasonable to expect that the value of γ/a at room temperature would give some indication as to its value at absolute zero. In this case, one would expect the characteristic temperature to pass through a minimum near $T/\beta = 0.2$, and then to rise slowly with increasing temperature.

It should be pointed out that it is in just this region near absolute zero that the Debye theory is ordinarily thought to be most nearly true. That is, it is for low-frequency (long wave length) waves that the motion of the atomic lattice should resemble most closely the motion of a continuum. This viewpoint is of course justified, but the range of temperature over which the Debye theory is valid extends only from absolute zero to about $T/\beta = 0.05$, a range which is almost negligible for practical purposes.

It may be of interest for further comparison with the Debye theory to

evaluate the characteristic temperature for a Debye distribution which has the same upper limit as the distribution function $G(\lambda)$. In this case, the distribution function would be of the form

$$F(\lambda) = A\lambda^3$$

and the total number of normal modes must be the same as for $G(\lambda)$. Using (4.4) one thus writes

$$\int_0^{\infty} F(\lambda) d\lambda = 2 = A\lambda^3/3 \int_0^{\infty} = 8/3A$$

or

$$A = 3/4.$$

Insertion of this value of A for $3k_0$ in the expression (6.9) yields

$$\theta = 2\beta.$$

Thus, a Debye frequency distribution which has the same upper frequency limit as does the distribution for the atomic case has a characteristic temperature equal to twice the value of the constant β .

6. Specific Heat of Silver

The results of the last paragraph will now be compared numerically with the observed specific heat of silver. First, the constant β which was defined in Equation (6.4) must be evaluated for silver at absolute zero. Using the numerical value of α at absolute zero as given by (5.19), β may be evaluated:

$$\begin{aligned} \beta^2 &= h^2 \alpha_0 / 2\pi^2 m k^2 \\ &= (6.62 \times 10^{-27})^2 \times 21.3 \times 10^8 / 2 \times 1.79 \times 10^{-22} \\ &\quad \times (1.38 \times 10^{-16})^2 \\ &= 1.39 \times 10^4 \end{aligned}$$

or

$$\beta = 118 \text{ deg.}$$

The experimental values for the Debye characteristic temperature of silver were taken from the work of Keesom and Clark⁽¹³⁾, and Eucken, Clusius and Woitinek⁽⁹⁾.

Inasmuch as the experimental values for the characteristic temperature are not the result of a direct measurement of the specific heat of the lattice itself, it is appropriate to describe the steps by which the characteristic temperature is obtained from the experimental data. These steps involve certain formulae which may in fact not be exactly correct.

If there are no difficulties in the experimental method which might cause systematic errors, such as an incorrect determination of the temperature scale or the presence of a gas whose heat of adsorption might contribute to the measurements, the quantity that is actually measured is the specific heat at constant pressure of metallic silver. These measurements at constant pressure are transformed into values of the specific heat at constant volume by means of the thermodynamic relation⁽⁷⁾,

$$(6.16) \quad C_p - C_v = k \alpha^2 MT / \rho$$

where

k is the bulk modulus of the material,

α is its volume coefficient of expansion,

M is its atomic weight,

T is the absolute temperature, and

ρ is its density.

Any inaccuracies introduced through the use of this expression result from a lack of knowledge of the temperature variation of quantities appearing on the right-hand side. The bulk modulus, for example, is customarily evaluated at low temperatures by extrapolating from considerably higher temperatures.

The specific heat at constant volume so obtained represents the total specific heat of the metal; that is, it includes the specific heat of the lattice, that of the conduction electrons, and any other contributions that might result from an interaction between the conduction electrons and the lattice or from excitation of nonconduction electrons.

Keesom and Clark⁽¹³⁾ subtracted from the above value, the specific heat of the (perfectly free) conduction electrons, which can be calculated from Sommerfeld's formula⁽¹⁷⁾:

$$C_e = \frac{\pi^2 n m k}{h^2} \left(\frac{8 \pi V}{3n N_0} \right)^{2/3} RT$$

where

n is the number of free electrons per atom,

m is the mass of an electron,

N_0 is Avogadro's number, and

the other symbols have their usual significance.

The specific heats that resulted after the subtraction of this term were then translated into equivalent Debye characteristic temperatures. Eucken, Clusius, and Voitinek did not correct for the conduction electrons, so that their characteristic temperatures are for the entire specific heat at constant volume.

Figure 20 shows the theoretical curve for $\gamma/a = -0.08$ (obtained by linear interpolation between the two curves of Figure 19) and the experimental values as given by the above authors. The values given by Keesom and Clark are smoothed values, whereas the others are not.

It is clear from an inspection of Figure 20 that in some respects the

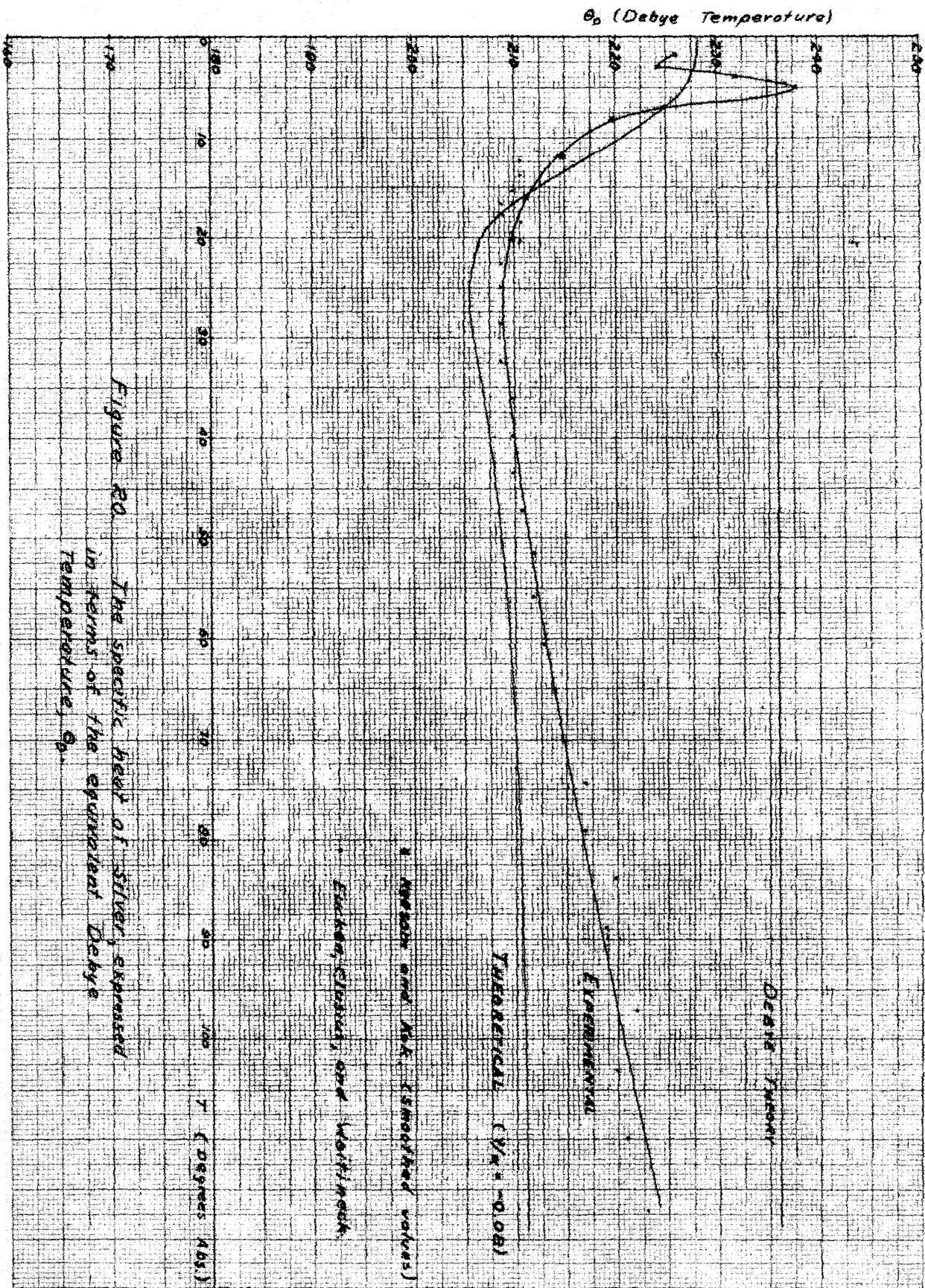


Figure 20 The specific heat of silver, expressed in terms of the equivalent Debye Temperature, θ_D .

experimental and theoretical curves agree, and that in others they do not. There is fair agreement between the two with regard to the rise of the characteristic temperature with decreasing absolute temperature below $T/\beta = 0.2$, and the existence of a minimum characteristic temperature at about this value of T/β . It is also evident that there is a radical difference in behavior between the two in the very-low-temperature range. Here, the theoretical curve attains a relatively broad maximum at absolute zero, while the experimental curve shows a very sharp maximum at about 5°K , with a second minimum at about 3.5°K . This same behavior is shown by the characteristic temperature of potassium chloride, which is an ionic crystal having no conduction electrons. This matter is discussed for both silver and potassium chloride by Keesom and Clark⁽¹³⁾.

Blackman⁽⁵⁾ deduced that the frequency spectrum of the sodium-chloride lattice increased more rapidly than a Debye spectrum in the low frequency region, and hence concluded that the characteristic temperature of this lattice should decrease from a maximum at absolute zero. This conclusion can also be drawn for the face-centered lattice, both from the actual curves of Figure 1 and from the positive values of the coefficients in the series expansions (4.10) and (4.11). For this reason, it seems quite clear that the very-low-temperature behavior of the characteristic temperature θ cannot be explained in terms of the differences between the frequency spectrum of a Debye continuum and that of an atomic lattice.

On the other hand, it seems reasonable to assume that the agreement between the experimental and theoretical curves in the range from 7°K to 50°K is not purely fortuitous, especially as the theoretical results were obtained by direct calculation, with no attempt to fit the experimental data as is often done in the Debye theory.

7. Conclusions

It was concluded in the last paragraph that the low-temperature anomalies found by Keesom and Clark have no simple explanation in terms of the vibrational spectrum of an atomic lattice. Furthermore, since the effect is very nearly the same for potassium chloride (an insulating, ionic crystal) as for silver, it is unlikely that the explanation lies in the properties of the conduction electrons.

Possibilities for further investigation are present. For example, it would be worthwhile to know whether there exist distribution functions $G(\lambda)$ which are everywhere positive and which yield the proper $\theta(T)$ curves for potassium chloride and silver. This could be done by solving the Equation (6.5) which is an integral equation of the first kind; or, since the region of interest is that of very low temperatures, such that $\beta/T \gg 1$, the function $G(\lambda)$ might be expanded in a power series, and the coefficients of the various terms evaluated with the use of Equations (6.6) and (6.8).

Another possibility for further investigation is the application of the continuum and lattice theories to the evaluation of other properties of crystals, such as thermal scattering of X-rays and the temperature variation of electrical resistance near absolute zero. Such a comparison would be rendered much easier by the existence of the distribution function which is obtained in the present work.

ABSTRACT

The equations of motion of the atoms of a face-centered, cubic crystal lattice are written, assuming central, Hooke's Law forces between each atom and its eighteen nearest neighbors, and the secular determinant defining the normal frequencies is obtained. This determinant is written as a product of third order determinants. The properties of the roots of the secular determinant are discussed, and it is shown that the surfaces of constant frequency have the symmetry properties (in reciprocal-vector space) of a body-centered cubic lattice. This fact is used to simplify the computation of the distribution of the normal frequencies. The frequency spectrum is found by actually modeling the constant frequency surfaces in plaster of Paris and measuring the volumes enclosed between successive surfaces. The frequency spectrum so obtained is used in the evaluation of the specific heat of a general crystal of the type treated, and numerical values are presented for the element silver. The present theory (that of Born and von Karman), is in much better agreement with the experimental values for temperatures below 100° K than is the Debye theory. Certain anomalies in the specific heat curves of silver and potassium chloride at temperatures below 10° K are not explicable in terms of the atomic model that is used.

BIBLIOGRAPHY

1. Blackman, M. Roy. Soc. Proc., 148, 384 (1935); 159, 416 (1937)
Camb. Phil. Soc. Proc., 33, 94 (1937)
2. Born, M. and von Karman, Th., Physik. Zeits., 13, 297 (1912); 14, 15 (1913)
3. Brillouin, L., Wave Propagation in Periodic Structures. McGraw-Hill Book Co.,
Inc. New York: 1946
4. Debye, P., Ann. Physik, 39, 789 (1912)
5. Dwight, H. B., Tables of Integrals and Other Mathematical Data. The Macmillan
Co. New York: 1934
6. Einstein, A., Ann. Physik, 22, 180,800 (1906); 34, 170 (1911)
7. Epstein, P. S., Textbook of Thermodynamics. John Wiley and Sons, Inc. New York: 1937
8. Eucken, A., Verh. deut. physik. Ges., 15, 571 (1913)
9. Eucken, A., Clusius, K., and Woitinek, H., Zeits. f. anorg. Chem., 203, 47 (1931)
10. Fine, P. C., Phys. Rev., 55, 355 (1939)
11. Fuchs, K., Roy. Soc. Proc. 153 A, 622 (1936)
12. Houston, W. V., Zeits. f. Physik, 48, 449 (1928)
13. Keesom, W. H., and Clark, C. W., Physica 2, 698 (1935)
14. Kellerman, E. W., Roy. Soc. Phil. Trans., A 238, 513 (1940)
15. Landolt-Bornstein, Physicalish = Chemische Tabellen, 5 Aufl. Ergbd. I, 702.
Julius Springer, Berlin: 1927.
16. Montroll, E. W., and collaborators, J. Chem. Phys. 10, 218 (1942); 11, 481 (1943);
12, 98 (1944).
17. Sommerfeld, A., Zeits. f. Physik, 47, 1 (1928)
18. Wooster, W. A., Textbook of Crystal Physics. Cambridge Univ. Press, London: 1938.